



*Università degli Studi della Basilicata*

PhD Programme

“APPLIED BIOLOGY AND ENVIRONMENTAL SAFEGUARD”

**“Research and development of innovative molecular sensor technologies for the monitoring of volatile organic compounds in wines”**

In the framework of the financial initiative “Innovative PhD agreement with specialization in enabling technologies in Industry 4.0” - Basilicata Region

Scientific  
Disciplinary Sector  
“AGR/11”

*PhD Coordinator*

Prof. Patrizia FALABELLA

*Tutor*

Prof. Sabino Aurelio BUFO

*Co-Tutor*

Prof. Patrizia FALABELLA

*PhD Candidate*

Donatella FARINA

Cycle XXXIII

# TABLE OF CONTENTS

<b>ABSTRACT .....</b>	<b>1</b>
<b>AIM.....</b>	<b>3</b>
<b>1. INTRODUCTION</b>	
<b>1.1 BIOSENSORS: NEW TECHNOLOGY IN ANALYTICAL TASK</b>	
1.1.1 What is a biosensor and how many types exist .....	5
1.1.2 Optical silicon biosensors .....	8
1.1.3 Features of a biosensor .....	11
1.1.4 Odorant binding proteins based biosensors .....	
1.1.4.1 OBPs based biosensors advantage .....	11
1.1.4.2 OBPs overview: structure and physiological role. ....	12
1.1.5 Application of biosensors .....	15
<b>1.2 WINE</b>	
1.2.1 Wine .....	16
1.2.2 Wine aroma compounds .....	20
1.2.3 Terpenes in wine .....	22
1.2.4 Wine aroma compounds analysis .....	27
<b>1.3 APHIDS AND THEIR OLFACTION</b>	
1.3.1 Aphids biology .....	28
1.3.2 Aphids pheromones .....	30
1.3.3 Aphids Odorant Binding Proteins .....	33
<b>1.4 BIOMIMICRY .....</b>	<b>34</b>

## 2. MATERIALS AND METHODS

### 2.1. ODORANT BINDING PROTEINS RECOMBINANT PRODUCTION

2.1.1 Identification of aphids Odorant Binding Protein .....	37
2.1.2 Expression of aphids Odorant Binding Proteins.....	38
2.1.3 Purification of aphids Odorant Binding Proteins.....	39

### 2.2 *In silico* EXPERIMENTS

2.2.1 Preparation of target proteins and ligand structures .....	40
2.2.2 Molecular docking .....	40
2.2.3 Binding pocket investigation .....	40

### 2.3 *In vitro* EXPERIMENTS

2.3.1 Fluorescence competitive binding assays .....	41
2.3.2 Fluorescence data analysis .....	41

### 2.4 BIOSENSOR DEVELOPMENT.....

### 2.5. BASILICATA'S WINE SAMPLING.....

## 3. RESULTS

### 3.1 *Apis*OBP7 SUBCLONING AND SEQUENCING OF ALL

RECOMBINANT PLASMIDS.....	45
---------------------------	----

### 3.2 ODORANT BINDING PROTEINS EXPRESSION.....

### 3.3 ODORANT BINDING PROTEINS PURIFICATION.....

3.4 MOLECULAR MODELING: aphids OBP structure, ligand selection and structure, <i>in silico</i> docking analysis .....	55
--	----

### 3.5 COMPETITIVE BINDING ASSAYS.....

### 3.6 BINDING POCKET ANALYSIS.....

3.7 OPTICAL BIOSENSORS OBP BASED. ....	69
<b>4. DISCUSSION .....</b>	<b>84</b>
<b>5. CONCLUSIONS AND FUTURE PERSPECTIVES.....</b>	<b>94</b>
<b>6. REFERENCES .....</b>	<b>96</b>
<b>SUPPLEMENTARY MATERIALS .....</b>	<b>108</b>
<b>APPENDIX</b>	
Appendix A: Sequences .....	115
Appendix B: Protocols .....	119
Appendix C: Solutions .....	125

## ABSTRACT

The scientific and social increasing demand for quantitative/qualitative determination of natural and artificial chemical species in different sector of human life (health, living environment, food, etc.) highlights the need for new strategies and new measurement methods. In particular, the agro-food industries need quick and sensitive tools to identify molecules in its final products or to monitor them during production processes. This need is due to the increase of food frauds. Indeed, in last decades, adulteration and falsification of food become a very serious problems also as regard human health.

Biosensors are cutting-edge and the cheapest tools that can satisfy the monitoring of food quality because they represent an intelligent combination of biological components, such as enzymes or bacteria, and technological components that detect physical and chemical changes and transmit them in the form of data.

Among agro-food chain products, wine plays an important role in world trade. Wine is one of the most appreciated beverages and it is a complex mixture of sugars, acid and odours that concur to give it characteristic flavour. Concerning flavours, specific volatile organic compounds (VOCs) in wine are able to give it fruity or floral aroma. These VOCs belong to terpenes class (monoterpenes and sesquiterpenes) and they all together contribute to wine aroma. Analysis of wine aroma is at the base of quality assessment and physicochemical parameters are important to be monitored in order to limit frauds or adulterations.

In an automated food production system, devices as biosensors are important to monitor and maintain product quality and uniformity based on aroma characteristics.

The nature is the principal source to discover new molecules that could be used to realize biosensors. In this context, insects represent the main source from which to be inspired because they constitute the largest animal phyla. Insects have an important part in all ecosystems considering their role in pollination, biological control and bioconversion. They are a resource of genes, molecules and processes that can inspire several technological innovations. Considerably sophisticated in insect is the “chemoreception” that is a process by which organisms respond to chemical stimuli in their environments that depends primarily on the senses of taste and smell. Chemoreception plays an essential role throughout the life cycle of insects that respond to different arrays of chemical, biological and environmental signals to locate and select food, mates, oviposition sites and avoid predators.

To interpret these signals, insects use a range of molecular components that are located in specialized structures called chemosensilla. The last ones are characterized by a variety of

forms and by one or more pores on their surface, that allow the access of molecules to the internal aqueous phase, the sensillar lymph, which surrounds the dendrites of sensory neurons. In the sensillar lymph, a large amount of small soluble proteins, Odorant Binding Proteins (OBPs) and Chemosensory Proteins (CSPs) are present.

Some aphids OBPs are able to bind the terpene (E)- $\beta$ -Farnesene that it is used as alarm pheromone. In *Acyrtosiphon pisum*, OBP3 and OBP7 are able to bind (E)- $\beta$ -Farnesene and they are responsible of alarm response. Recently, *Acyrtosiphon pisum* OBP9 was found to be involved in perception of this compound. Even *Megoura viciae* use (E)- $\beta$ -Farnesene as alarm pheromone and its perception is mediate by OBP3.

*Acyrtosiphon pisum* OBP3 are able to bind also farnesol, structurally related to (E)- $\beta$ -Farnesene and *Megoura viciae* OBP3 is able to bind limonene. Farnesol and limonene are listed as wine terpenes.

Starting from this consideration, aphids OBPs were produced through recombinant procedures and used to develop a possible biosensor able to bind terpenes in wine. Beside farnesol and limonene, already tested with aphids recombinant proteins, others wine terpenes were tested with *Acyrtosiphon pisum* OBP3 and *Megoura viciae* OBP3. A preliminary *in silico* analysis of aphid OBPs, including also *Acyrtosiphon pisum* OBP9 and OBP7, was conducted to select other terpenes useful for a rational design of the biosensor. Terpenes selected were geraniol, nerol and citronellol.

Concerning biosensor assembly, the choice was to produce optical silicon biosensors. Optical sensors are more versatile than others because they can be made from different materials (silicon, glass, polymers, etc.) and among materials, silicon has gained attention and popularity in recent years because of its ease fabrication, special optical properties and its versatile surface chemistry. Moreover, silicon is readily available, low cost and biocompatible.

*Acyrtosiphon pisum* OBP3 was the first protein used to optimize the optical biosensor assembly protocol because of its previous functional characterization. For biosensor development, Porous Silicon (PSi) surfaces were used and the flow sensing was used as a strategy to verify the behavior of sensing in *real time*. OBP was adsorbed onto oxidized surface simply flowing the protein on surface and farnesol was tested in different concentration (range: 10  $\mu$ M – 400  $\mu$ M). Even if results are not conclusive, they are encouraging considering that terpenes are very small molecules that give a small change in the refractive index.

## AIM

This PhD work is focused on the research and development of innovative technologies useful in winemaking industries. Particularly, the main interest was to study how to create a biosensor able to detect aroma compounds in wines. The necessity to create a ease-to-use, low cost and rapid device able to detect small volatile organic compounds (VOCs) involved in wine aroma is due to huge increase of frauds in wine market and it will be also useful for winemakers to improve products in early stage of winemaking.

To date, aroma wine analysis is conducted using “classical” methods like gas chromatography that require time and the availability of expensive instrument. Moreover, these analyses require a pre-concentration of volatiles before gas chromatography step.

Therefore, the idea at the base of this PhD research was to identify biological element that could be used to develop a biosensor for the monitoring of VOCs in wine.

Insect Odorant Binding Proteins (OBPs) seemed to be the most suitable biological elements to reach this goal. OBPs are small protein involved in olfactory perception and they are good candidate for their use in sensing devices for odours. Indeed, they possess interesting characteristics like their compact structure, their soluble nature and small size; they are extremely stable to high temperature, refractory to proteolysis and resistant to organic solvents. In particular, aphids OBPs were selected because these insects naturally perceive terpenes such as limonene, farnesol and others. They use terpenes as pheromone but also to localized host plant. The focus was on *Acyrtosiphon pisum* OBP3, OBP7, OBP9 and *Megoura viciae* OBP3 because all these OBPs are able to bind E- $\beta$ -farnesene (a terpene). Moreover, among them, *Apis*OBP3 is able to bind also farnesol (an analog of E- $\beta$ -farnesene), a wine terpene.

In this PhD work, aphids OBPs were structurally characterized with innovative Molecular modeling tools to verify if they are able to bind terpenes specifically present in wine (in addition to farnesol). Then, they were produced through recombinant DNA techniques, purified by chromatography and analyzed with biochemical binding assays.

Subsequently, a key aim of research was the attempt to develop an optical biosensor OBP based using innovative surface made of silicon.

Just recently, Porous silicon (PSi) have been studied as biosensor element and the attempt during the period abroad of PhD course (at Nanophotonic technology Center of Valencia, Spain) was to optimize a protocol for optical OBP-based biosensor assembly. For this aim, the adsorption procedure was preferred to immobilization for two reason: incompatibility of protein buffer with coupling agents using in immobilization procedure and the chemical

“simplicity” of this procedure (no chemical agent could interfere with the structure of protein). To date, this PhD research represent the first attempt to use OBP on PSi surface and we focused on the optimization of biosensor assembly. In fact, even if Porous silicon have a lot of advantage, they suffering of negative aspect as the pores size and the thickness of oxide layer. This two parameter are not always controllable and could affect the protein adsorption. Moreover, the direct detection of small molecules (like terpenes) is very difficult, owing to the small change in the refractive index induced by the binding of those analytes on the sensor surface.

To conclude, PSi represent a good candidate as biosensor support but more studies are require to develop a standardized protocol, particularly for the direct monitoring of small molecules.



# INTRODUCTION

## 1.1 BIOSENSORS: NEW TECHNOLOGY IN ANALYTICAL TASK

### 1.1.1 What is a biosensor and how many types exist

Sensing tools are used for a multitude of application in every conceivable analytical tasks such as disease monitoring, drug discovery, food safety, process control and pollutants detection in environment.

The scientific and social increasing demand for quantitative determination of both natural and artificial chemical species, considering their diffusion and their effects on the environment and on living agents, highlights the need for new detecting strategies and new measurement methods. This has stimulated the development of chemical sensors, and more recently of biosensors.

In the last decades, the growth in the field of biosensors has been particularly remarkable because these tools join the sensitivity/specificity of biology and physiochemical transducers to achieve complex and precise measurement in an easy-to-use format.

The “father of biosensors” is Leland C. Clark who invented the first biosensor for glucose detection in 1962. This device was based on glucose oxidase enzyme. It was the first attempt to join the selectivity given by the electrode with the characteristic specificity of an enzyme.

A biosensor is a compact analytical device incorporating a biological sensitive element able to measure biological or chemical reactions by generating signals proportional to the concentration of analyte in the reaction.

A biosensor is composed (Bhalla et al 2016) by:

- Bioreceptor. It is a molecule that specifically recognizes the analyte. The process of signal generation upon interaction of the bioreceptor with the analyte is termed biorecognition.
- Transducer. It is an element that converts one form of energy into another. In a biosensor the transducer role is to convert the biorecognition event into a measurable signal. This event is called signalization. Signal is usually proportional to the amount of analyte–bioreceptor interactions.
- Electronics. This is the part of a biosensor that processes the transduced signal and converts it in a digital form.

- Display. The display consists of a user interpretation system such as the liquid crystal display of a computer or a direct printer that generates numbers or curves understandable by the user.

A schematic representation of these elements is shown in Figure 1.

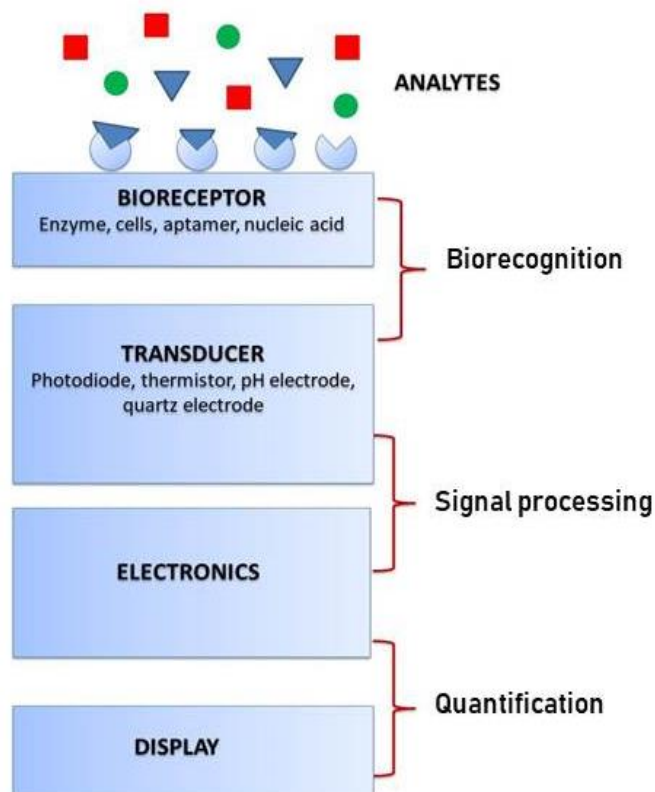


**Figure 1.** A schematic representation of a biosensor

Different types of biosensors exist, depending on the bioreceptor used. Biorecognition can be based on (Chambers et al., 2008):

- Receptor. Receptors are transmembrane and soluble proteins responsible for physiological process in cells, binding specific molecules called ligand. Although receptors are attractive biosensor recognition elements due to their ligand specificity and affinity, they are not often used as bioreceptor because of purification protocol difficulties and their instability. This is not the case of soluble proteins.
- Enzyme. This type of biosensor is very attractive because of a variety of measurable reaction products. A problem associated with enzymes as bioreceptor is expression difficulties.
- Antibody. Antibody based biosensors are the most widespread systems. They use sensitivity and specificity of antibody-antigen interactions.

- Aptamer. This type of biosensor is based on nucleic acids (RNA or ssDNA) that recognize their target by shape (conformation).
- Peptide nucleic acid. Peptide nucleic acid (PNA) is an artificially synthesized polymer similar to DNA or RNA in which the deoxyribose phosphate backbone is replaced by a pseudo-peptide polymer to which the nucleobases are linked. Since the backbone of PNA contains no charged phosphate groups, the binding between PNA/DNA strands is stronger than the binding between DNA/DNA strands due to the lack of electrostatic repulsion.
- Lectins. They are proteins binding glycans and represent excellent bioreceptor because of their high affinity for saccharide moieties via multivalent interactions.
- Molecular imprint. A molecularly imprinted polymer is a polymer that has been processed using the molecular imprinting technique which leaves cavities in the polymer matrix with an affinity for a molecule. The process usually involves an initiating polymerization of monomers in the presence of a template molecule that is extracted afterwards, leaving behind complementary cavities.

Concerning transducer, there are three general categories of biosensors depending on the type of the generated output (Pelosi et al., 2018). They can convert a biorecognition event into a:

- a) Mass change. Piezoelectric biosensors are considered as mass-based biosensors (Malhotra et al., 2017). Piezoelectric platform or piezoelectric crystal is a sensor part working on the principle of oscillations change due to a mass bound on the piezoelectric crystal surface.
- b) Optical signal. When optical biosensors detect analyte, there is a change in light absorption, fluorescence or scattering (Malhotra et al., 2017). Surface plasmon resonance (SPR) spectroscopy belong to label-free optical biosensing technologies. The SPR method is based on optical measurement of refractive index changes associated with the binding of analyte to bioreceptor immobilized on metal or semiconductor layer. Local surface plasmon resonance (LSPR) is a particular type of SPR, based on gold nanoparticles: the electromagnetic field remains localized in a nanoscale region around the nanoparticle-dielectric interface. In fact, while the penetration depth of the plasmon field for SPR is 200-1000 nm, it is 15-30 nm for LSPR (Turner, 2013).
- c) Electronic signal. A change in current, voltage or impedance occurs when a bioreceptor binds a ligand. This change is dependent on ligand concentration.

Whatever the application or type of biosensor, three steps are important for its functionality:

- a) Immobilization of biochemical substance (DNA, protein, cell, etc.) in a way it is able to interact with analyte;
- b) Transduction process that convert the interaction between biochemical substance and analyte into an electrical signal;
- c) Signal processing.

Immobilization is a very important and delicate phase in biosensor development since that the bioreceptor need to be functionally active and stable when attached to the support matrix. It is necessary for the biological component exhibit maximum activity in its immobilized micro-environment.

Immobilization procedures are different and depend on the approach used. Biological component may be (Barker, 1989):

- Entrapped in a gel matrix (alginate, gelatin, collagen).
- Immobilized on pretreated supports through cross-linking or covalent bonding.
- Absorbed into substance such as alumina, cellulose, silica gel, DEAE cellulose, DEAE Sephadex, etc.

Concerning proteins, they can be immobilized through (Pelosi et al., 2018):

1. Amine bond between activated carboxyl groups on the surface and the amino groups of protein.
2. Thiourea bond between the amino groups of protein and isothiocyanate immobilized on surface.
3. His-tag added to protein that react with nickel ions on surface.
4. Extra cysteine residue on protein N-terminus that react with an activated surface.

### **1.1.2 Optical silicon biosensors**

In a biosensor, the binding of analyte by the biological element, can modify electrical proprieties of device (electronic biosensors) or mass (quartz microbalance based biosensors) or refractive index (optical biosensors).

In recent years, there has been great interest into development of optical sensors rather than traditional ones, because of their property. For example, the first advantage of using an optical sensor opposed to traditional electrical based sensors is that electrical sources are not required and they operate at environmental temperature (Griol et al., 2019). These features allow use of these biosensors in analysis of dangerous products such as explosive and in extreme environmental conditions.

Optical biosensors are able to translate changes in the propagation velocity of light through a

medium that contains biological material into a signal that is quantifiable (Banuls et al., 2013). In fact, the variation of the refractive index can be evaluated and can be correlated with the concentration of the analyte and with the affinity constant of the interaction, resulting in a quantitative value of the interaction (Estevez et al., 2011).

An optical transducer is, by definition, a device made of a material that is light active. This means that, after the molecular interaction between the probe and the target, some feature of the light coming from or through the transducer changes as much as possible. The absorption, the phase, the intensity, or whatever other property of the propagating light is therefore monitored and correlated with the biomolecular event under investigation.

Optical sensors are more versatile than others because they can be made from different materials (silicon, glass, polymers, ect.) (Banuls et al., 2013).

Among materials, silicon has gained attention and popularity in recent years because of its ease fabrication, special optical properties and its versatile surface chemistry (Dhanekar and Jain, 2013). Moreover, silicon is readily available, low cost and biocompatible (Dhanekar and Jain, 2013; Escorihuela et al., 2012).

Concerning silicon surface, porous silicon (PSi) sensing structures are appreciated as biosensors element. PSi is nanostructured material composed of a network of pores (ranging from macro, micro to nano sizes, depending on application) and nanocrystallites in the silicon (Caroselli et al., 2017, Dhanekar and Jain, 2013), like a sponge. This particular morphology provide a higher interaction volume and an enormous internal surface.

The PSi fabrication process is very ease and one of the common, simple and efficient methods is based on an electrochemical etching procedure. The PSi structure is obtained by electrochemical dissolution of doped crystalline silicon wafers in a hydrofluoric acid (HF) - based solution (49% HF and ethanol) (Terracciano et al., 2019). The etching process requires a thorough pre-cleaning of silicon wafer by a chemical procedure for removal of any unwanted deposition on the silicon wafer. Then, it is subject to a galvanostatic electrochemical etching process comprises of an etching cell, silicon wafer (anode), a constant current source, platinum wire (cathode) and an electrolyte (Dhanekar and Jain, 2013). The current is allowed to flow for a fixed duration called as etching time. Modulating parameters such as current density, type and concentration of crystalline silicon, and the composition of electrolyte solution makes it possible to obtain porous structures with specific morphological and optical properties. Freshly etched PSi samples expose hydrogen, having Si-H, Si-H<sub>2</sub> and Si-H<sub>3</sub> or Si-H<sub>x</sub> hydrides on the surface. These groups are very responsive, reactive and metastable (Dhanekar and Jain, 2013). During fabrication or storage in ambient/laboratory, air induces impurities in PSi such as oxygen, carbon etc. The oxidation of PSi causes a

significant change in the refractive index of the material, interfering with transduction signal of PSi optical biosensors. A common method to prevent PSi from degradation is to intentionally grow an oxide layer on the surface via thermal oxidation, which reduces or completely removes the Si–H from the entire skeleton, substituting it for SiO<sub>2</sub>.

To provide greater stability and protection against dissolution, the oxidized surface could also be chemically modified with alkyl silanes. Modification of PSi surface (functionalization) is important also for the following bioreceptor immobilization. The specific detection of analytes is based on the functionality of the bioreceptor and that is why immobilization techniques is a key point to consider during biosensor assembly. Most of the bio functionalization methods for silicon surfaces employ self-assembled silane-based layer to which conjugate the biological element. The reaction is based on the condensation between siloxanes of organosilane and hydroxyl moieties present on the surface (Banuls et al., 2013). Organosilanes used for silicon surface modifications are functionalized at the terminal with different reactive groups (NH<sub>2</sub>, SH, epoxy, isocyanate- ended organosilane) which are used to bind a biological molecule such as antibody or receptor.

Chemical modification of PSi are synthesized in Figure 2.

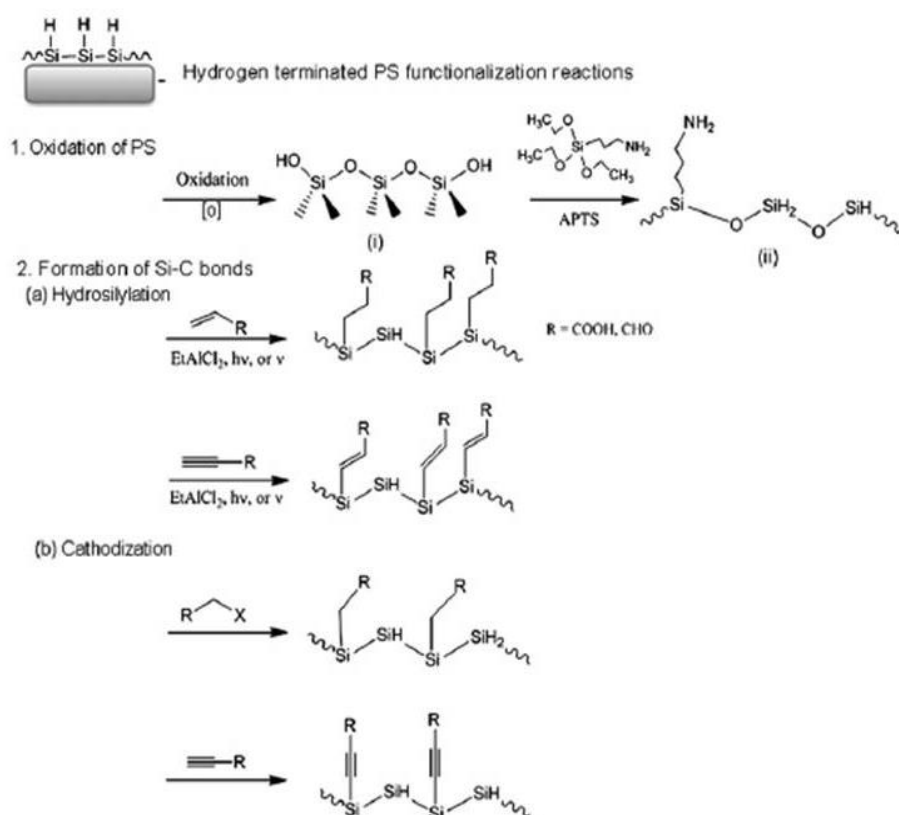


**Figure 2.** Some PSi modifications. Image from Dhanekar and Jain, 2013

These silicon surfaces are usually used for optical biosensor assembly.

Every substance that penetrates into the sponge-like matrix of a PSi layer changes its refractive index so that the optical spectrum of the sample also changes. The shift of the optical spectrum depends on two parameters: the pore-filling ability and the value of the refractive index of the substance. The first is strictly determined by the chemical nature of the substance, such as hydrophilicity or hydrophobicity, viscosity and so on; while the second is an intrinsic characteristic of the substance considered. This is the reason why a PSi device is only a specific optical sensor, (i.e., it gives different responses to different substances) but is not selective, which means that it would not be able to recognize a component in a complex mixture. The selectivity could be realized introducing a biological element, as protein or enzyme, in the system.

### **1.1.3 Features of a biosensor**

A biosensor has the following attributes (Bhalla et al., 2016):

- Selectivity. It is the ability to detect a specific analyte in a sample where there are other molecules.
- Reproducibility. It is biosensor ability to generate identical responses for a duplicated experimental set-up.
- Stability. It is determined by environment around the biosensing system. It consists in bioreceptor susceptibility to ambient disturbance. Stability can be affected by temperature, pH, bioreceptor affinity and its degradation.
- Sensitivity. It is the minimum amount of analyte detected by a biosensor.
- Linearity. It is maximum linear value of the sensor calibration curve. Linearity of the sensor must be high for the detection of high substrate concentration. A term associated with linearity is linear range, which is the range of analyte concentrations for which the biosensor response changes linearly with concentration.

### **1.1.4 Odorant Binding Proteins based biosensors**

#### **1.1.4.1 OBPs based biosensors advantage**

Bioreceptor could be a cell, a tissue, a nucleic acid or a protein. Particularly, proteins are very likely the best candidates as sensing elements with the required selectivity although these are subject to denaturation and degradation. They require a moist environment to keep their

structure and functionality.

Recently, proteins have attracted increasing interest as a sensing elements and particularly proteins of olfactory system: membrane-bound olfactory receptors (ORs) and soluble odorant binding proteins (OBPs).

OBPs are the most promising biosensing elements because of their features:

1. soluble nature
2. stability
3. efficient expression (high yield in bacterial system)
4. easy purification (anion-exchange chromatography following by gel filtration)
5. Possibility of site directed mutagenesis in order to modify the specificity for odorant molecules.

#### **1.1.4.2 OBPs overview: structure and physiological role.**

Olfaction is one of the oldest senses. Indeed, the detection of chemicals such as odorant and pheromones has always been important in evolution, allowing the organisms to identify food, potential mating partners, dangers and enemies. It is clear that olfactory system is essential for the survival of most animals.

Odorant are rich in information and animals have evolved sophisticated olfactory systems to detect and interpret them.

The functional organization of the olfactory system is similar in organisms ranging from insects to mammals (Su et al., 2009). In both vertebrate and invertebrate, odorants interact primarily with receptors on the membrane of a specialized sensory cells activating a signal pathway that arrives to higher centers of the brain where it is processed.

In vertebrate, olfaction happens mainly in nose through olfactory epithelium in the dorsal nasal cavity (Su et al., 2009) and its sensory neurons send projection to olfactory bulb. Volatile odorants surround the cilia of olfactory neurons where they are detected by odorant receptor (ORs).

In mammalian nose, five types of chemosensory G protein coupled receptors (GPCRs) have been identified (Meyerhof and Korsching, 2009) and, among these, odorant receptors (ORs) are the largest family discovered. These are expressed in the main mammalian olfactory epithelium and bind small, volatile odorous molecules.

Vertebrate ORs are classified in nine groups ( $\alpha, \beta, \gamma, \delta, \epsilon, \zeta, \eta, \theta, \kappa$ ) and have different chemical receptive range: some ORs have a broad receptive range, whereas others have a narrow receptive range (Kaupp, 2010).

In general, vertebrate ORs work interacting with odorants through residues in helices 2-7.



Olfaction in insects rely on a repertoire of chemosensory receptors that is smaller than that in mammalian. The specialized organs for insect sensing, especially for olfaction, are antennae. Antennae contain sensilla where olfactory neurons (ORNs) are located.

Insect olfactory sensilla are characterized by a variety of shapes and by one (uniporous sensilla) or more pores (multiporous sensilla) on their surface to provide the access of molecules to the inner aqueous phase, the sensillar lymph, that surrounds the dendrites of sensory neurons.

In insects, three different types of chemosensory receptors have been identified:

- Olfactory receptors (ORs)
- Gustatory receptors (GRs)
- Ionotropic glutamate receptors (IRs).

Insect ORs adopt a membrane topology that is reverse of vertebrate GPRCs and their signaling mechanism is entirely different. Insects ORs are ligand-gate ion channels.

A special feature is that in insect neurons, a universal co-receptor named OR83b is express beside common ORs.

OR83b, also called ORCO, is highly conserved across insect orders, dimerizes with odorant and pheromone receptors, and is required for efficient localization of these proteins to dendrites of sensory neurons.

Animal olfactory system is based also on Odorant Binding Proteins (OBPs) (Figure 3). In fact, most airborne odorants are hydrophobic meanwhile ORNs operate in an aqueous environment. OBPs are present in high concentration around the dendrites of olfactory neurons (ORNs) both in vertebrate and in insects. These proteins are believed to solubilized and transport odorants.

Vertebrate OBPs are structurally characterized by a  $\beta$ -barrel motif composed of antiparallel  $\beta$ -sheets. They are usually present as homodimer. The binding pocket is located inside the barrel.

In insect, two different classes of soluble polypeptides have been identified: OBPs and CSPs (chemosensory proteins).

These proteins bind reversibly odorant molecules and pheromones, allowing to delivery their chemical message to the membrane-bound receptors (Pophof, 2004; Pelosi et al., 2006; Grosse-Wilde et al., 2006).

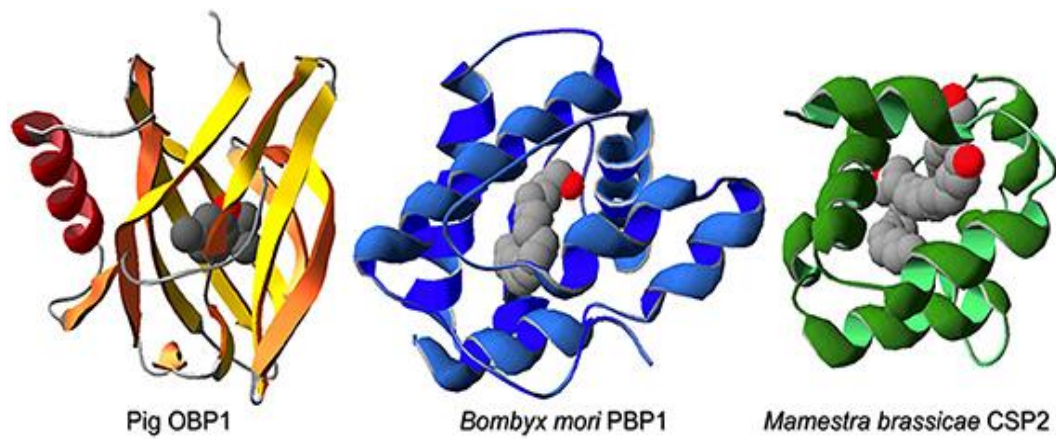


**Figure 3.** Structure of proteins involved in olfactory system. From left: OBP of vertebrates (pig), PBP of insect (*Bombyx mori*), CSP of insect (*Mamestra brassicae*)

In Lepidoptera, OBPs have been classified into: pheromone-binding proteins (PBPs), general odorant-binding proteins (GOBPs) and antennal specific proteins (ASPs) or antennal-binding protein (ABPs). PBPs are preferentially expressed in pheromone sensitive sensilla, GOBPs are mainly found in basiconica sensilla, that generally respond to plant odours (Steinbrecht et al., 1995; Laue et al., 1994; Zhang et al., 2001), while ABPs are highly expressed in antennae and their specific function is still unclear (Krieger et al., 1996).

However, OBPs present six conserved cysteines that stabilize the three-dimensional structure by three interlocked disulphide bridges and CSPs have only four conserved cysteine residues establishing two small loops between adjacent residues. CSPs are also smaller and better conserved between species from different orders than OBPs (Pelosi et al., 2006).

Insects OBPs share very little amino acid sequence similarity to vertebrate OBPs as they mainly contain  $\alpha$ -helical domains. They are divergent across and within species, with percent of conserved amino acid residues as low as 8% in some cases.

Insect OBPs are small (13-17 kDa) water-soluble proteins consisting of 130-150 amino acids (Vieira and Rozas, 2011; Leal, 2013). They are expressed with a signal peptide that is removed during processing and is not found in protein mature form. OBPs can be classified in short-chain OBPs (about 100 amino acids), medium-chain OBPs (about 120 amino acids) and long-chain OBPs (about 160 amino acid) (Leal et al., 1999)

OBPs are divided into four groups according to their primary protein sequences (Fan et al., 2011):

- Classical OBPs: six cysteine residues; three disulphide bonds formed by six cysteine.
- Plus-C OBPs: two or three cysteine add to classical six cysteine residues; one highly conserved proline residue, at least 2 conserved cysteines.
- Minus-C OBPs: a smaller number of cysteine residues.

- Atypical OBPs: six or more cysteine residues and a long C-terminus.

One important issue, related to the physiological function of OBPs, is whether these proteins can selectively bind and discriminate between the thousands of different semiochemicals presented to the olfactory repertory (Zhou, 2010).

Reversible binding of pheromones and other odorants to insect OBPs has been demonstrated in several insect species and some evidences support their selective binding. One example is the first OBP structure determined, the PBP from the moth *Bombyx mori* (Sandler et al., 2000). It has been studied both in its crystallized form by X-ray diffraction spectroscopy (Sandler et al., 2000) and in solution, using NMR techniques (Damberger et al., 2000; Horst et al., 2001). The structure is very compact, mostly made of  $\alpha$ -helical domains (six conserved helices). The six cysteines form three disulphide bridges C1-C3, C2-C5, C4-C6, which enforce the organization of the  $\alpha$ -helices in the *B. mori* PBP structure. Helices  $\alpha_1$ ,  $\alpha_2$ ,  $\alpha_4$ ,  $\alpha_5$  and  $\alpha_6$  form a conical shaped cavity for odorants, the “binding pocket”, and helix  $\alpha_3$  closes one end of this pocket. The molecule of bombykol, the sex pheromone of silkworm moth *B. mori*, is the specific ligand of this PBP; it is bound by numerous intermolecular forces, not simply general hydrophobic interactions, in this pocket (Klusak et al., 2003), whose access requires some conformational changes.

Therefore, apart from acting as carriers, OBPs might also contribute to the specificity of the detection by their selective binding of a fraction of the volatile compounds that enter the sensillum (Renou, 2014).

### **1.1.5 Application of biosensors**

Biosensors are low cost, small size, quick and easy-to-use devices. That is why biosensors have found potential application in a lot of fields.

Indeed, biosensors are used in clinical and diagnostic field (i.e glucose oxidase-based sensor) and also in the industrial processing, environmental monitoring, agricultural and food industry.

In particular, interest in research and development of electronic systems able to perceive aromatic compounds found in different matrices (air, water, food, beverage, biological fluids) has increased enormously in the last decades and has pushed research towards the construction of electronic “noses” (e-nose).

An electronic nose is a biomimetic system. It is designed to imitate the functioning of the olfactory systems, such as that of mammals or more specifically the human one. An electronic nose typically consists of several integrated and/or interfaced components including a gas-sensors array, a data-processing and analysis unit. The gas-sensor array is composed by

individual sensors which convey the electronic outputs (after compound recognition) to a transducer able to convert electronic outputs in digital values. At the end, e-nose is able to produce a distinct EASP (electronic aroma signature pattern). EASP identification is possible because of comparison with the reference database.

Electronic nose sensor design is frequently inspired by biological olfactory system: natural olfactory elements are analyzed and modelled, serving a basis for designing biological e-nose device (Wilson, 2013)

In an automated food production system, devices as biosensors or e-noses are important to monitoring and maintaining product quality and uniformity based on aroma characteristics. Specific volatile organic compounds (VOCs) released from food are responsible for the characteristic aroma of food products.

One of the most important and widely-studied applications of electronic nose in the food industries concerns analysis of wine aroma to detect quality and physiochemical parameters that are important to ensure its quality and to limit frauds or adulterations (Baietto and Wilson, 2015).

## **1.2 WINE**

### **1.2.1 Wine**

Grape is one of the most appreciated fruits in the world. It can be consumed as such or as a main ingredient for the preparation of drinks (wine and fruit juices) and other products (Beres et al., 2017).

Botanically, grape is a fruit of plant genus *Vitis* and it is composed by berries that grow in clusters from 15 to 300 units. The berry is composed by (Fregoni M. et al., 2008):

- epicarp (peel), membranous with cuticle, without stomata;
- mesocarp, cells full of juice;
- endocarp, containing seed.

Each component of the berry is characterized by a different amount of chemicals (Figure 4)

The peel contains mainly tartaric acid, anthocyanins, tannins, aromas and enzymes.

The pulp (mesocarp and endocarp) contains sugars (glucose and fructose), tartaric acid, malic acid, pectin, nitrogen compounds and minerals.

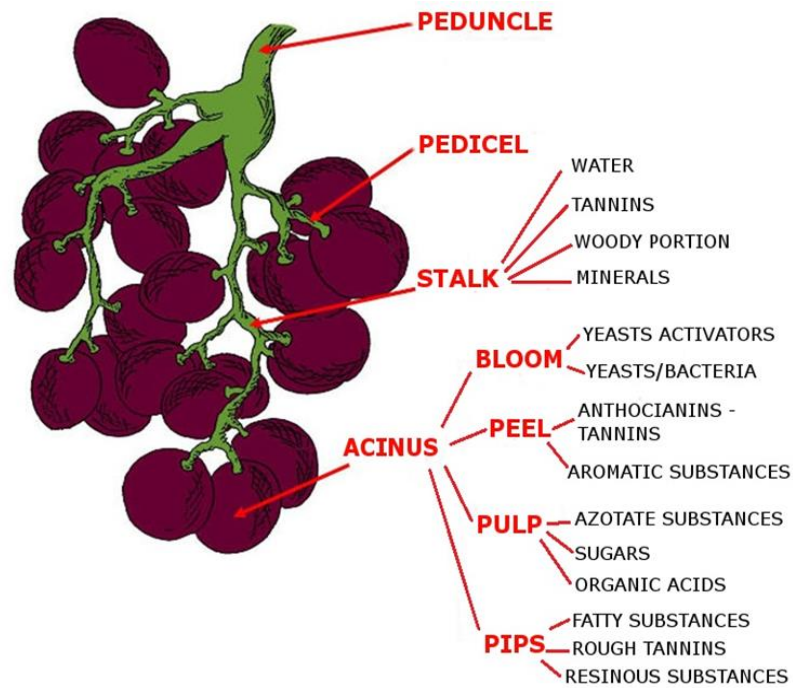


**Figure 4.** Different distribution of chemicals in the grape.

During the grape ripening, several chemical changes affect the berry such as:

- hormones changes;
- increase of berry size;
- changes in tissue consistency and berry softening;
- bloom appearance;
- accumulation of color pigments in the peel;
- polyphenols increase;
- sugars accumulation;
- acids reduction;
- synthesis of aromatic substances;
- changes in nitrogen compounds content;
- vitamins increase;
- minerals changes.

All these modifications are responsible of final product quality.

Grape has multiple uses in human nutrition: table grape is important as part of a balanced diet because of the presence of insoluble sugars in high concentration but it can be used also for preparation of jams, desserts or it can be dried.

Despite the variety of application, the most famous and appreciated use of grape remain winemaking.

Vinification is one of the oldest food processing procedures conducted by human.

Wine has existed for more than 7000 years and winemaking born thanks to the observation of damaged berries that, due to a spontaneous fermentation process, have produced an alcoholic substance with a particular taste (Chambers and Pretorius, 2010).

Winemaking is the conversion of grape juice into wine operated by micro-organisms, in particular by yeasts.

During vinification, micro-organisms produce or consume different compounds (Perez-Torrado et al., 2017) through their metabolism reactions, leading to the formation of a compound (wine) that will have different features depending on the type of reactions that they occurred and based on the starting product.

Winemaking starts with grape harvesting and destemming. From berries pressing, must (liquid) is obtained that will be used for fermentation.

The choice of a suitable fermentation technology is carried out according to the typological and qualitative objectives that are to be obtained in the final product.

Indeed, fermentation depends on wine “color”. Red wine fermentation use both must and the solid part. It is based on prolonged contact of the must with pomace, mainly to extract color and tannins from peel. White wine fermentation is base only on must fermentation (Beres et al. 2017).

Must composition is very important to determine the quality of wine. It is composed by a large variety of chemical compounds present in different concentration which are altered during and at the end of fermentation.

Chemical compounds in must are:

- water (its rate ranges from 60/65% to 85/88%);
- sugars (glucose, fructose and sucrose are main sugars while others are present in a low concentration such as ribulose and ribose);
- acids (the most representative are tartaric, malic and citric acids);
- nitrogen compounds (organic and inorganic nature);
- phenolic compounds (phenols, flavonoids, anthocyanins, tannins, flavones);
- minerals;
- vitamins;
- enzymes;
- colloids (arabans and pectines);

Winemaking occurs because micro-organisms convert glucose into ethanol and carbon dioxide. This metabolic reaction is called alcoholic fermentation (Figure 5).

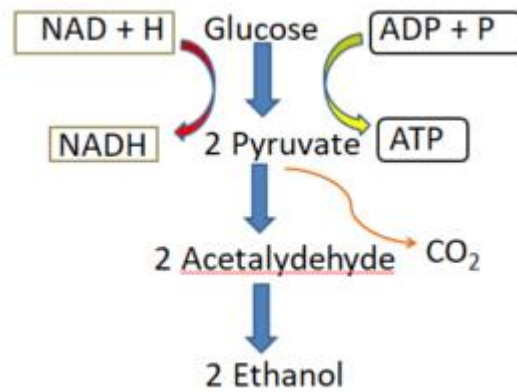


**Figure 5:** Alcoholic fermentation

Other type of fermentation that occur during winemaking are malolactic and maloalcoholic fermentation (Figure 6). Malolactic fermentation is a process in winemaking in which tart-tasting malic acid, naturally present in grape must, is converted to softer-tasting lactic acid. This fermentation is most often performed as a secondary fermentation and it is performed by bacteria belonging to genus *Lactobacillus*.

Instead, maloalcoholic fermentation is due to yeasts belonging to genus *Schizosaccharomyces* and consists on malic acid conversion into ethanol.

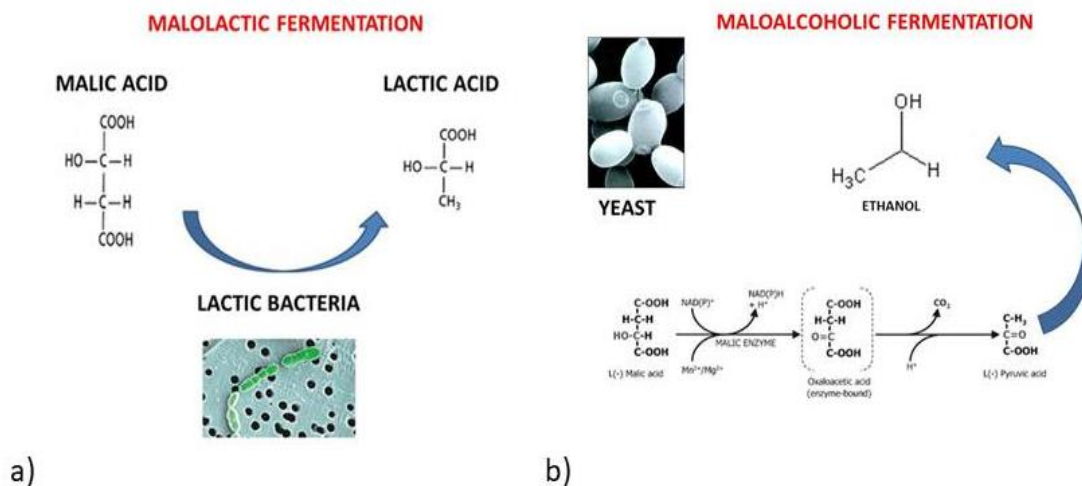


**Figure 6.** Malolactic (a) and Maloalcoholic (b) fermentations

Therefore, fermentation depends on type of micro-organism present at the beginning. Nowadays, winemakers select the most suitable yeast to start fermentation, in order to reduce the risk of contamination by other microorganism that could affect wine negatively and also,

in order to generate specific characteristics in wine (Perez-Torrado et al., 2017).

Yeasts are main microorganism involved in winemaking and they are responsible of aroma and other wine characteristic.

In his review, Fleet (2003) resumes relationship between yeast and wines aroma.

Yeasts contribute positively to wines aroma because they produce:

- ethanol and other solvents thanks to which aromas are solubilized;
- enzymes that release aromas from their precursors;
- secondary metabolites such as acids, esters, aldehydes, alcohols and Sulphur compounds.

*Saccharomyces cerevisiae* is the most used yeast even though it is not prevalent on wine grape (Fleet, 2003).

In the modern winemaking, pure culture of selected *Saccharomyces cerevisiae* are added to must, after pressing, to start fermentation (Chamber and Pretorius, 2010). This type of fermentation is defined “induced” (Fleet, 2003).

In some cases, fermentation is conducted using yeast naturally present on grape surface. This type of fermentation is called “indigenous”.

The choice of yeast genus to start winemaking is important to fight challenges of process such as the modification of chemical composition of wine aroma.

Indeed, there are a lot of factors that influence aromatic profile of grape and wine.

### **1.2.2 Wine aroma compounds**

As a rule, flavor can be defined as neurophysiological response to food or other substances that involve senses of taste and smell.

Sense of smell is very important in human feed. Odors (or aromas) are involved, partially, in food choice on the base of attractiveness and acceptance.

An odor is caused by one or more volatilized chemical compounds, generally found in low concentrations, that humans and animals can perceive by their sense of smell.

A chemical compound is an odor when it is sufficiently volatile to be transported to the olfactory system. Precisely for this reason, most of odors are volatile organic compounds (VOCs).

VOCs are a class of chemical compounds emitted as gas by solid or liquid. VOCs are numerous, varied, ubiquitous and play an important role in communication between plants or plants and animals.

They include aliphatic and aromatic hydrocarbons, aldehydes, esters, ethers and alcohols. All these compounds are characterized by volatility that is the tendency of a substance to evaporate at normal temperatures, reaching the maximum level of stability.



Aroma is one of the most important influencing elements during a wine tasting and it defines wine characteristic and quality. In fact, every wine carries in itself a great variety of flavors and numerous odorous anticipate the taste and define whether a wine is pleasant or not.

A great variety of volatile organic compounds is responsible of wine bouquet complexity. Indeed, VOCs are present in wines in different concentration, polarity and volatility degree (Mauriello et al., 2009).

For example, VOCs are responsible for fruity and floral flavor of wines.

According to their origins, wine aroma compounds can be divided in:

- varietal aromas;
- pre-fermentation aromas;
- fermentation aromas;
- post-fermentation aromas.

Varietal aromas are related to grape variety.

*Vitis vinifera* is the main grape used in winemaking but other type of grape are used and each has its “floral” or “fruity” characteristics that influenced wine aroma (Fleet, 2007).

Varietal aromas are divided into:

- primary aromas. These aromas are present in grapes already in a free form;
- secondary aromas. These are present in grapes in the form of aglycons (conjugated aromas). They become free during pre-fermentation, fermentation and aging phases.

Against this background, grapes can be classified into aromatic and non-aromatic grapes and they differ each other by aroma compounds content.

In aromatic grapes, free aromas are present in concentration higher than their odor threshold and then immediately detectable during tasting.

Instead, in non-aromatic grapes free aromas are present in concentration lower than their odor threshold and consequently not detectable during tasting.

Pre-fermentative aromas are produced during grape pressing as a consequence of enzymatic reaction that involved acyl-glycerols in cells membranes.

Instead, fermentative aromas are forming during fermentation by yeasts.

Finally, post-fermentative aromas are compounds forming at the end of fermentation when glucose and fructose in the must are totally consumed. In this phase of winemaking, lactic acid bacteria, yeasts auto-lysis, conservation and aging procedures affect wine aroma and make it more complex. In fact, after fermentation, yeasts release molecules that interact with those of wine and before blotting, wine is subjected to various treatments, such as clarification and stabilization that expose it to air causing many oxidative reactions. Moreover the container selected for aging or storing is a parameter to consider. For example, the extracts

from the wood barrel contribute to flavour.

Furthermore, some compounds are directly odorous while others are present in form of precursor and became active during fermentation (Marais, 1983; Zhu, 2016; Fregoni et al., 2008).

Therefore, wine aromas are the result of combination (D'Onofrio, 2011) of:

- grape metabolism depending on viticultural environment (vineyard, weather, soil, cultivation techniques);
- pre-fermentative biochemical processes (redox reaction, hydrolysis, etc.) that occur during pressing and maceration;
- metabolism reaction of micro-organism involved in alcoholic and malolactic fermentation
- chemical reaction that occur during evolution and aging.

Consequently, wine aroma profile is expression of multiple factors that together contribute to define aromatic character of a wine, strictly connected to vineyard, territory and seasonal trend.

### **1.2.3 Terpenes in wine**

Aromatic grapes are characterized by a significant content of terpenic compound belonging to classes of mono-, di- and tri-hydroxylate alcohols, ethers and acids.

Monoterpene and sesquiterpene hydrocarbons have also reported.

Terpenes (monoterpenes and sesquiterpenes) are main responsible of varietal aromas together with C<sub>13</sub>-norisoprenoids, benzenoids, volatile thiols, methoxypyrazines, aliphatic alcohols and aldehydes with six carbon atoms (D'Onofrio, 2011).

In Nature, terpenes are a wide class of secondary metabolites produced by plants and animals.

They are based on multiple units of isoprene (Figure 7), an unsaturated hydrocarbon with 5 carbon atoms. For this reason, they are also called isoprenoid (Hopkins and Huner, 2007).

Depending on the number of isoprene units, terpenes are classified into monoterpenes (2 units), sesquiterpenes (3 units), diterpenes (4 units), triterpenes (6 units), tetraterpenes (8 units).

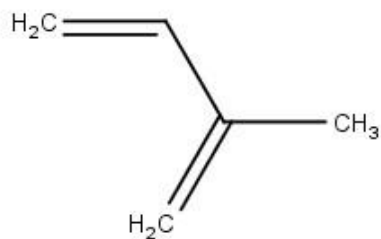


**Figure 7.** Isoprene

Therefore, most of the natural terpenes can be sketched starting from “isoprene units”. This consideration constitutes an important unifying theory for this wide class of compounds. Even if the biosynthesis of terpenes really occurs through enzymatic reactions starting from mevalonic acid (Figure 8), precursor of the isoprene.

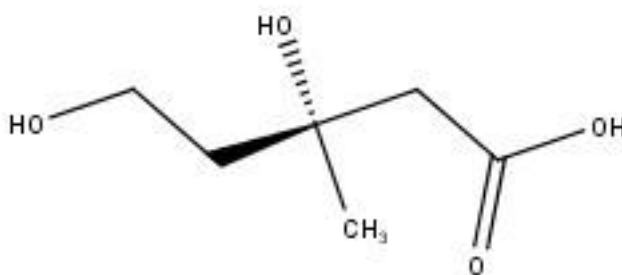


**Figure 8.** Mevalonic acid

Mevalonic acid is then phosphorylated using ATP, forming mevaloil pyrophosphate. This compound is then decarboxylated to form acid 3-isopentenyl pyrophosphate (IPP). Thanks to a proton transposition reaction, IPP becomes 3,3-dimethylallylpyrophosphoric acid (DMAP) which is the effective alkylating agent in the biosynthesis of isoprenoids and the biological form of the isoprene unit. A schematic representation of terpenes synthesis is shown in Figure 9.

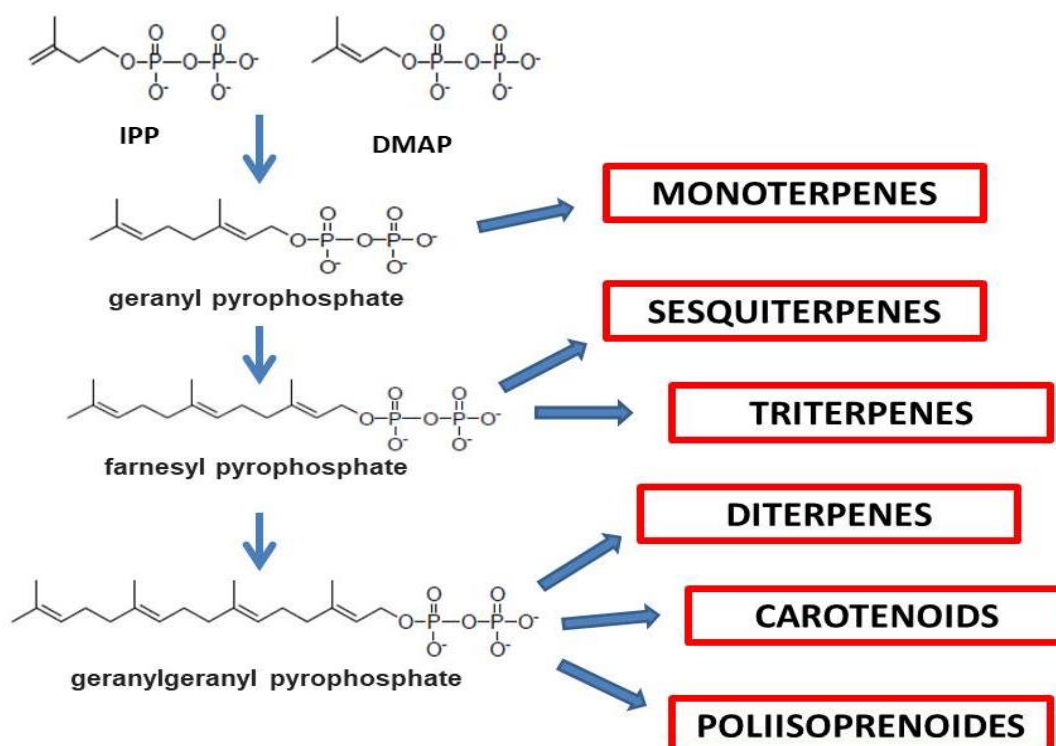


**Figure 9.** Schematic representation of terpenes precursors and synthesis of isoprenoid compounds.

An extraordinary feature of natural terpenes is the amazing number of existing carbocyclic structures. In fact, terpenes can also be cyclical, beside linear form.

During terpene synthesis, isoprene units are generally joined in a tail-head arrangement while the tail-tail arrangement is less common (Hopkins and Huner, 2007).

In wines, monoterpenes and sesquiterpenes are only terpenic compounds able to confer them the distinctive aroma.

Monoterpenes, with 10 carbon atoms, derive from a common precursor called geranyl pyrophosphate. To date, over 500 monoterpenes have been isolated/identified that differ in their carbon skeleton and functionalization degree. Monoterpenes could have acyclic or cyclic skeletons (mono-, bi- and tri- cyclic structures) with rings of 5 and 7 elements.

The interaction between IPP and DMAPP leads to the formation of geranyl pyrophosphate (GPP) that have also two linear isomers (Figure 10), neryl pyrophosphate (NPP) and linalyl pyrophosphate (LPP).

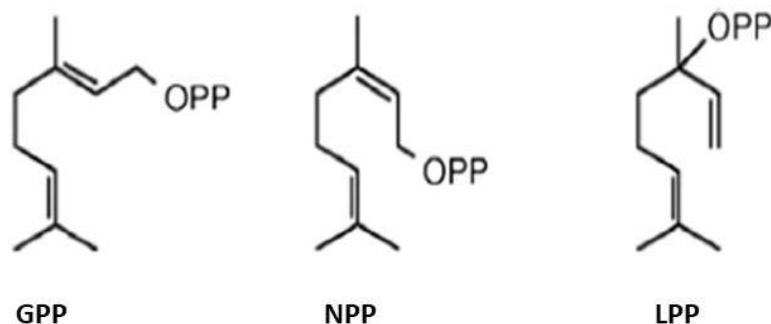


**Figure 10.** Monoterpenes precursors

GPP, NPP and LPP can be the starting point for the formation of various linear or cyclic monoterpenes.

Linalool, geraniol, nerol and citronellol are oxygenated derivatives terpenes most frequently found in nature. Beside, geranium acid has been found in free form and is present in many types of grapes. The importance of cyclic monoterpene ethers as compounds that contribute to the aroma has been recognized only during the last decade and in particular after the discovery and identification of rose oxide and linalool oxides.

Sesquiterpenes are plants and fungi secondary metabolites that have 15 carbon atoms.

Precursor of these compounds is trans-trans-farnesyl pyrophosphate (TTFPP) which originates by condensation of geranyl pyrophosphate and isopentenyl pyrophosphate.

Isomerization of TTFPP in TCFPP (trans-cis-farnesyl pyrophosphate) is responsible for the different conformation forms. Hence, two distinct classes of compounds with different carbocyclic skeletons are generated. Sesquiterpenes are characterized by complex structures due to the incorporation of very different skeletons, with numerous oxygenated functions and the presence of multiple carbon-carbon bonds.

Terpene hydrocarbons are very volatile compounds and therefore responsible for the immediate aromatic sensation during wine tasting.

Aromatic grapes have an extremely varied content of terpenes (free or glycosylated) but they can be referred to two groups: grapes with a prevalence of linalool (and its derivatives) and grapes with a prevalence of geraniol (and its derivatives). A third group, less numerous, is related to  $\alpha$ -terpineol and its derivatives (Di Stefano, 2013).

Difference between aromatic and non-aromatic grapes is to be understood referred only to organoleptic characteristics and its natural content of free and conjugated terpenols.

Non-aromatic grapes contain themselves terpenes related to three groups abovementioned. A

study of terpenes profile of these grapes could provide valuable information on biosynthetic trends.

The knowledge about terpenes profiles of the aromatic varieties revealed particularly important in oenology as regard the different behavior of the grapes (e.g. prevalence of geraniol or linalool) towards the activity of the yeasts and consequently of the technique to be adopted for the winemaking, particularly concerning the starter yeast to use. In fact, yeast metabolism could modify terpenes molecules influencing the complexity of wine aroma. For example, *Saccharomyces cerevisiae* is responsible of conversion of geraniol into geranyl acetate but also citronellyl- and neryl-acetate (Steyer et al., 2013). To date, studies show that also non-*Saccharomyces* yeast are able to modify wine aroma profile. Hence, the final aroma of wine could be affected by multiple causes starting from the initial content of terpenes.

There are over 4000 terpenes but among them, only those with 10 atoms of carbons (monoterpenes) or 15 atoms of carbons (sesquiterpenes) are odorous (D'onofrio, 2011; Fregoni et al., 2008).

Monoterpenes are simple hydrocarbons, aldehydes (linalale, geranial), alcohols (linalool, geraniol), acids (linalic acid, geranic acid) and esters (linalyl acetate).

The most odorous monoterpenes are linalool, nerol, geraniol (rose),  $\alpha$ -terpineol (camphor), citronellol (lemon), hotrienol (lime), limonene (citrus).

In grapes, most of these monoterpenes occur as nonvolatile precursor. They are conjugated to glucose or disaccharides. Their potent volatility and fragrance are released on hydrolysis of this linkage by yeast or *Aspergillus niger*  $\beta$ -glucosidase (Fleet, 2007).

Since the 1960s, attempts have been made to identify the molecules responsible for the wine aroma. The pioneering works of Usseglio-Tomaset (1966) had proved that the linalool was the terpenic alcohol responsible for the aroma of Muscat. Terrier (1972) also identified nerol and geraniol in wines. Rapp et al. (1980) identified other terpenes: 2,6 – dimethyl-3,7-octadien-2,6-diol and 3,7-dimethyl -1,7-octadien-3,6-diol.

In addition to these terpenic compounds present in Muscat, there are others found in aromatic grapes such as citronellol,  $\alpha$ -terpineol, rose oxide, nerol oxide, linalool oxide (D'Onofrio, 2011) and hotrienol (Marais, 1983).

All these molecules are the most frequent representatives of monoterpenes in wines.

Sesquiterpenes are present in the grapes exclusively in free form and have been identified as hydrocarbons with resinous odor or as alcohols.

Two sesquiterpenes identified in wines are farnesol and  $\beta$ - caryophyllene (D'Onofrio, 2011).

All terpenes aforementioned are only some (but the main) of the terpenic compounds present in the grapes and in wines derived from them. Others have been reviewed by Marais (1983).

#### 1.2.4 Wine aroma compounds analysis

The identification of chemical components involved in wine aroma is often a challenge.

Over 1000 volatile compounds are present in wines and their concentration range from several mg/L to less than a few ng/L (Polaskova et al., 2008).

Because their volatility, gas chromatography (GC) is most widely technique used for aroma compounds analysis.

Some more abundant compounds can be analyzed through direct injection in a GC – flame ionization detector meanwhile those present in low concentration need to be pre-concentrate.

Historically, wine volatiles have been isolated using distillation or solvent extraction techniques that are time and labor expensive (Polaskova et al., 2008).

For these reason, new techniques are emerged during years and new rapid analysis are used to date.

Analytical tools for analysis of wine volatiles actually are (Polaskova et al., 2008; Munoz-Gonzalez et al., 2011):

- SPME – GC; Solid-Phase Micro Extraction consists of a needle with a retractable fiber coated with a polymeric sorbent material that is pierced through the septum of a vial containing the sample. The assembly is transferred to the GC where carrier gas allow the desorption of volatiles.
- SBSE – GC; Stir Bar Sorptive Extraction consist on magnetic stir bar coated with polymeric sorbent placed in the sample and stirred for a defined time to extract nonpolar analytes. After extraction, stir bar is subject to desorption and volatiles analyze through GC.
- SPDE – GC; Solid – Phase Dynamic Extraction uses a syringe equipped with a modified needle in which a polymer adsorbent is placed. The extraction of volatiles from sample is performed by successive movements of syringe plunger. The following desorption is carried out in the GC.
- GC – O; Gas Chromatography – Olfactometry is based on the “human assessor” that sniffs the eluent of the chromatograph column annotating time.

These techniques were introduced in the past and thanks to them, progresses are made concerning wine aroma analysis.

However, an improvement of analytic techniques and the development of new tools, such as biosensors, could led us to understand better the complexity of wine “bouquet” that actually is not completely understood.

## 1.3 APHIDS AND THEIR OLFACTION

### 1.3.1 Aphids biology

Aphid' is the common name for insects belonging to the superfamily Aphidoidea, within the order Hemiptera and they are major pest of many plants (Guerrieri and Digilio, 2008). They belong to the order of Rynchota or Hemiptera, where the Aphidoidea superfamily includes more than two thousands species of aphids, with variable size from one millimeter to few centimeters in length and in different colors and shapes.



**Figure 11.** Aphids

They cause damages to their host plant either directly by feeding on their phloem sap, or indirectly by transmitting viruses. They have mouth appendages elongated into a stylet bundle with which they suck lymph and cellular juices causing changes in plant tissues.

Aphids (Figure 11) are small, soft-bodies insects with complex life cycles (Figure 12) including sexual/asexual reproduction tradeoff. In fact, aphids present a unique biological feature: they are able to alternate parthenogenesis (this type of reproduction does not need any male intervention, it can generate clonal individuals in a few day) and bi-parental reproduction (based on males and females mating). In the family Aphididae, the annual cycle generally includes a single sexual generation with males and females that mate. Then, fertilized eggs are released in winter by females. Overwintering eggs are characterized by cold hardiness (Guerrieri and Digilio, 2008) and they rise, in the spring, to a wingless “foundress” that, in turn, give birth partogenetically to further partogenetic females (winged or wingless, depending on environment) which continue to reproduce asexually during summer (Hales et al., 1997).

In autumn, when the day is shorter and temperatures are colder, females asexually produce a generation of sexual females and males (Mackay et al., 1983; Lees, 1990) and then the sexual/asexual reproduction tradeoff starts again.



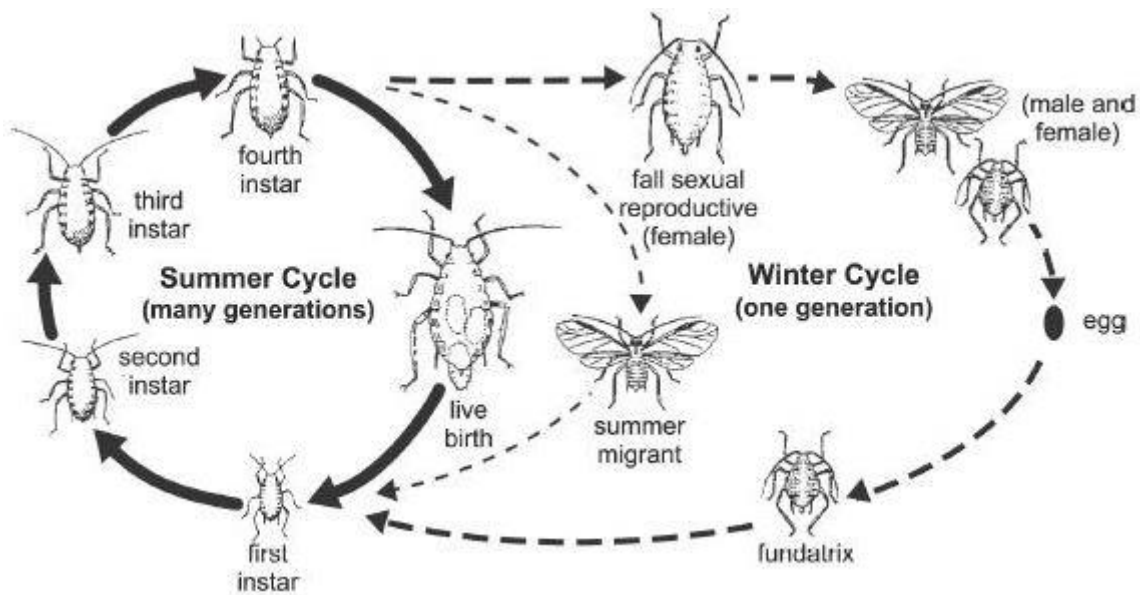


**Figure 12.** Schematic aphids life cycle

In some aphids clones, the sexual generation can no longer be induced and clones gradually diverge each other because of accumulation of mutation (Hales et al., 1997).

Three main development cycles can be distinguished, sometimes founded within the same species:

- holocyclic, cyclic viviparous parthenogenesis alternating with sexual reproduction;
- anholocyclic, absence of sexual reproduction;
- paraholocyclic, occasional appearance of sexual reproduction.

About a third of aphid species include obligate parthenogenetic lineages together with typical cyclical parthenogenetic ones (Simon and Peccoud, 2018).

Aphids tend to include sexual cycle in more extreme environment while parthenogenesis is preferred in stable environment; generally the sexual forms are induced by short photoperiod and temperature and host plant condition plays also a determining role (Hales et al., 1997).

The aphids life cycles can be also distinguished depending on whether they spend all their life on the same host plant species or migrates from a primary host to secondary host plant, with a winter host and a spring-summer host. In the first case, life cycle is defined autoecious while the second is called heteroecious cycle.

Positive signals associated with host plant or negative ones associated with non-host plant are perceived by aphids through antennal olfactory sensilla (Dixon, 1998).

Aphids can be apterous or winged depending on the presence/absence of wings. Winged morphs may appear as a response to crowding or to the complete exploitation of the host plant (Guerrieri and Digilio, 2008).

Cyclical parthenogenesis and the production of winged or wingless morph are to the base of

aphids' geographical and adaptations because these features led aphid to respond rapidly to environmental natural or anthropogenic changes (Simon and Peccoud, 2018).

Moreover, different aphid species can coexist on the same plant and in some cases, species of the same genus are able to share the same host plant using different feeding sites (Guerrieri and Digilio, 2008).

### **1.3.2 Aphids pheromones**

Chemoreception is the physiological process occurring in certain receptor cells that detect and discriminate different chemicals. Insect have developed sophisticated communication mechanisms based on secretion and perception of semiochemicals.

A semiochemical is a chemical substance or a mixture that carries a message for purpose of communication. Two types of semiochemicals can be distinguished: allelochemicals and pheromones (Figure 13). They have interspecific and intraspecific functions, respectively (Gullan and Craston, 2014). Allelochemicals are divided into several classes (Figure 13): allomones give an adaptive advantage to the emitting organism; synomones give benefit both sender and receiver; kairomones confer an advantage to the receiving organism (Ryan, 2002). For example, many phytophagous insects find their host plants by the chemical fingerprint of secondary plant substances that they use as kairomones; mosquitoes locate vertebrate hosts for blood meals by using as kairomones the carbon dioxide and other chemicals produced during normal vertebrate metabolism; the parasitic mite *Varroa jacobsoni* is attracted to honey bee drone larvae by fatty acid esters present in the bee larvae, and the rabbit flea uses the hormones of its rabbit hosts as a kairomone to locate the rabbit, and also to mature its reproductive system (Klowden, 2013)

Pheromones can also be classified into different types, depending on their functions and effects (Figure 13): sex pheromones, alarm pheromones, trail marking pheromones, territory marking pheromones, egg marking pheromones and aggregation pheromones (Beck et al., 2017).

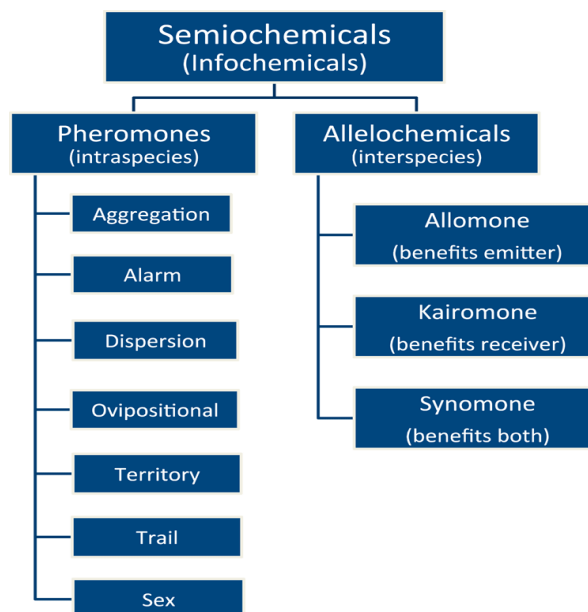


**Figure 13** Different types of semiochemicals

According to its definition, a pheromone is a fluid substance secreted by an organism which causes a highly specific behavioural response when perceived by an individual of the same species.

Pheromones are usually mixtures of substances with high volatility, produced by tegumental glands and secreted in very small quantities.

Aphids use two types of pheromones for their chemical communication: sex and alarm pheromones.

In aphids, mating females attract males by producing of sex pheromone secreted from glands located on the hind tibiae (Hales et al., 1997). The release of pheromone has circadian rhythm and it is a mixture of the monoterpenoids (4aS,7S,7aR)- nepetalactone and its related alcohol (1R,4aS,7S,7aR)-nepetalactol (Birkett and Pickett, 2003) (Figure 14).

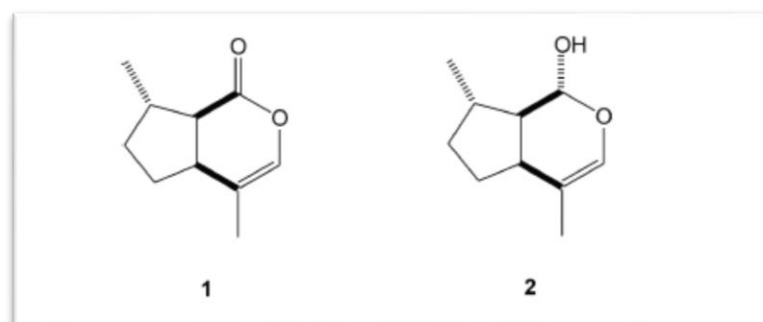


**Figure 14.** Aphids pheromones; (4aS,7S,7aR)- nepetalactone (1) and (1R,4aS,7S,7aR)-nepetalactol (2)

These two compounds are present in different ratios in each aphid species. The relative quantity of these pheromones seem to be extremely important for communication between sexes, because it is species-specific and males recognize females of their own species among those of other species thanks to this ratio (Hardie et al. 1992; Dawson et al., 1996, Hales et al., 1997).

The alarm pheromone is released from the cornicle secretion (Pickett et al, 1992) in response to a danger situation, such as attacks by natural enemies (predators or parasitoids) and induces the feeding arrest and an immediate dispersal effect among individuals of colony, that move away or drop from plant (Pickett et al., 1992). In fact, for their anatomical characteristics, aphids are easy prey to parasites and predators and the main defence technique is the escape, activated from the alarm pheromone (Pickett et al., 1992; Dixon, 1998). Cornicle secretion also contain triglycerides which appear to function as mechanical defences by gluing appendages (mouthparts, antennae, ovipositor, etc.) of natural enemies permanently or temporarily incapacitating the attacker. Therefore, the emission of cornicle droplets interfere predation events in two way: mechanically and depositing pheromone droplets directly onto the predator (Vandermoten et al., 2012).

Although aphids comprise a great variety of species, most of them produce and utilize the same alarm pheromone, the sesquiterpene (E)- $\beta$ -farnesene (EBF) (Figure 15) (Pickett et al., 1992; Francis et al., 2005; Dewhirst et al., 2010).

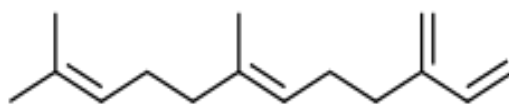


**Figure 15.** The sesquiterpene (E)- $\beta$ -farnesene (EBF), also known as (E)-7,11-dimethyl-3-methylene-1,6,10-dodecatriene

EBF is also a plant component of volatile blends: many plants also emit EBF as component of constitutive volatile blends (Agelopoulos et al., 2000) or those induced by herbivore feeding (Turling and Ton, 2006) or by mechanical damage (Agelopoulos et al., 1999)

The response to the alarm pheromone, that involves sixth antennal segment (Pickett et al., 1992), can be influenced by different factors, such as environmental temperature and aphid-life stage, producing a more or less intense reactivity of aphids to its release ( Roitberg and Myers, 1978).

In addition to the dispersal effect, the alarm pheromone seems to mediate indirectly the production of winged offspring of the pea aphid. It was suggested that EBF leads to a “pseudo crowding effect”, increasing the number of tactile stimuli among individuals of a colony (Sloggett and Weisser, 2004; Kunert et al., 2005).

Furthermore, this pheromone can act as a kairomone, attracting the aphid natural enemies such as aphid parasitoids, triggering attack behavior in the parasitoids, obviously serving as a stimulant for host recognition (Micha and Wyss, 1996)

Finally, more than one study suggests that EBF is emitted by one individual aphid and amplification of the alarm signal with release of pheromone by other aphids of colony does not occur, though the amount of pheromone emitted by an aphid is small (Hatano et al., 2008; Verheggen et al., 2008), highlighting the power of this semiochemical also at low concentrations.

### **1.3.3 Aphids Odorant Binding Proteins**

Despite the great number of aphids species, a single alarm pheromone, (E)- $\beta$ -farnesene, is produced and utilised by most aphids. Francis et al. (2005) have analysed 23 species of aphids and among them, 21 contain EBF in their pheromonal blend.

EBF is a volatile hydrocarbon and as pheromone it is perceived at molecular level by insect. Very recently, odorant binding proteins (OBPs) have been shown to be essential for pheromone and odour perception in insect (Matsuo et al., 2007).

Insect OBPs are small (13-17 kDa) water-soluble proteins consisting of 130-150 amino acids (Vieira and Rozas, 2011; Leal, 2013) folded in an  $\alpha$ -helix structures. OBPs are divergent across and within species, with percent of conserved amino acids as low as 8% in some cases. A pattern of six cysteines, connected in the native protein by three interlocking disulphide bridges, represents odorant binding proteins signature (Pelosi et al., 2005) even if other type of OBPs with modification of this pattern exist.

Unlike OBPs from other orders of insect that are greatly divergent, aphids OBPs are highly conserved, with differences between species limited to only few amino acid substitutions (Qiao et al. 2009). Probably, this unusual high conservation is due to the fact that several aphid species, although phylogenetically distant, utilise the same alarm and sex pheromones (Qiao et al. 2009).

Several studies have been conducted to identify odorant binding proteins that could mediate EBF perception in aphids.

In their work, Qiao and colleagues (2009) have identified, in *Acyrtosyphon pisum*, one OBP able to bind EBF: recombinant *Apis*OBP3 has been tested in biochemical assay (competitive

binding assays) and it showed a good affinity to the following chemical compounds, EBF, farnesol and 3,7- dimethyloctyl acetate. These data indicate that the aphid OBP3 is involved in detecting and recognising the alarm pheromone EBF. These *in vitro* assays were confirmed also with RNAi (Zhang et al., 2017).

Another odorant binding protein is also able to bind EBF in *Acyrtosyphon pisum*. This protein is called OBP7 and particularly interesting is the fact that OBP7 is similar to OBP3 in its binding pocket, although they share only a 15% of amino acid sequence (Sun et al., 2012).

The binding pocket of *Apis*OBP3 is composed by five hydrophobic amino acids (Ile 43, Leu 48, Leu 64, Val 104 and Leu 108) on opposite  $\alpha$  – helical domains that interact with branched chains of terpenoids. A sixth residue Tyr 84 interacts with the two double bonds at one end of EBF (Qiao et al., 2009). Also *Apis*OBP7 present a set of branched residues in its binding pocket and an aromatic residue Phe52 (Sun et al., 2012). Although the two aromatic amino acids are situated on opposite sides in the binding pocket, their position is the same in relation to other residues.

The aphid *Megoura viciae* also uses EBF as alarm pheromone but it is not the only terpene in pheromone blend. In fact, in this aphid alarm signal is constituted also by  $\alpha$  - pinene,  $\beta$  – pinene and limonene (Pickett et al., 1992).

Also in *Megoura viciae* EBF is perceived by OBP3, a six  $\alpha$  – helices protein characterized by a groove in the surface formed primarily from the N – terminal region of the chain and parts of helices  $\alpha$ 1 and  $\alpha$ 2; there is a tyrosine (Tyr30) inserted deeply into groove and forming a hydrogen bond with Phe5 (Northey and al., 2016). These two amino acids, together with Val 27 and Tyr 105, participate to form the putative binding protein (Northey and al., 2016).

## 1.4 BIOMIMICRY

"Everything you can imagine, nature has already invented it." - Albert Einstein

Human life has not only developed from nature but has always been connected with it.

Biomimicry is the science based on the study of biological processes and their transfer from the natural to the artificial world. Man is inspired by nature and from it he finds solutions to the most varied problems.

The first ever to refer to biomimicry was Leonardo Da Vinci, when in his studies on flying machines he took the flight of birds as example.

A more recent example is VELCRO® brand. Velcro is the trade name of a fast-closing device for clothes, bags and so on. It all started in the 1940s when the Swiss engineer Georges de Mestral, upon returning home for a walk in the woods with his dog, noticed cockleburrs

attached to his pant and to the fur of his dog. To understand how these elements remain glued to his socks, Georges de Mestral studied them with a microscope and he noticed tiny hooks on the ends of the thorns which were certainly responsible for the adhesion of the achenes to the surfaces. Subsequently, de Mestral developed a closure system consisting of two elements: a linear cloth strip with tiny hooks that could mate with another one with tiny slots; the two elements temporarily attached until they were mechanically separated.

Velcro continues today to produce and market closure systems. (Hargroves and Smith, 2006).

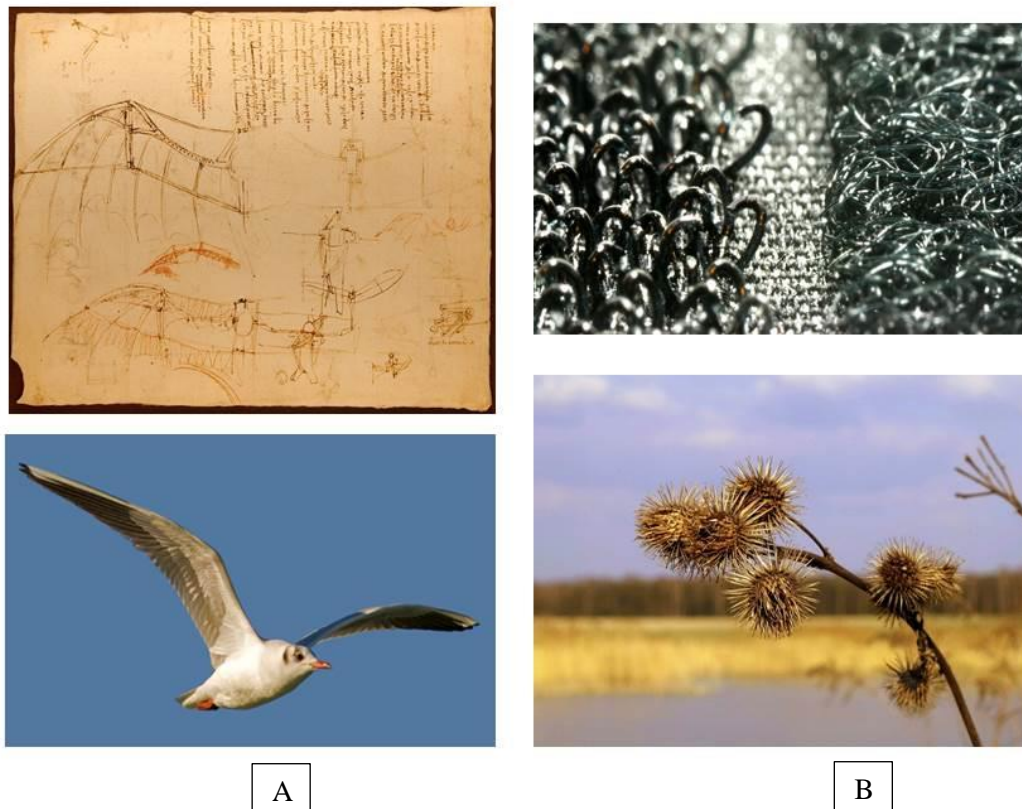


**Figure 16.** Biomimicry examples. **A.** Leonardo's flying machines; **B.** VELCRO®

Biomimicry is an emerging discipline that aimed at finding more sustainable solutions to human challenges through nature emulation (Figure 16).

Mimicking a biological system for the creation of biology-inspired technology happens in multiple ways, which can be categorized by: principle, morphology, behaviour, manufacture, or any combination of these (Stroble et al. 2009).

Important sources of inspiration are animal and insects particularly. Insects include the greatest number of species in Nature and they have solved a variety of technical, during evolution, thanks to a several specialized structures and processes. These features have been

considered and mimicked in bio-material production processes, stimulating new grounds in technology. For these reasons, within years, insect life events, behavior, physiologies and morphologies, have been investigated more in detail, in order to provide innovative solutions in human life.

Insect solution may be applied in several technological areas (Figure 17) such as materials science and technology, optics, sensors and robotics (Gorb, 2011).

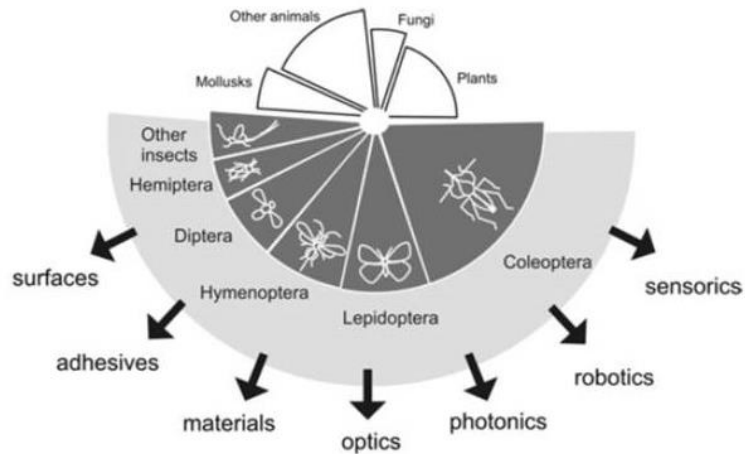


**Figure 17.** Insect as a source for biomimetic ideas (Gorb, 2011)

An example of insect solution for technology applications is cuticle. Cuticle is at the base of insect exoskeleton and it is composed by chitin and protein. In particular, chitin is structural polymer found in crystalline form. Chitin crystals always occur in insects as bundles of micro fibrils with a diameter of 25-30 Å. Insect cuticle may inspire new materials with its helicoidally arrangement and its proprieties such as flexibility, great extensibility and reasonable strength (Gorb, 2011).

Insects may be also a source for biomimetic ideas in sensors assembly. Mechanoreceptors and chemoreceptors are used by insect to perceive mechanical and chemical stimuli respectively. Insect chemoreception is one of the most studied physiological processes and a better understanding of insect olfactory or gustatory or pheromone perception could improve the performance of biologically inspired systems such as biosensors for monitoring chemicals.



## 2. MATERIALS AND METHODS

### 2.1 Odorant Binding Proteins recombinant production

#### 2.1.1 Identification of aphids Odorant Binding Proteins: *Acyrtosiphon pisum* OBP3, *Acyrtosiphon pisum* OBP9, *Acyrtosiphon pisum* OBP7 and *Megoura viciae* OBP3

Aphids OBPs sequence (*Acyrtosiphon pisum* OBP3, *Acyrtosiphon pisum* OBP9, *Acyrtosiphon pisum* OBP7 and *Megoura viciae* OBP3) (Appendix A.1) were previously cloned in expression vectors, at Insects Physiology and Molecular biology Laboratory, University of Basilicata (Potenza). Concerning *Acyrtosiphon pisum* OBP7 it was necessary to change the expression vector ( from pET-5b to pET-22b) because of expression troubles. First of all, pET22b was double digested with NdeI/EcoRI (New England Biolabs, MA,USA) and then dephosphorization (Appendix B.1) was conducted to prevent plasmid from closing on itself. Simultaneously, *Acyrtosiphon pisum* OBP7- pET5b, already available, was double digested too, using the same restriction enzymes. Fragment corresponding *Apis*OBP7 was purified using Quantum Prep Freeze N-Squeeze DNA Gel Extraction Spin Columns (Bio-Rad, Hercules, CA, USA) according to manufacture protocol (Appendix B.2) and subsequently used for ligation reaction. Ligation reaction was performed according to a molarity equation (Sambrook et al., 1989) and using a 1:3 ratio of insert, 1 $\mu$ L Ligase buffer (10X), 2  $\mu$ L T4 DNA Ligase (400000 U/mL) (New England Biolabs, MA, USA). The incubation was carried out at 16°C in a water bath over-night and, then the enzyme was inactivated at 65°C for 10 min.

The total volume of ligation reaction mixture was used to transform *Escherichia coli* DH5- $\alpha$  chemically competent cells (Appendix B.3). This final transformation process has allowed the recombinant *Apis*OBP7/pET-22b plasmid to take up into chemically competent cells for propagation and storage. After ligation reaction, positive screening was conducted through miniprep procedure (FastPlasmid Mini Kit, 5 PRIME) (Appendix B.4) of suspected positive clones and then a PCR was conducted using plasmidic DNA as template and vector primers (Appendix A.2): T7 Promoter Primer (#69348-3) and T7 terminator primer (#69337-3).

Recombinant plasmids (*Apis*OBP3-pET30b, *Apis*OBP9-pET45b, *Apis*OBP7-pET22b and *Mvic*OBP3-pET17b) were sent to Macrogen Europe (Amsterdam, The Netherlands) for sequencing, to ensure that the OBP sequence were not affected by mutations. The sequencing primer used was T7 Promoter Primer (#69348-3) for all constructs.

## 2.1.2 Expression of aphids Odorant Binding Proteins.

Once sequencing results were obtained, recombinant plasmids were used separately to transform *Escherichia coli* DH5 $\alpha$  cells (Appendix B.3) and the single colony of each transformation, grown on agar plate (Appendix C.1) containing appropriate antibiotic (ampicillin or kanamycin), was used to perform a midi-prep, according to the manufacturer's instructions (PureLink™ HiPure Plasmid Midiprep Kit, Invitrogen K210004) (Appendix B.5). Quantitative evaluation of midi-preps was carried out by reading 1  $\mu$ l of each sample at the NanoDrop® 1000 Spectrophotometer.

Midi-preps were subsequently used for *Escherichia coli* BL21 (DE3) cells transformation (Appendix B.3) to perform *in vitro* expression of recombinant proteins.

Recombinant protein production depends on using cellular machinery, in which proteins are synthesized, modified and regulated. The bacterium *Escherichia coli* has been the most popular expression platform for over two decades. The advantages of using this organism as host are mostly the fast growth kinetics and consequently a high amount of recombinant protein. For protein production, IPTG (Isopropyl  $\beta$ -d-1-thiogalactopyranoside) (ThermoFisher, 15529019) as inducer has been used. The addition of IPTG when the bacterial culture had reached a value of O.D.<sub>600</sub>=0.6 allows the cells to use most of their resources for the production of the target protein. The concentration used for *Acyrtosiphon pisum* OBP3, *Acyrtosiphon pisum* OBP7, *Acyrtosiphon pisum* OBP9 and *Megoura viciae* OBP3 expression was 0.4 mM. Different times from induction were tested to identify the better one. Generally, insect OBPs are produced as inclusion bodies (IBs) when overexpressed by *Escherichia coli* (Northey et al., 2016). Solubilization of inclusion bodies was accomplished by DTT addition and refolding using cysteine-cystine redox reaction (Appendix B.7), according to protocols that have been verified to afford the proteins in their active forms (Ban et al., 2003; Kruse et al., 2003).

After induction of recombinant proteins, Denaturing Lysis Buffer (Appendix C.2) containing 8M Urea was used for the purpose of breaking cells and samples were centrifuged at 4000 rcf for 20 minutes to eliminate cells debris.

Then, 10 mM dithiothreitol (DTT) in Tris-HCl, pH 8.0 was added to supernatant and samples were incubated for 60 minutes. After the time was up, 100 mM cysteine in 0.5 M NaOH was added and an incubation of 10 minutes at room temperature occurred. The cysteine-cystine refolding protocol was completed adding 5 mM cysteine in 100 mM Tris-HCl, pH 8.0 and incubating samples, at 4° C for 16 hours, under stirring. Then samples were extended dialysed against appropriate buffer to be purified.

*Acyrtosiphon pisum* OBP3 and *Megoura viciae* OBP3 were dialysed against Tris Buffer 50 mM pH 7.4 (Appendix C.4), *Acyrtosiphon pisum* OBP7 against Tris Buffer 50 mM pH 7.4 and Tris Buffer 30 mM pH 8 while *Acyrtosiphon pisum* OBP9 against Native Lysis buffer (Appendix C.3) containing imidazole.

### **2.1.3 Purification of aphids Odorant Binding Proteins.**

Anion-exchange chromatography (Appendix B.9) was performed to purify *Acyrtosiphon pisum* OBP3, *Acyrtosiphon pisum* OBP7 and *Megoura viciae* OBP3, using DEAE-Sepharose (DCL6B100, Sigma-Aldrich). This resin is based on diethylaminoethanol (DEAE) covalently linked to Sepharose (a polysaccharide polymer).

Anion-exchange chromatography is a process that separates substances based on their charges using an ion-exchange resin containing positively charged groups, such as DEAE.

Proteins were purified using Tris buffer pH 7.4 (Appendix C.4) as elution buffer.

At the first, resin was equilibrated with Tris buffer pH 7.4 without NaCl (Buffer A) and then sample was loaded into the column. After incubation, protein elution was performed using the same buffer used to equilibrate resin (Buffer A) and then a wash using Tris buffer 50 mM, pH 7.4 with 1M NaCl (Buffer B) was conducted to eliminate bacterial protein bound to the resin. Chromatography fractions were analysed through electrophoresis in denaturing conditions (Appendix B.8).

Gel filtration resin (Sephadex G-50, G50150, Sigma-Aldrich) (Appendix B.10) was also used to try to purify *Acyrtosiphon pisum* OBP7 because anion exchange did not work. Tris Buffer 30 mM pH 8 (Appendix C.4) was used as elution buffer. The principle of this purification is that particles of different sizes elute through a stationary phase at different rates. Gel filtration chromatography separates proteins, peptides, and oligonucleotides on the basis of size. Molecules move through a bed of porous beads, diffusing into the beads to greater or lesser degrees. Smaller molecules diffuse further into the pores of the beads and therefore move through the bed more slowly, while larger molecules enter less or not at all and thus move through the bed more quickly. Sephadex G-50 resin has a fractionation range of 1500–30000 Da, compatible with aphid proteins produced.

Instead, Ni-NTA Agarose resin was used to perform *Acyrtosiphon pisum* OBP9 because this protein was cloned with adding of 6xHis tag located at N-terminal of protein.

The stationary phase consists of a silica matrix associated with nitrilotriacetic acid (NTA), a trivalent chelating agent, which binds the nickel ions by three coordination bonds, leaving the remaining three coordination sites free for the bond of the imidazole ring histidine. Two

successive purifications were necessary to obtain protein without contaminants into elution fraction.

*Acyrtosiphon pisum* OBP9 was purified using the batch procedure that consists in binding the protein to the Ni-NTA resin in solution and then packing the protein–resin complex into a column for the washing and elution steps. This strategy promotes efficient binding of the 6xHis-tagged protein. The first purification was conducted under denaturing condition and elution fractions were subsequently dialysed against Native Lysis Buffer (Appendix C.3) and then used for the following in batch purification under native condition (Appendix B.11).

After purification, proteins were dialysed against Tris Buffer pH 7.4 for following *in vitro* assay.

## **2.2 *In silico* experiments**

### **2.2.1 Preparation of target proteins and ligand structures**

The primary structure of aphids OBPs was analyzed using the ExPASy Compute pI/MW tool ([https://web.expasy.org/compute\\_pi](https://web.expasy.org/compute_pi)) that provided physicochemical parameters: theoretical isoelectric point (pI) and molecular weight (MW)

The three-dimensional crystal structure of aphids OBPs was predicted by Homology Modelling using I-TASSER (Iterative Threading ASSEmbly Refinement), a server for protein structure and function prediction. The amino acidic sequences of the recombinant proteins of interest in this study, without signal peptide, was used as template. Only one representative conformation of the modelled OBPs was selected among different models with the best (highest) C-score.

### **2.2.2 Molecular docking**

The molecular docking analysis was performed to obtain possible conformations of protein–ligand complexes and to predict ligand orientation. Docking simulations were performed by employing SwissDock (<http://www.swissdock.ch/>) program and the cluster analysis was performed using UCSF CHIMERA (<http://www.rbvi.ucsf.edu/chimera>). Clusters were analyzed according to their binding energy values (kcal/mol) and  $\Delta G$ . The best conformation was chosen with the lowest binding energy.

### **2.2.3 Binding pocket investigation**

Aphids Odorant Binding Proteins were analyzed using CASTp 3.0 (Computed Atlas Surface Topography of proteins) to identify the number of pockets and the amino acids involved in

the formation of ligand binding pocket. This analysis was useful for the subsequent development of the nanobiosensor and in particular for biofunctionalization of porous silicon surfaces.

Moreover, the knowledge about binding pocket amino acids composition allowed to speculate about their role in the ligand binding.

## **2.3 *In vitro* experiments**

### **2.3.1 Fluorescence competitive binding assays**

Fluorescence competitive binding assays were employed for monitoring *in vitro* interaction between OBPs and wines terpenes, in order to obtain a number of parameters, such as binding affinity and association/dissociation rate constants for a functional and structural characterization of the target protein, useful for the subsequent development of the nanobiosensor. In this study, a simple fluorescence-based binding assay has been used for initial screening of the most representative wines terpenes. Consequently, the binding properties of *Acyrtosiphon pisum* OBP3, *Megoura viciae* OBP3 and *Acyrtosiphon pisum* OBP9 towards compounds were analyzed. Each protein was dissolved in 50 mM Tris-HCl buffer pH 7.4 and emission fluorescence spectrum was recorded between 380 and 450 nm on Cary Eclipse Fluorescence Spectrophotometer.

Reference value is 407 nm at which to take the values for Fluorescence intensity. The choice of this wavelength as reference value was due to 1-NPN property. When excited in aqueous buffer without OBPs, this probe emitted a maximum of fluorescence at 470-480 nm while the peak shift to 406-410 nm when protein is introduced in the cuvette. This shift in the emission wavelength is accompanied by a several-fold increase in the intensity.

A quartz cuvette with a 1 cm light path was used and slits for excitation and emission were fixed at 5 nm and 10 nm, respectively.

To measure the affinity of ligands, 2  $\mu$ M NPN (Sigma-Aldrich - 104043) as fluorescent reporter was added to a 2  $\mu$ M solution of the protein dissolved in 50 mM Tris-HCl pH 7.4. The mixture was then titrated with each competitive ligand at concentration ranging from 0 to 16  $\mu$ M. Tested ligands were farnesol (Sigma-Aldrich - 43348), geraniol (Sigma-Aldrich - W250716), nerol (Sigma-Aldrich - 50949) and citronellol (Sigma-Aldrich - W230901).

### **2.3.2 Fluorescence data analysis**

For determining binding constants, the intensity values corresponding to the fluorescence emission at 407 nm were plotted against free ligand concentrations.

Ki (Northey et al., 2016) and Kd (Sun et al., 2012) were used as affinity parameters. Ki

refers to inhibition constant, while  $K_d$  means dissociation constant. Both terms are used to describe the binding affinity that a small molecule or macromolecule has for an enzyme or receptor.  $K_d$  measures the equilibrium between the ligand-protein complex and the dissociated components. The  $K_i$  inhibition constant also represents a dissociation constant, but more narrowly for the binding of an inhibitor to an enzyme. That is, a ligand whose binding reduces the catalytic activity of the enzyme.

GraphPad6 was used to determine the equilibrium dissociation constant  $K_i$  ([http://www.graphpad.com/guides/prism/6/curvefitting/index.htm?reg\\_one\\_site\\_competition\\_ki.htm](http://www.graphpad.com/guides/prism/6/curvefitting/index.htm?reg_one_site_competition_ki.htm)) of ligand by measuring its competition for NPN and nonlinear regression curve fitting to the one site competitive binding model. This model fits the  $K_i$  of the ligand directly using the fixed concentration of NPN and the dissociation constant for NPN ( $K_{dNPN}$ ) obtained from a direct fluorescence titration and nonlinear regression curve fitting to one site binding model  $Y = B_{max} * X / (K_{dNPN} + X) + NS * X$  ( $X$  is the NPN concentration,  $B_{max}$  is the maximum specific binding in the same units as  $Y$ ,  $NS$  is the slope of nonspecific binding in  $Y$  units divided by  $X$  units).

The analysis assumes that the protein has one binding site and 100% active, and that the binding is reversible and at equilibrium.

Instead,  $K_d$  was calculated using Sigma Plot™ 13 Software. The dissociation constant ( $K_d$ ) for the OBPs/ligand complex was calculated using the following equation  $K_d = [IC_{50}] / (1 + ([1-NPN] / K_{d-PROBE}))$  for each ligand, where  $[IC_{50}]$  is the probe concentration required to occupy 50% of pockets in vitro and causing a decay of fluorescence to half-maximal intensity,  $[1-NPN]$  is the free probe concentration used and  $K_{dNPN}$ , the dissociation constant for the protein/probe complex.

## 2.4 Biosensor development

The biosensor development was carried out in collaboration with the Nanophotonic Technology Center (NTC) of Valencia (Spain). The aim of the collaboration was to realize a biosensor based on photonic technology. Photonic technology is recognized as one of the main candidates for the development of future high performance biosensing devices. This is due to the several advantages that it presents when compared to other technologies, such as high sensitivity, compactness and high integration level, shorter time to result, label-free detection, use of very low sample and reagents volumes, and their immunity to electromagnetic interferences.

For biosensor assembly, Porous silicon surface were used. Porous silicon (PSi) is a form of the chemical element silicon that has introduced nanopores in its microstructure, rendering a

large surface to volume ratio compared to planar silicon surface. The refractive index of porous layers is determined by the porosity and each porous sample has an its own optical spectrum. Any change occurring in the pores caused by analytes adsorption leads to a direct reflection on the spectral shift.

PSi sample was mounted in a custom-made methacrylate cell, which was connected to a vacuum pump (TSE system pump) able to start the flowing and to a solution container. The flow rate was 20  $\mu\text{l}/\text{sec}$ .

The optical change in refractive index was monitored using Ocean Optic HR4000, Halogen Light source (450 – 900 nm), connected to a spectrometer and the related software Ocean View. Data collected with this setup were analyzed using MatLab software.

Terpenes were diluted using an organic solvent because of their hydrophobic nature (methanol or ethanol).

All experiment were conducted using in flow sensing because it was useful to monitor variations in refractive index of porous layer in *real time*. In fact, using this strategy, it was possible monitoring the evolution of sensing signal at the same time, including the entrance of protein into pores. This was necessary because it was the first time that OBPs were used for PSi optical biosensor. Another advantage of flow cells is that the sample is not removing from the experimental setup and consequently a source of inaccuracy is removed.

Even if a lot of immobilization procedure are available in literature, adsorption was the first choice of biosensor development because it was necessary to minimize the effect of protein solution buffer (Tris- Buffer). In fact, all protein immobilization procedures require ECD/NHS that are not compatible with the Tris Buffer. Moreover, adsorption is the most simple procedure, without the use of chemical that could influence negatively and permanently the structure of protein.

PSi used were oxidized PSi. The oxidized surface are not affected by water oxidation and for this reason were selected as biosensing surface.

## **2.5 Basilicata's wine sampling**

Different types of wines were sampled in the two winery partners of the PhD Program, (“Cantine del Notaio” and “Consorzio Viticoltori Associati del Vulture – Cantine di Barile”) to be analysed with the biosensor.

“Cantine del Notaio” is located in Rionero in Vulture (Potenza, Basilicata, Italy). It has paid a special attention to the choice of vineyards and counts 40 hectares, (approx. 99 acres) distributed amongst the most characteristic and renowned hillsides in the Mount Vulture

area, (Rionero, Barile, Ripacandida, Maschito and Ginestra), and possess vines more than a hundred years old. These areas have different soils, (sand, volcanic residue, medium consistency or clay) but the same layer of volcanic tufo in common, and a pedoclimatic exposition which allows a perfect ripening of the grapes, amongst the very latest ones to be harvested (mid-October to mid-November).

In this winery, Aglianico del Vulture was sampled as wine. In detail:

- Aglianico del Vulture, red wine, 2018 (steel barrel)
- Aglianico del Vulture (“L’atto”), red wine, 2018 (bottled wine)
- Aglianico del Vulture (“Il repertorio”), red wine, 2017 (bottled wine)

The “Consorzio Viticoltori Associati del Vulture” is a winery located in Barile (Potenza, Basilicata) and it brings together the oldest wineries and vineyards of Vulture that have made the history of oenology in Basilicata. The consortium structure is equipped with modern oenological equipment that allows to produce 20000 hectolitres of wine of which 50000 are aged in oak barrels located in a cave.

In this winery, different types of wines were sampled. In detail:

- Aglianico del Vulture, red wine, 2019 (steel barrel)
- Aglianico del Vulture, red wine, 2019, sweet filtered (steel barrel)
- Aglianico del Vulture, rose wine, 2019 (steel barrel)
- Malvasia, white wine, 2019 (steel barrel)



### 3. RESULTS

#### 3.1 *Apis*OBP7 subcloning and sequencing of all recombinant plasmid.

All selected aphids OBPs sequence (*Acyrtosiphon pisum* OBP3, *Acyrtosiphon pisum* OBP9, *Acyrtosiphon pisum* OBP7 and *Megoura viciae* OBP3) were previously cloned at Insects Physiology and Molecular Biology Laboratory, University of Basilicata, in expression vectors (pET-vectors).

Concerning *Apis*OBP7, a first small-scale expression experiment, showed no optimal protein production and a sub-cloning procedure was performed. The OBP sequence was moved in a new expression vector (pET22b), available at the Insects Physiology and Molecular Biology Laboratory. The fragment corresponding to *Apis*OBP7 sequence was recovered from the original clone (*Apis*OBP7 – pET5b) performing a double digestion with NdeI and EcoRI and ligated into pET-22b vector, previously digested with the same enzymes and dephosphorylated. Screening of positive clones was performed using Mini-prep and PCR in tandem.

PCR was carried out using plasmidic DNA obtained from Mini-prep of colonies as template and vector primers T7 promoter and T7 terminator as primer forward and reverse, respectively. An additional negative control was prepared for PCR reaction and it consisted in using empty pET-22b as template.

PCR samples were analyzed on 0.8% agarose gel and the size of amplicons was verify (Figure 18). The size of amplicon is different depending on template. If template is the recombinant vector, that is plasmid with protein sequence insert in the multiple cloning site (MCS), the amplicon is larger in size than amplicon obtained using non-recombinant vector as template.

In the case of pET-22b, the sizes of amplicons attended were approximately 309 bp and 583 bp concerning non-recombinant e recombinant plasmid respectively.

309 bp is due to the number of nucleotides between T7 primers (forward and reverse) used to perform PCR while 583 bp of is due to sum of these nucleotide (they became 208 after vector linearization using NdeI and EcoRI) and the *Apis*OBP7 nucleotide sequence (375 bp).

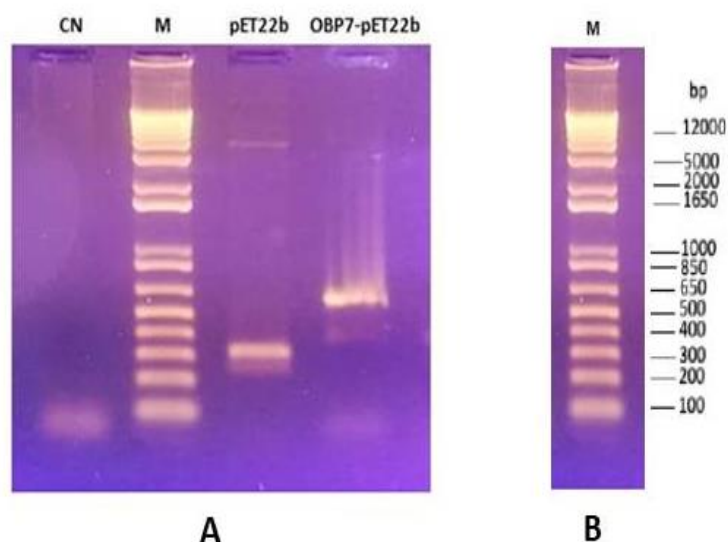


**Figure 18.** A) agarose gel of PCR product **CN**: negative control consisting in reaction mix without template; **M**: 1 Kb Plus DNA Ladder (Invitrogen, #10787018); **pET22b**: negative control consisting in reaction mix with empty vector as template; **OBP7-pet22b**: recombinant vector. **B**) details of marker used.

Recombinant vectors carrying aphids Odorant Binding Proteins, already available at Physiology and Molecular biology Laboratory of University of Basilicata, and the recombinant vector *Apis*OBP7 - pET22b were sequenced using Macrogen Sequencing Service. Sequencing results were aligned with OBP sequence deposited in data bank to verify the quality of recombinant clones. Alignment was conducted considering both nucleotide and amino acids sequences using blastn and tblastp respectively (available at <https://blast.ncbi.nlm.nih.gov/Blast.cgi>). For each recombinant clone, alignments are shown in Appendix A.3.

### 3.2 Odorant Binding Proteins expression.

After sequencing, recombinant plasmids were initially propagated in DH5 $\alpha$  chemically competent *E. coli* cells, that do not contain the T7 RNA polymerase gene, thus eliminating plasmid instability due to the production of proteins potentially toxic to the host cell.

Midi-prep of each recombinant plasmid was performed starting from a single colony to get more plasmid DNA useful for expression experiments.

The DNA obtained was therefore evaluated quantitatively and qualitatively. This evaluation was carried out using the spectrophotometer and agarose gel electrophoresis respectively.

Once established the quality and quantity of midi-prep, each recombinant plasmid was then transferred singularly into expression hosts, BL21 (DE3) chemically competent *E. coli* cells,

that provide a source of T7 RNA polymerase gene, whose expression is induced by Isopropyl  $\beta$ -D-1-thiogalactopyranoside (IPTG), a molecular mimic of allolactose which trigger transcription of the lac operon, to induce gene expression under the control of the lac operator.

After the IPTG-induction, recombinant protein was extracted using Denaturing Lysis Buffer containing 8M Urea (Appendix B.6) and samples were analyzed using SDS-Page (Appendix B.8). Recombinant proteins were checked on polyacrylamide gel according to predicted molecular weight.

Molecular weight and isoelectric point of recombinant proteins were calculating using Compute pI/Mw tool available at [https://web.expasy.org/compute\\_pi/](https://web.expasy.org/compute_pi/) and they are listed in the following Table 1.

<b>PROTEIN</b>	<b>MOLECULAR WEIGHT (kDa)</b>	<b>ISOELECTRIC POINT</b>
<i>Acyrthosiphon pisum</i> OBP3	13.34	5.20
<i>Acyrthosiphon pisum</i> OBP7	14.27	8.86
<i>Acyrthosiphon pisum</i> OBP9	15.89	6.76
<i>Megoura viciae</i> OBP3	13.38	5.20

**Table 1.** Molecular weight and isoelectric point of all recombinant proteins

Expression of recombinant proteins was firstly optimized. For this reason, small-scale time course experiments were conducted. The first OBP produced was *Apis*OBP3. Concerning the expression of this protein, two time of induction were selected and two concentration of IPTG were compared (Figure 19). The best condition is achieved using 0.4 mM of IPTG and two hours of cell culture incubation. Considering this result, the expression experiments of other OBPs were performed using a fixed concentration of IPTG and changing the time of incubation.

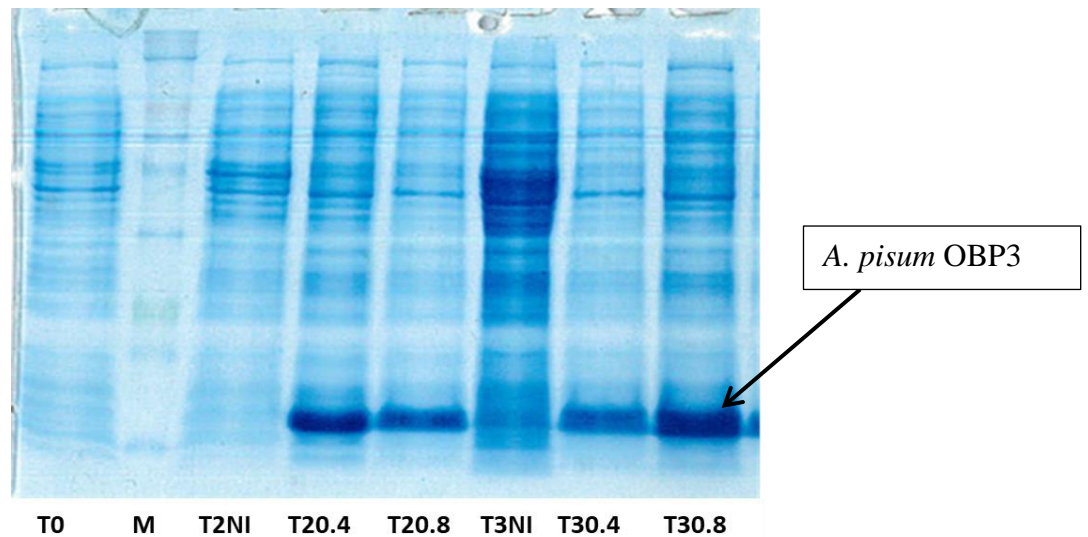


**Figure 19.** *Apis*OBP3 time course expression experiment. **T0**: time before addition of IPTG; **M**: ColorPlus Prestained Protein Marker (New England BioLabs #P7709S); **T2NI**: 2 hours of cells growing without IPTG; **T2 0.4**: 2 hours after induction with IPTG 0.4 mM; **T2 0.8**: 2 hours after induction with IPTG 0.8mM; **T3NI**: 3 hours of cells growing without IPTG; **T3 0.4**: 3 hours after induction with IPTG 0.4mM; **T3 0.8**: 3 hours after induction with IPTG 0.8mM.

Therefore, *Apis*OBP7 was expressed using 0.4 mM IPTG and collecting samples up to 4 hours after induction. The best time was 3 hours after induction (Figure 20).

In both cases (*Apis*OBP3 and *Apis*OBP7 expression), recombinant proteins were found in supernatant obtained after denaturing protocol extraction (Appendix B.6).

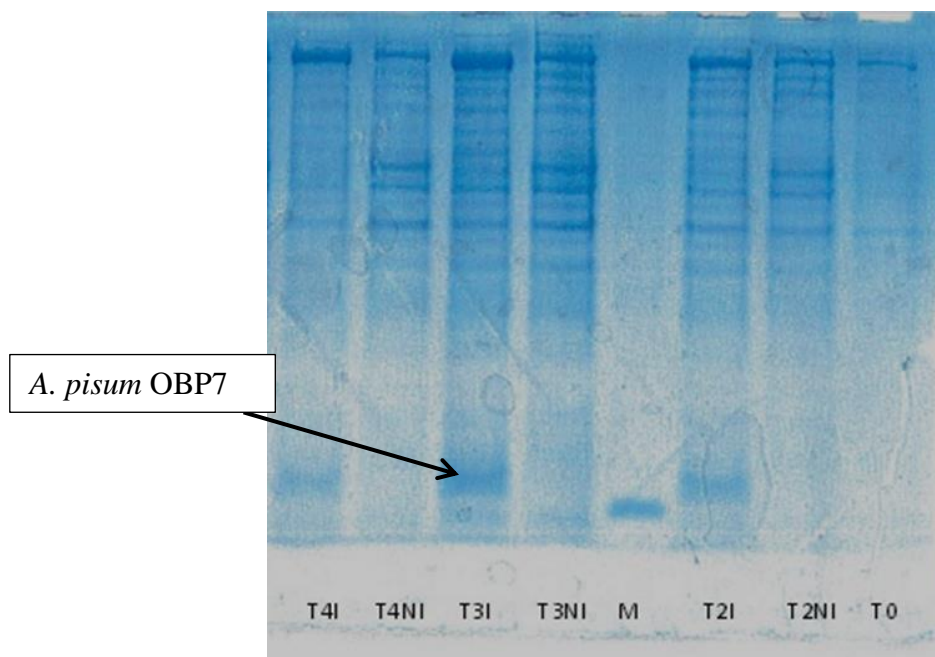


**Figure 20.** *Apis*OBP7 time course expression experiment. **T0**: time before addition of IPTG; **M**: in this experiment *A. pisum* OBP3 was used as molecular weight marker; **T2NI**: 2 hours of

cells growing without IPTG; **T2I**: 2 hours after induction with IPTG 0.4 mM; **T3NI**: 3 hours of cells growing without IPTG; **T3I**: 3 hours after induction with IPTG 0.4mM; **T4NI**: 4 hours of cells growing without IPTG; **T4I**: 4 hours after induction with IPTG 0.4mM.

Time course experiments were performed also regarding *Apis*OBP9 (Figure 21) and *Mvic* OBP3 (Figure 22).

In both cases, recombinant proteins were found in supernatant and pellet obtained from denaturing protocol extraction. The presence of recombinant protein in both fractions can be explained assuming that the volume of Urea used for cell disruption was not enough to solubilize also the inclusion bodies (IBs) and recombinant proteins precipitated with membrane detritus. Indeed, OBPs are located in IBs when overexpressed in bacterial host system.

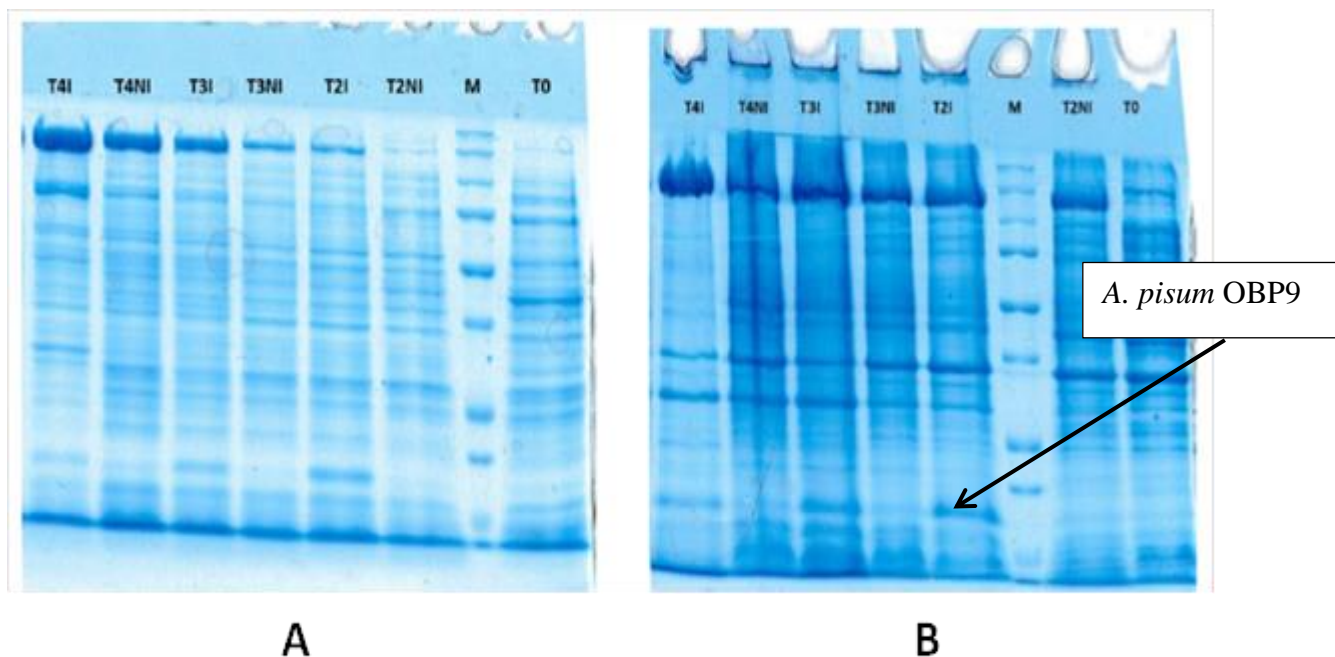


**Figure 21.** *Apis*OBP9 time course expression experiment. **A** and **B** represent urea treatment supernatant and pellet respectively. **T0**: time before addition of IPTG; **M**: ColorPlus Prestained Protein Marker (New England BioLabs #P7709S); **T2NI**: 2 hours of cells growing without IPTG; **T2I**: 2 hours after induction with IPTG 0.4 mM; **T3NI**: 3 hours of cells growing without IPTG; **T3I**: 3 hours after induction with IPTG 0.4mM; **T4NI**: 4 hours of cells growing without IPTG; **T4I**: 4 hours after induction with IPTG 0.4mM

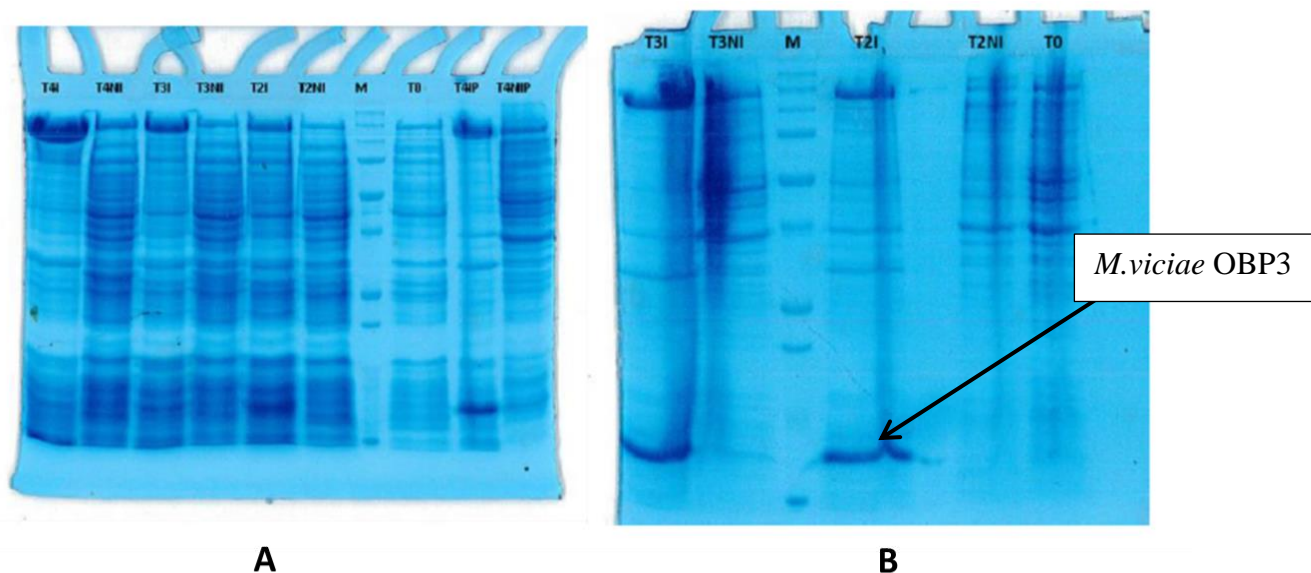


**Figure 22.** *Mvic*OBP3 time course expression experiment. **A** and **B** represent urea treatment supernatant and pellet respectively. In **A**, **T4IP** (4 hours after induction) and **T4NIP** (4 hours without) are pellet samples. **T0**: time before addition of IPTG; **M**: ColorPlus Prestained Protein Marker (New England BioLabs #P7709S); **T2NI**: 2 hours of cells growing without IPTG; **T2I**: 2 hours after induction with IPTG 0.4 mM; **T3NI**: 3 hours of cells growing without IPTG; **T3I**: 3 hours after induction with IPTG 0.4mM; **T4NI**: 4 hours of cells growing without IPTG; **T4I**: 4 hours after induction with IPTG 0.4mM

### 3.3 Odorant Binding Proteins purification

After Urea lysis, samples were treated with the “oxido-shuffling” reagents (cysteine-cystine) and then were dialysed against appropriate buffer to be purified.

*Acyrtosiphon pisum* OBP3 and *Megoura viciae* OBP3 were dialysed against Tris Buffer 50 mM pH 7.4 , *Acyrtosiphon pisum* OBP7 against Tris Buffer 50 mM pH 7.4 and Tris Buffer 30 mM pH 8 while *Acyrtosiphon pisum* OBP9 Native Lysis buffer containing imidazole.

*Apis*OBP3 was successfully purified using ionic exchange chromatography (Figure 23). A polypropylene column was filled using 1 mL of DEAE Sepharose resin and the sample was incubated at room temperature for 15 minute to promote the binding. Then, two buffer were used to elute recombinant protein. The first buffer was 50 mM Tris Buffer pH 7.4 (Buffer A) and the second buffer was Tris Buffer 50 mM pH 7.4 with 1M NaCl (Buffer B).

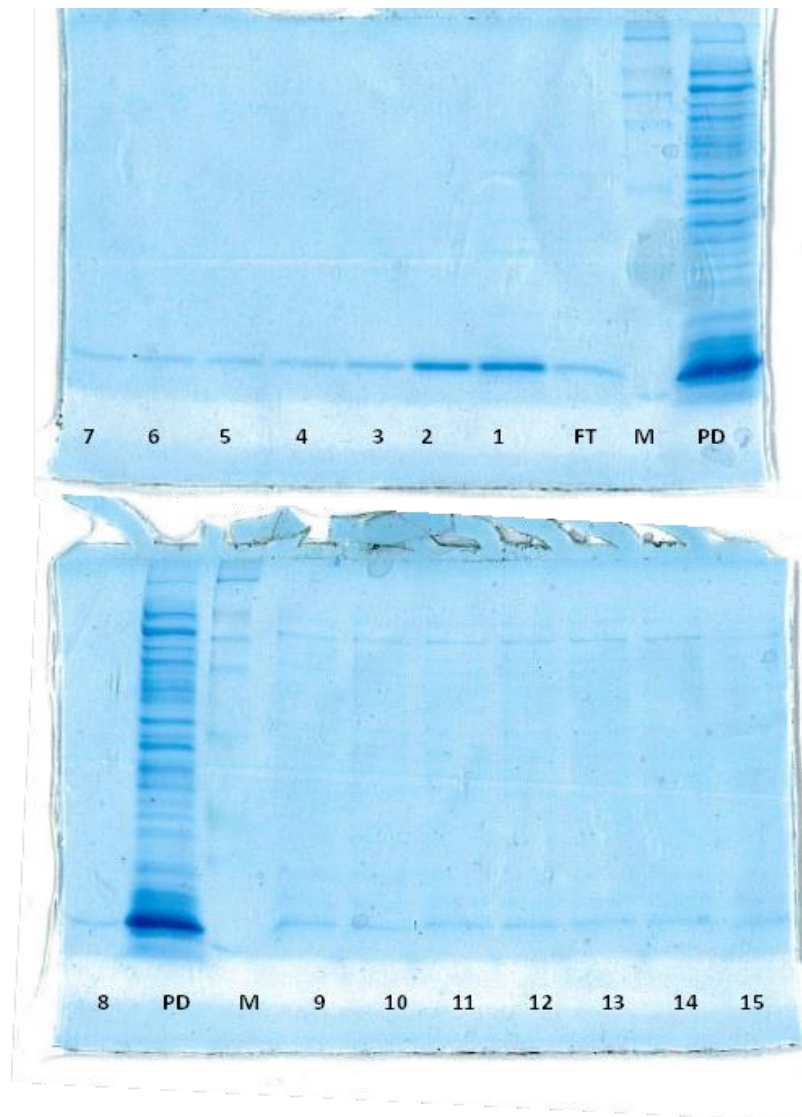


**Figure 23.** Purification of recombinant *ApisOBP3*. **PD**: post dialysis; **M**: ColorPlus Prestained Protein Marker (New England BioLabs #P7709S); **FT**: flow through; **1-8**: elution with BUFFER A; **9-15**: elution with BUFFER B.

Recombinant *ApisOBP3* was found in all fraction but it was mainly in FT and 1-7 elution fractions (Figure 23). Moreover, these fractions were cleaner than others, containing only recombinant protein. The cleanest fractions were collected together and quantified through the Bradford assay. The total yield of recombinant protein was 600  $\mu\text{g}$  (from an initial bacterial culture of about 300 mL).

A similar purification procedure has been exploited also for *MvicOBP3* protein (Figure 24) with a total yield of recombinant protein equal to 680  $\mu\text{g}$  (from an initial bacterial culture of about 300 mL).

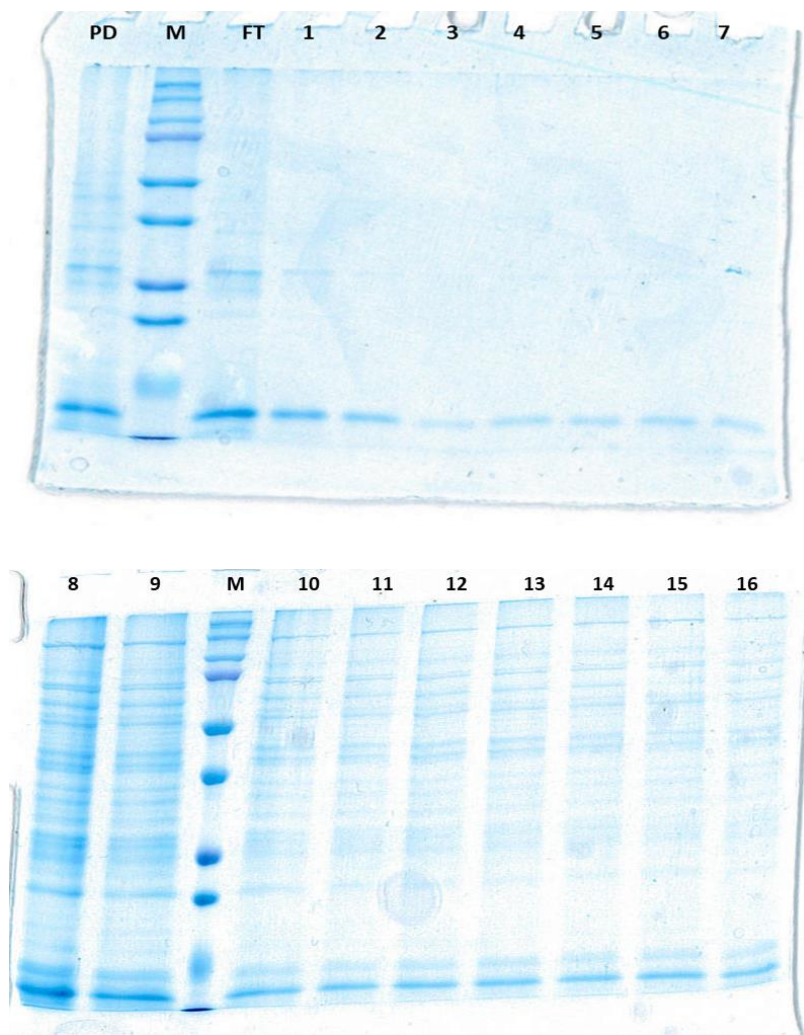


**Figure 24** Purification of recombinant *MvicOBP3*. **PD**: post dialysis; **M**: ColorPlus Prestained Protein Marker (New England BioLabs #P7709S); **FT**: flow through; **1-7**: elution with BUFFER A; **8-16**: elution with BUFFER B. Recombinant *M.viciae* OBP3 was found in all fraction but 1-7 elution fractions were cleaner than others, containing only recombinant protein.

At the beginning, also *ApisOBP7* was purified through ionic exchange resin but it did not work. The used procedure was the same of *ApisOBP3* and *MvicOBP3*. OBP7 was eluted using the same buffers (Figure 25) and also changing the pH of buffer (Figure 26) but the attempts were unsuccessful. Chromatography fraction where recombinant protein was present contain also bacterial proteins.



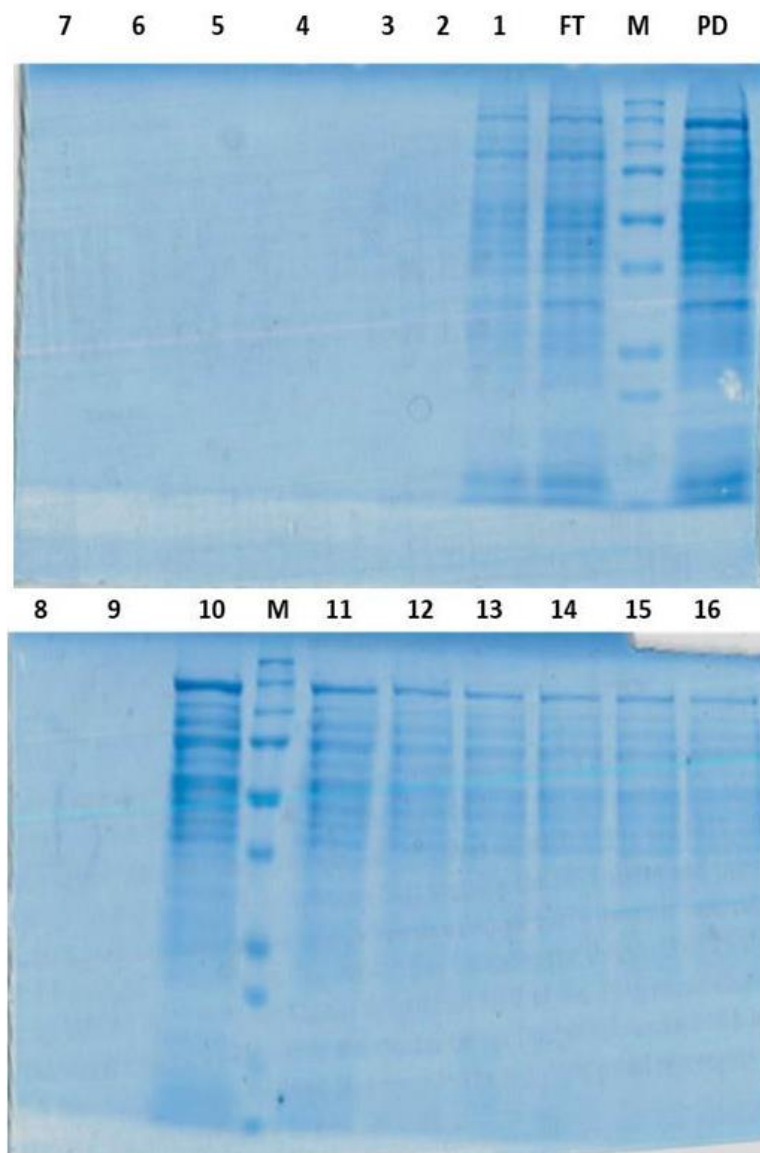


**Figure 25.** Anion exchange chromatography of recombinant *ApisOBP7*. **PD**: post dialysis; **M**: ColorPlus Prestained Protein Marker (New England BioLabs #P7709S; **FT**: flow through; **1-9**: elution with BUFFER A; **10-16**: elution with BUFFER B

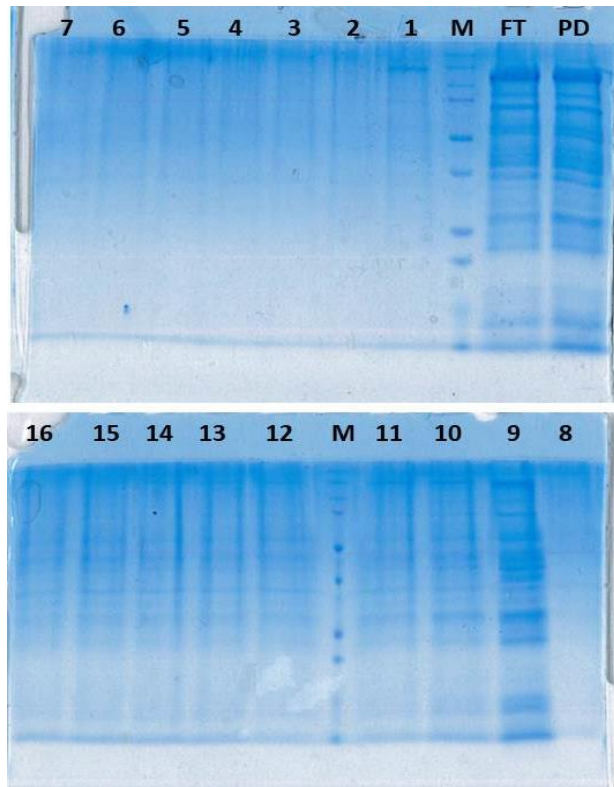


**Figure 26 .** Anion exchange chromatography of recombinant *ApisOBP7*. **PD**: post dialysis; **M**: ColorPlus Prestained Protein Marker (New England BioLabs #P7709S; **FT**: flow through; **1-8**: elution with Tris Buffer 50 mM pH 10.8 ; **9-16**: elution with Tris Buffer 50 mM/ 1M NaCl pH 10.8

Gel filtration chromatography was also used to try to purify *ApisOBP7* because anion exchange did not work. Tris Buffer 30 mM pH 8 was used as elution buffer. Also in this case, purification of recombinant protein was not successful (Figure 27).

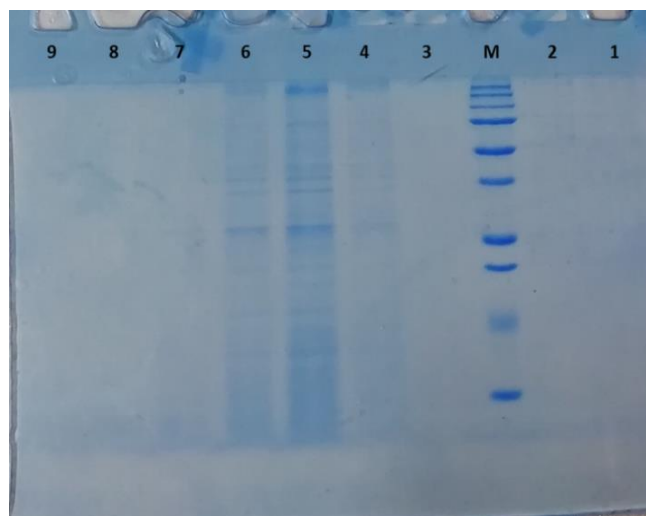


**Figure 27** Gel filtration chromatography of recombinant *ApisOBP7*. **M**: ColorPlus Prestained Protein Marker (New England BioLabs #P7709S; **1-9**: 1,5 mL elution fraction collected using Tris Buffer 30 mM as mobile phase.

Concerning *Apis*OBP9, it was purified using the Ni-NTA resin. This type of purification was possible to be performed because the recombinant protein was cloned with His-tag. Two Ni-NTA purification *in tandem* were required to obtain a clean fraction containing only the recombinant protein (Figure 28). All the fractions were put together and quantified through Bradford assay (total yield equal to 710  $\mu$ g, starting from 200 mL of initial bacterial culture)

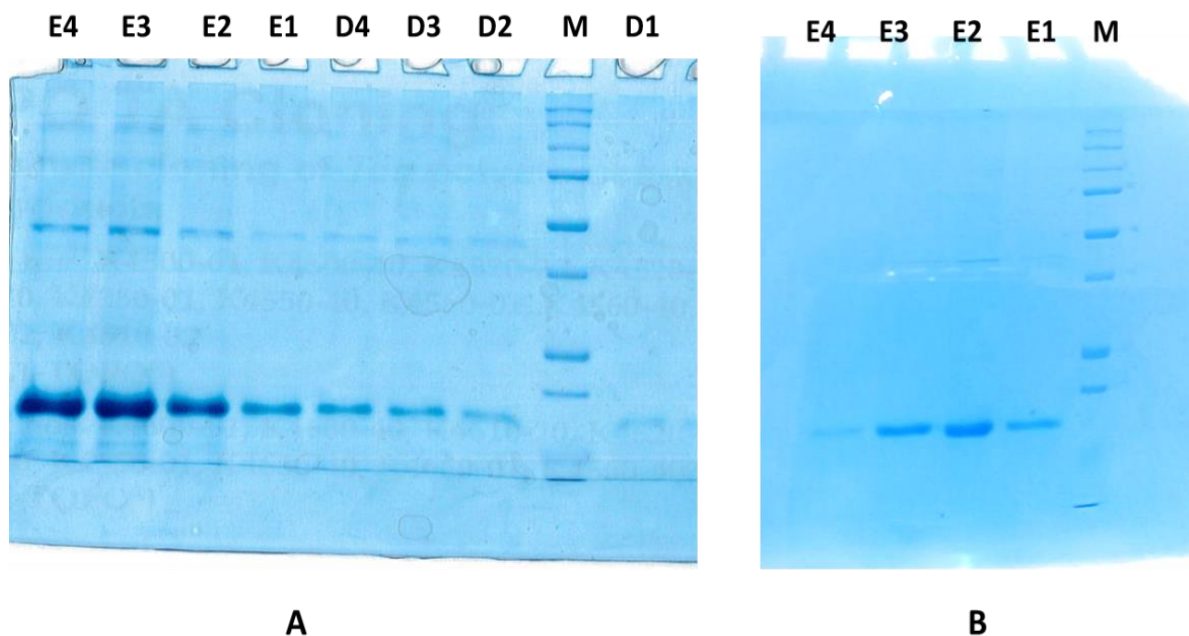
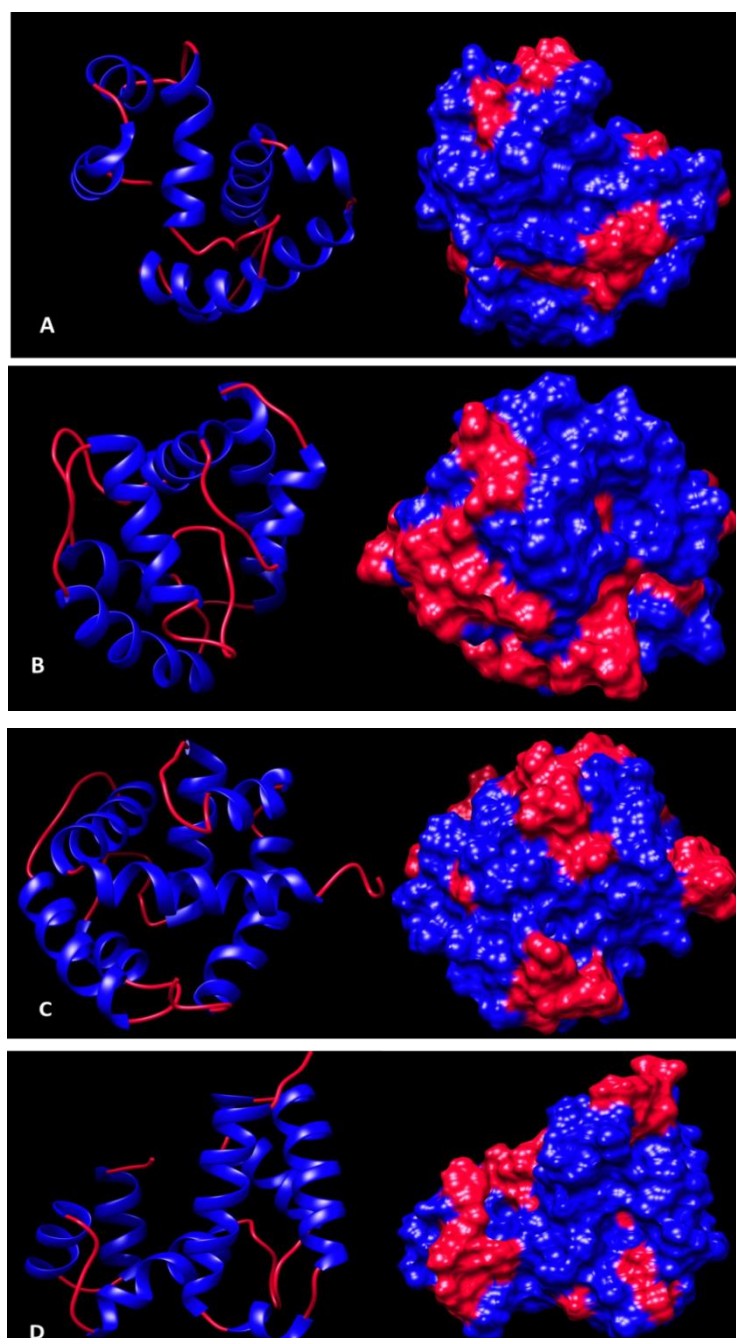


**Figure 28.** Ni-NTA purification of recombinant *Apis*OBP9. **A.** The first purification in batch following manufacture's protocol. It was performed under denaturing condition. **D1-D4:** elution fraction obtained using Buffer D (denaturing elution buffer, Appendix C.4); **E1-E4:** elution fraction obtained using Buffer E (denaturing elution buffer, Appendix C.4). **B.** The second purification in batch. It was performed under native condition, after dialysis of samples obtained from the first purification, using a suitable buffer. **E1-E4:** elution fraction obtained using Buffer E (Appendix B.11 and C.4).

After dialysis against 50mM Tris Buffer (pH 7.4), all purified recombinant proteins were subsequently used in competitive binding assays to test their affinity to some volatile organic compounds.

### 3.4 Molecular modeling: aphids OBP structure, ligand selection and structure, *in silico* docking analysis

Starting from amino acid sequences, *Apis*OBP3, *Apis*OBP7, *Apis*OBP9 and *Mvic*OBP3 were *ab initio* modelled using I-TASSER webserver and then visualised using UCSF CHIMERA (Figure 29).

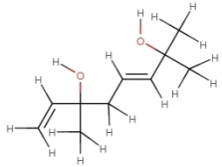
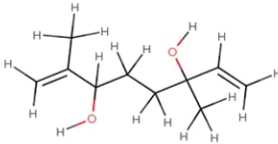
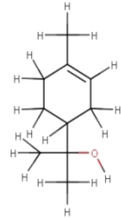
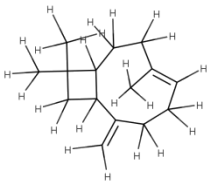
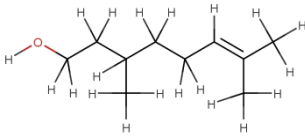
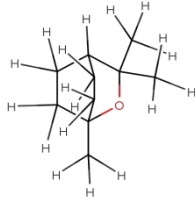
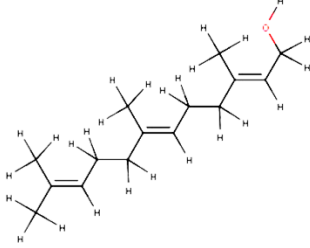
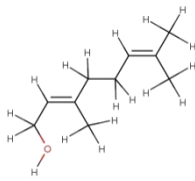


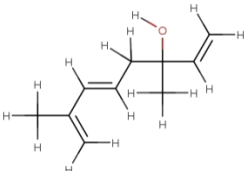
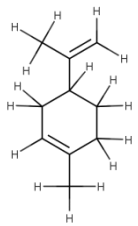
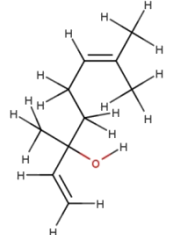
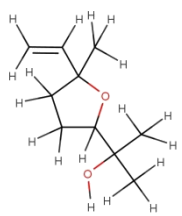
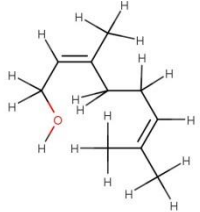
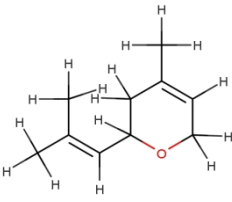
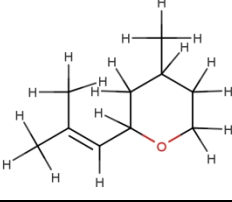
**Figure 29.** Three-dimensional structures of aphids OBPs. **A.** *ApisOBP3*; **B.** *ApisOBP7*; **C.** *ApisOBP9*; **D.** *MvicOBP3*. **Left:** secondary structure with  $\alpha$ -helix (blue) and coil (red); **Right:** OBPs surface, blue corresponds to  $\alpha$ -helix regions while red corresponds to coiled regions.

Protein structures were subsequently used for molecular docking. Molecular docking technique was used to calculate the interaction energies and the binding affinity of the complex formed by OBP and the chemical structures of identified terpenes in wine.

At first, wine terpenes were identified with a bibliographic approach. Many reviews about wine aroma are available in PubMed (<https://www.ncbi.nlm.nih.gov/pubmed/>) and the most

representative terpenes in wine are listed below (Table 2).

<b>TERPENES</b>	
<b>Name</b>	<b>Structure</b>
2,6 – dimethyl – 3,7 – octadien – 2,6 – diol	
3,7 – dimethyl – 1,7 – octadien – 3,6 – diol	
$\alpha$ - terpineol	
$\beta$ - caryophyllene	
Citronellol	
Eucalyptol	
Farnesol	
Geraniol	

Hotrienol	
Limonene	
Linalool	
Linalool oxide	
Nerol	
Nerol oxide	
Rose oxide	

**Table 2.** List of terpenes found in wines

Structures of identified terpenes were obtained using MarvinSketch software (<https://chemaxon.com/products/marvin>) and the interaction of each terpenes with aphids

OBPs was evaluated using SwissDock software and UCSF CHIMERA.

Binding energy and  $\Delta G$  values are reported in Tables 3 - 6

<b>TERPENE</b>	<b>ENERGY kcal/mol</b>	<b><math>\Delta G</math> kcal/mol</b>
2,6 – dimethyl – 3,7 – octadien – 2,6 – diol	-12,66	-6,50
3,7 – dimethyl – 1,7 – octadien – 3,6 – diol	-19,59	-6,56
$\alpha$ – terpineol	-21,62	-6,52
$\beta$ - caryophyllene	28,72	-5,86
Citronellol	-27,40	-6,60
Eucalyptol	-1,56	-5,96
Farnesol	-34,31	-7,14
Geraniol	-27,59	-6,79
Hotrienol	-11,52	-6,39
Limonene	-26,22	-6,37
Linalool	-19,91	-6,31
Linalool oxide	-1,80	-6,53
Nerol	-27,63	-6,66
Nerol oxide	-20,66	-6,44
Rose oxide	-17,65	-6,45

**Table 3.** *Apis*OBP3 – terpenes *in silico* affinity

<b>TERPENE</b>	<b>ENERGY kcal/mol</b>	<b><math>\Delta G</math> kcal/mol</b>
2,6 – dimethyl – 3,7 – octadien – 2,6 – diol	-12,07	-6,42
3,7 – dimethyl – 1,7 – octadien – 3,6 – diol	-16,25	-6,14
$\alpha$ – terpineol	-17,94	-6,27
$\beta$ – caryophyllene	29,28	-6,46
Citronellol	-23,18	-6,25
Eucalyptol	-2,10	-6,25
Farnesol	-29,58	-6,87
Geraniol	-23,60	-6,19
Hotrienol	-8,00	-5,98
Limonene	-23,69	-6,21
Linalool	-17,11	-6,21
Linalool oxide	1,00	-6,09
Nerol	-23,78	-6,29
Nerol oxide	-17,70	-6,28
Rose oxide	-17,47	-5,95

**Table 4.** *Apis*OBP7– terpenes *in silico* affinity

<b>TERPENE</b>	<b>ENERGY kcal/mol</b>	<b><math>\Delta G</math> kcal/mol</b>
2,6 – dimethyl – 3,7 – octadien – 2,6 – diol	-10,26	-6,15
3,7 – dimethyl – 1,7 – octadien – 3,6 – diol	-16,09	-6,03
$\alpha$ – terpineol	-17,59	-6,07
$\beta$ - caryophyllene	29,03	-6,41
Citronellol	-24,41	-6,49
Eucalyptol	-2,80	-6,33
Farnesol	-28,53	-6,57
Geraniol	-22,97	-6,18
Hotrienol	-9,00	-5,96
Limonene	-21,85	-5,96
Linalool	-16,78	-6,12
Linalool oxide	-1,23	-6,39
Nerol	-23,42	-6,40
Nerol oxide	-16,37	-6,03
Rose oxide	-18,34	-6,06

**Table 5.** *Apis*OBP9 - terpenes *in silico* affinity

<b>TERPENES</b>	<b>ENERGY kcal/mol</b>	<b><math>\Delta G</math> kcal/mol</b>
2,6 – dimethyl – 3,7 – octadien – 2,6 – diol	-14,40	-6,71
3,7 – dimethyl – 1,7 – octadien – 3,6 – diol	-19,12	-6,58
$\alpha$ – terpineol	-20,84	-6,51
$\beta$ - caryophyllene	29,00	-6,69
Citronellol	-25,75	-6,66
Eucalyptol	-5,60	-6,59
Farnesol	-35,68	-7,48
Geraniol	-26,81	-6,58
Hotrienol	-13,36	-6,60
Limonene	-24,10	-6,11
Linalool	-22,36	-6,58
Linalool oxide	-2,78	-6,53
Nerol	-26,52	-6,63
Nerol oxide	-20,94	-6,53
Rose oxide	-18,22	-6,64

**Table 6.** *Mvic*OBP3 - terpenes *in silico* affinity



Molecular docking results were exploited to select terpenes to be used in competitive binding assays. Terpenes were selected on the basis of the binding energy value associated to complex OBP-terpenes. Most of the complexes formed by OBP and terpene had energy values similar to each other and for these reason these values were compared to the energy value associated to OBP/ $\beta$ -farnesene complex. Indeed, all OBPs are able to bind  $\beta$ -farnesene with good affinity (Sun et al., 2012; Qiao et al., 2009; Northey et al., 2016; Falabella et al., data unpublished). Energy values of each OBP/  $\beta$ -farnesene complexes is listed in Table 7.

<b>OBP - <math>\beta</math>-FARNESENE COMPLEX</b>	<b>ENERGY kcal/mol</b>	<b><math>\Delta G</math> kcal/mol</b>
<i>Acyrtosiphon pisum</i> OBP3	-32,84	-7,16
<i>Acyrtosiphon pisum</i> OBP7	-28,23	-6,60
<i>Acyrtosiphon pisum</i> OBP9	-25,55	-6,52
<i>Megoura viciae</i> OBP3	-32,32	-7,34

**Table 7.** Energy values of OBP/ $\beta$ -farnesene complex. These values were used as reference.

### 3.5 Competitive binding assays

The selected terpenes were nerol, geraniol, citronellol and farnesol. The choice of these terpenes was firstly correlated to the energy value derived from molecular docking analysis. Indeed, complexes formed by each OBP and these terpenes have an energy value closer to OBP/ $\beta$ -farnesene (e.g. *Apis*OBP3/  $\beta$ -farnesene has an energy value of -32,84 while *Apis*OBP3/nerol has an energy value equal to -27,63). Moreover among these compounds, geraniol and nerol are isomers and it was interesting to test the selectivity of the proteins against these isomers. All these compounds were used for *in vitro* assays to test the affinity of the proteins towards each of them. To investigate the aphids OBPs binding affinities, competitive binding assays were used. These assays are based on competition to the binding site in the protein between a fluorescent probe (N-Phenyl-naphthalen-1-amine; 1-NPN) and a free ligand. When excited in aqueous buffer at 337 nm, 1-NPN produces a very weak fluorescent peak at 480 nm; in presence of OBPs, the emission wavelength is shifted to 407 nm, accompanied by a several-fold increase in the intensity. These assays represent the most popular protocol to test OBPs affinity to ligands.

Competitive binding assays were performed using 2  $\mu$ M of protein (dissolved in 50 Tris

Buffer pH 7.4), 2  $\mu\text{M}$  of 1-NPN and an increasing concentration of terpene (0-16  $\mu\text{M}$ ). According to *in silico* data, *Acyrtosiphon pisum* OBP3 was tested with nerol, geraniol and citronellol (Figure 30), *Acyrtosiphon pisum* OBP9 was tested with farnesol, nerol and citronellol (Figure 31) and *Megoura viciae* OBP3 was tested with farnesol, nerol and geraniol (Figure 32). Concerning results, an increase of fluorescence, instead of decrease, occurred regardless of what protein was used. An attempt using an higher concentration of fluorescence probe was performed but results were the same: an increase of fluorescence (data not shown). Although there was an increase in fluorescence rather than a decrease, inhibition and dissociation constants were alike calculated, using the fluorescent value at 407 nm plotted against free ligand concentrations.  $K_i$  and  $K_d$  were calculated for each protein/ligand (Supplementary materials. Section 5).

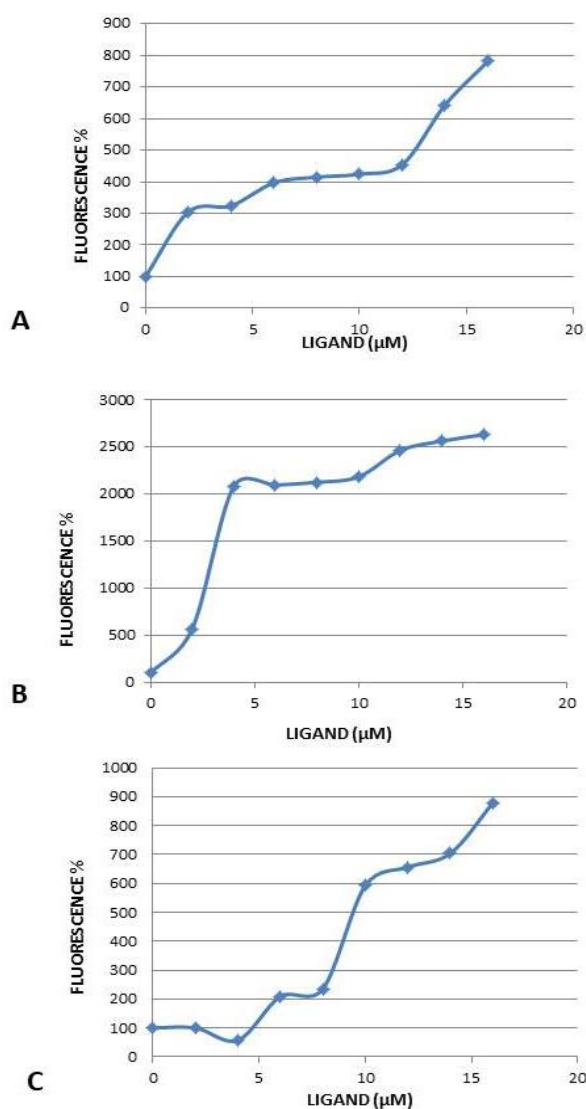


**Figure 30.** *Apis*OBP3 competitive binding assay results. Terpene tested **A.** Nerol **B.** Geraniol **C.** Citronellol. The concentration of ligand was plotted against fluorescence percentage.

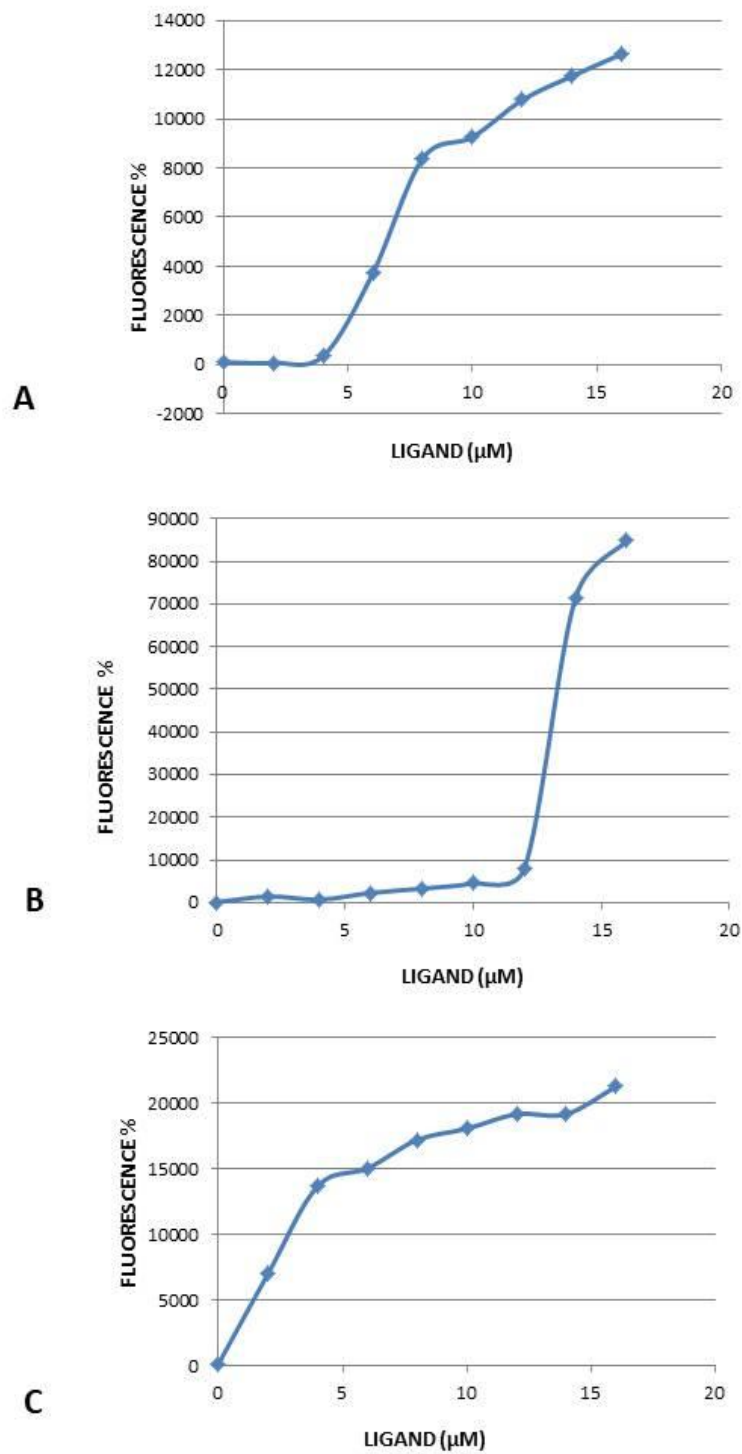


**Figure 31.** *Apis*OBP9 competitive binding assay results. Terpene tested: **A.** Farnesol **B.** Nerol **C.** Citronellol. The concentration of ligand was plotted against fluorescence percentage.

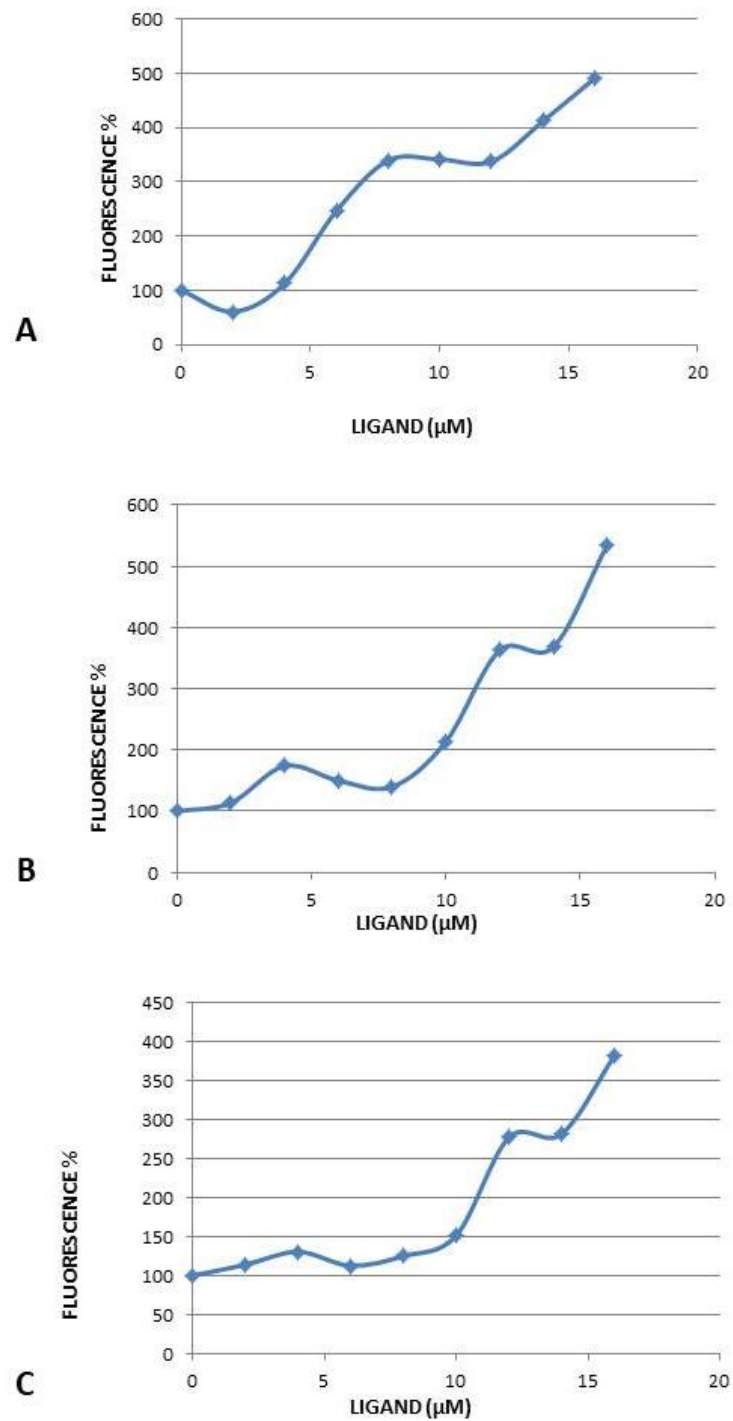


**Figure 32** *MvicOBP3* competitive binding assay results. Terpene tested: **A.** Farnesol **B.** Nerol **C.** Geraniol. The concentration of ligand was plotted against fluorescence percentage.

### 3.6 Binding pocket analysis

Biosensor assembly is based on immobilization of a biological element (protein, cell or aptamers) on a transducer surface. The biological element is responsible of analyte recognition and it must be in the right conformation to solve its role. For this reason, an analysis of binding sites in aphids' OBPs was necessary to understand the strategy of immobilization of protein on transducer surface.

The amino acids sequences of OBPs were analyzed through the software CASTp. In particular, this software identifies all pockets and voids on a protein structure and provides detailed delineation of all atoms participating in their formation.

Amino acids hypothetically involved in *Apis*OBP3 binding pocket are showed in Figure 33 while CASTp analysis of *Apis*OBP9 and *Mvic*OBP3 are showed in Figure 34 and Figure 35, respectively.

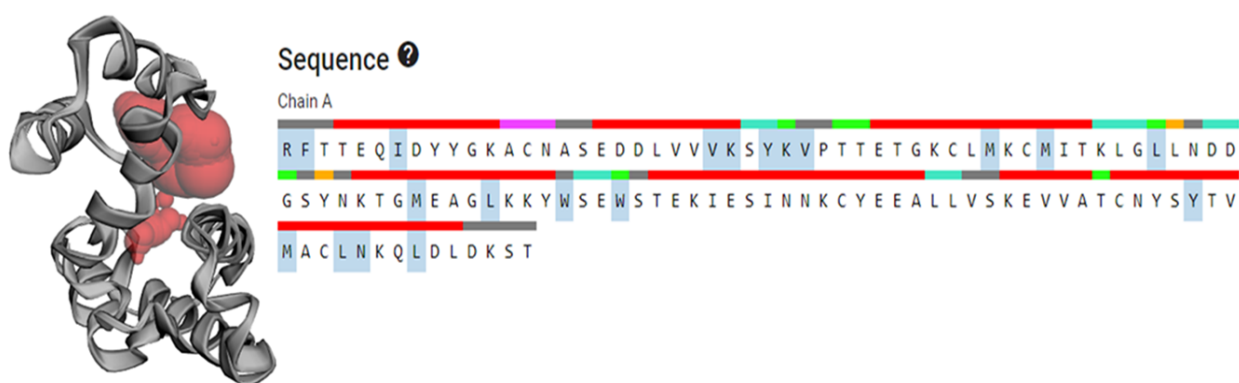


**Figure 33.** *Apis*OBP3 CASTp analysis. In blue are shown amino acids involved in binding pocket formation.



**Figure 34** *Apis*OBP9 CASTp analysis. In blue are shown amino acids involved in binding pocket formation.



**Figure 35.** *MvicOBP3* CASTp analysis. In blue are shown amino acids involved in binding pocket formation.

Details about binding pocket in OBPs, obtained using CASTp software, were useful also for understanding the involvement of amino acids in the interaction with ligands.

SwissDock/CHIMERA analysis predicted the correct binding mode between a protein and a ligand. For this reason, the OBP/ligand complexes were further analyzed through CHIMERA, underlining binding pocket in the three-dimensional structure and visualizing the interaction between ligand and binding pocket residues.

The analysis included *ApisOBP3* interacting with farnesol (Figure 36A), citronellol, geraniol and nerol (Figure 37), *ApisOBP9* interacting with citronellol, farnesol and nerol (Figure 38) and *MvicOBP3* interacting with limonene (Figure 36B), farnesol, geraniol and nerol (Figure 39).

Only these OBP-ligand complexes were analyzed in their binding pocket interaction because of the preliminary selection of terpenes (see Results, 3.4 Molecular modeling: aphids OBP structure, ligand selection and structure, *in silico* docking analysis).

*ApisOBP3*/farnesol and *MvicOBP3*/limonene were analyzed in their binding pocket according to literature (Qiao et al. 2009, Northey et al. 2016).

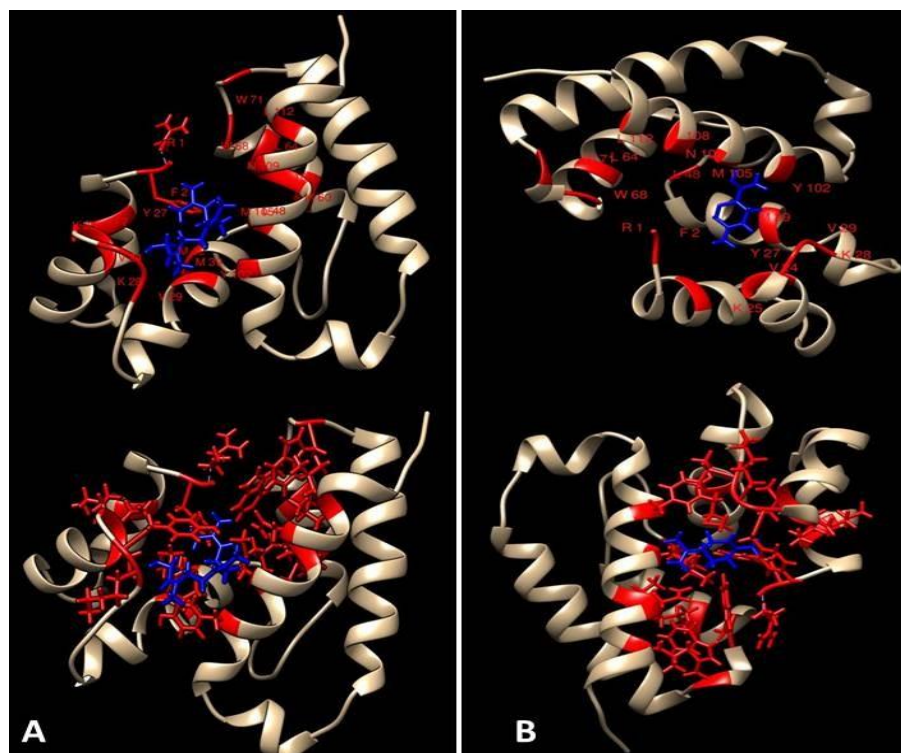


**Figure 36.** CHIMERA visualization of *Apis*OBP3/farnesol (**A**) and *Mvic*OBP3/limonene (**B**) complexes. In this figure, complexes with a more negative energy are shown. The upper side of figure shows OBP-ligand interaction with binding pocket underlined in red and named with 1-letter method and position in chain. The side below shows the lateral chain of the binding pocket amino acids.

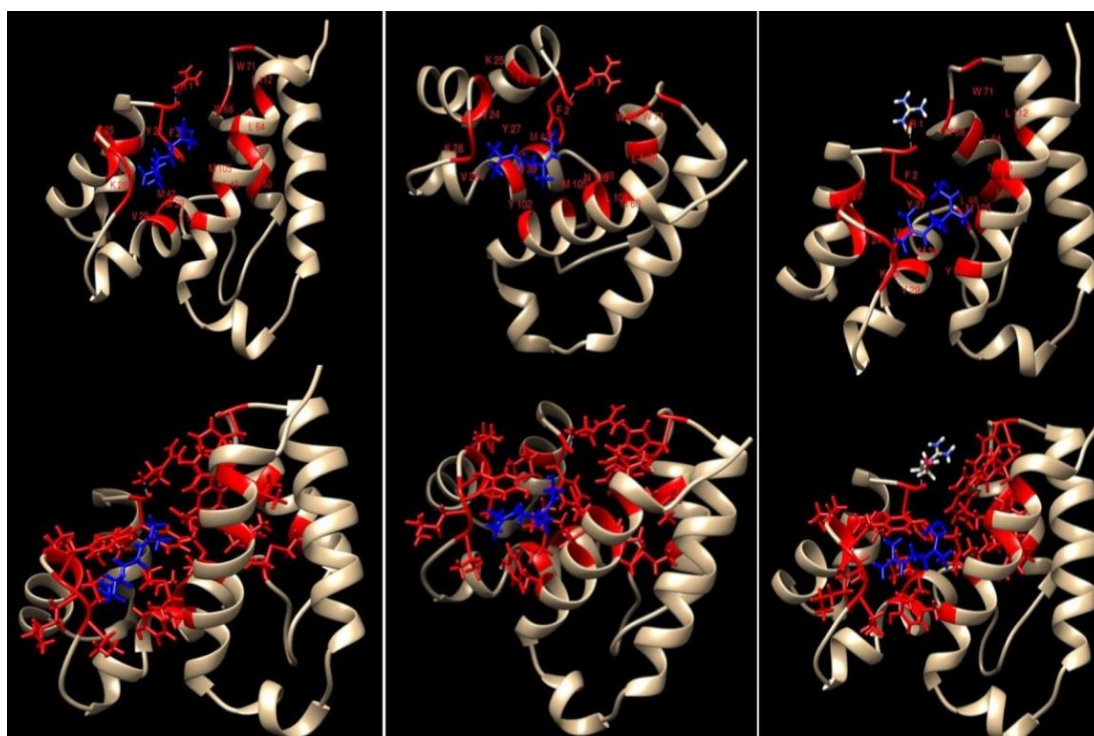


**Figure 37.** CHIMERA visualization of *Apis*OBP3/citronellol (**left**), *Apis*OBP3/geraniol (**central**) and *Apis*OBP3/nerol (**right**). In this figure, complexes with a more negative energy are shown. The upper side of the figure shows OBP-ligand interaction with binding pocket underlined in red and named with 1-letter method and position in chain. The side below shows the lateral chain of the binding pocket amino acids.

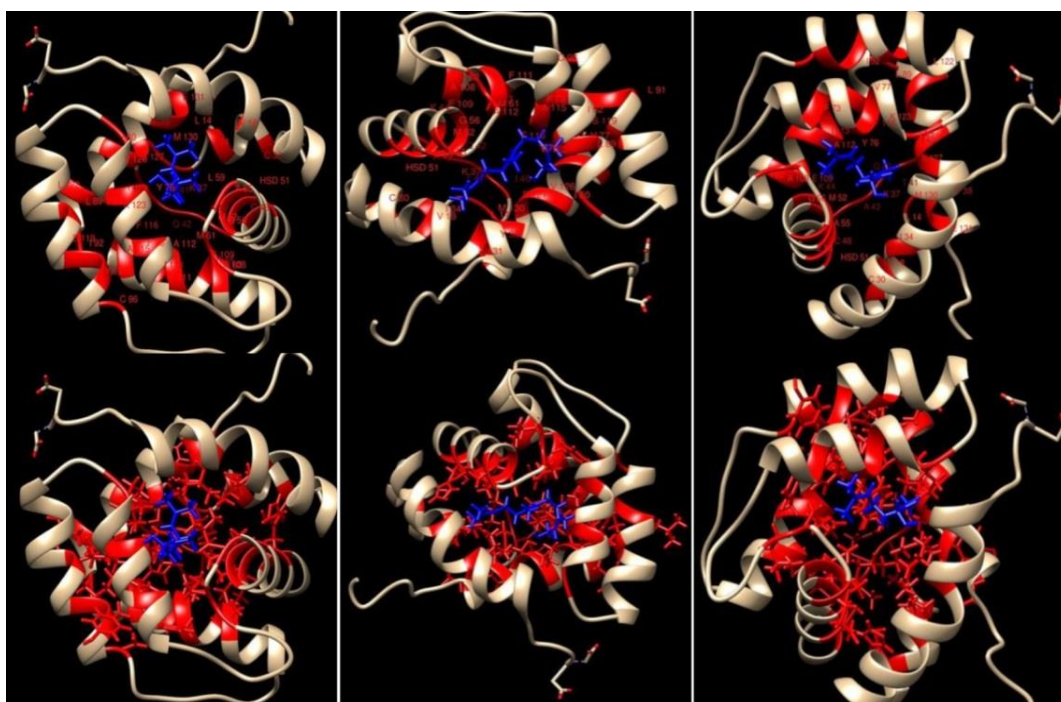


**Figure 38.** CHIMERA visualization of *ApisOBP9*/citronellol (**left**), *ApisOBP9*/farnesol (**central**) and *ApisOBP9*/nerol (**right**). In this figure, complexes with a more negative energy are shown. The upper side of figure shows OBP-ligand interaction with binding pocket underlined in red and named with 1-letter method and position in chain. The side below shows the lateral chain of the binding pocket amino acids.

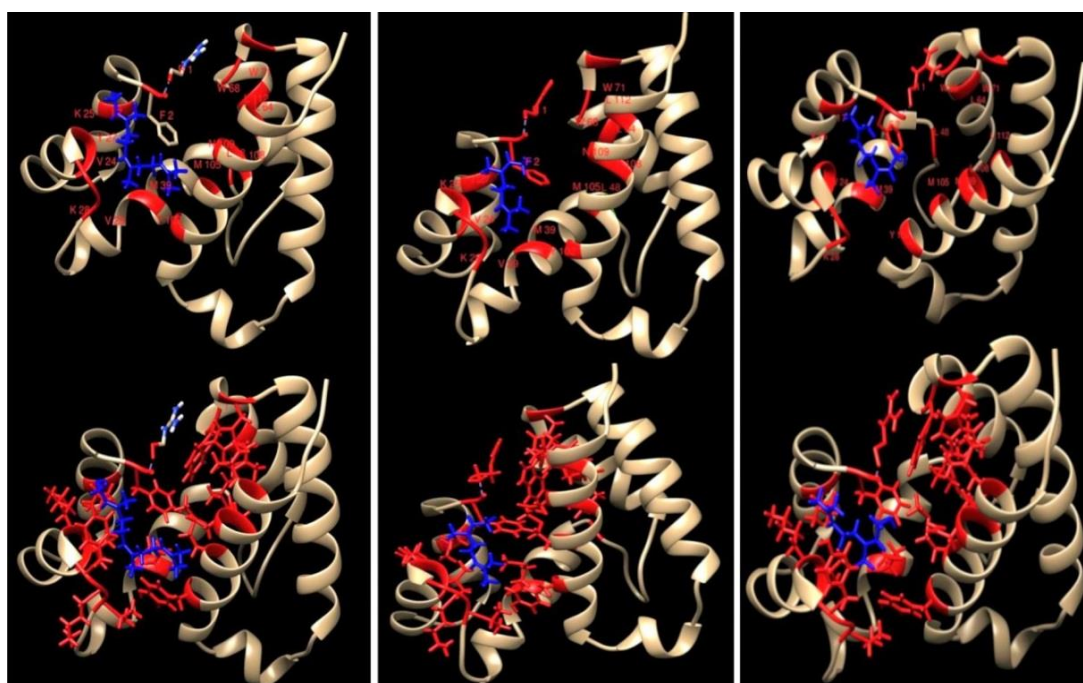


**Figure 39.** CHIMERA visualization of *MvicOBP3*/farnesol (**left**), *MvicOBP3*/geraniol (**central**) and *MvicOBP3*/nerol (**right**). In this figure, complexes with a more negative energy are shown. The upper side of figure shows OBP-ligand interaction with binding pocket underlined in red and named with 1-letter method and position in chain. The side below shows the lateral chain of the binding pocket amino acids.



### 3.7 Optical biosensors OBP based

*Apis*OBP3 was the first protein used for P*Si* biosensor assembly. The choice of use firstly *Apis*OBP3 was due to previous functional characterization of this protein and its recorded ability to bind farnesol (Sun et al., 2012). Hence, initial experiments have involved this protein and farnesol. This was useful to optimize the biosensor assembly protocol.

P*Si* samples used were oxidized samples (Figure 40). For all sample used in this PhD research, the oxidation procedure was the thermal oxidation (the standard for porous silicon). The oxidation step creates a SiO<sub>2</sub> layer that covers the pores inner surface and make the sample more stable to atmospheric oxygen and water solutions. If this step is bypassed, prolonged exposure render the surface prone to oxidation by atmospheric oxygen and promotes instability in the surface and it is undesirable for many applications.

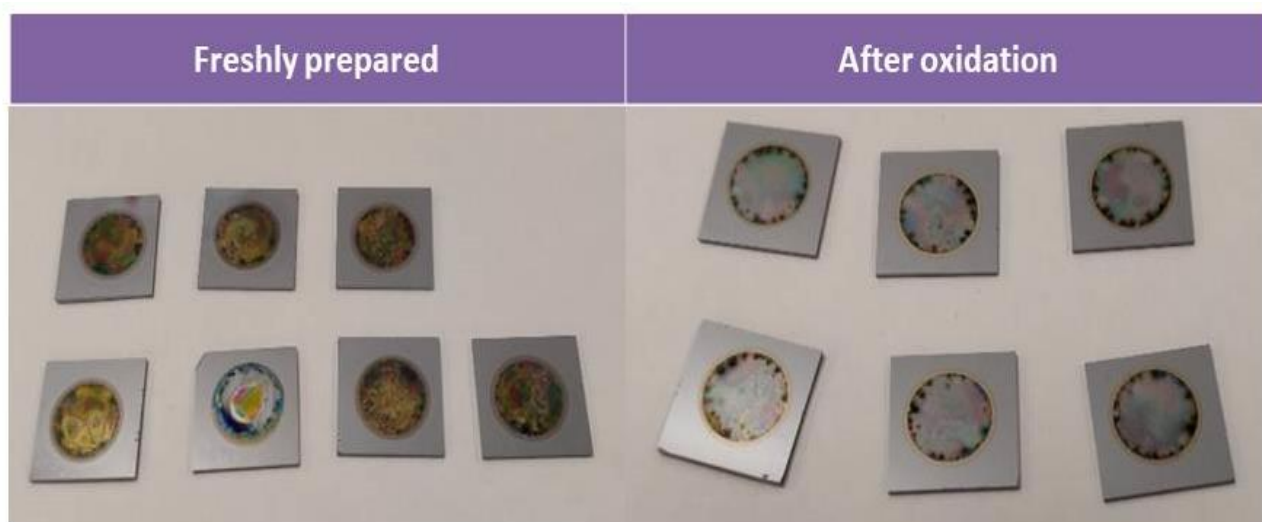


**Figure 40.** Porous silicon samples before and after the thermal oxidation.

Before use, samples were also characterized through microscope. An exhaustive example of sample surface used at Nanophotonic Technology Center of Valencia is shown in Figure 41.

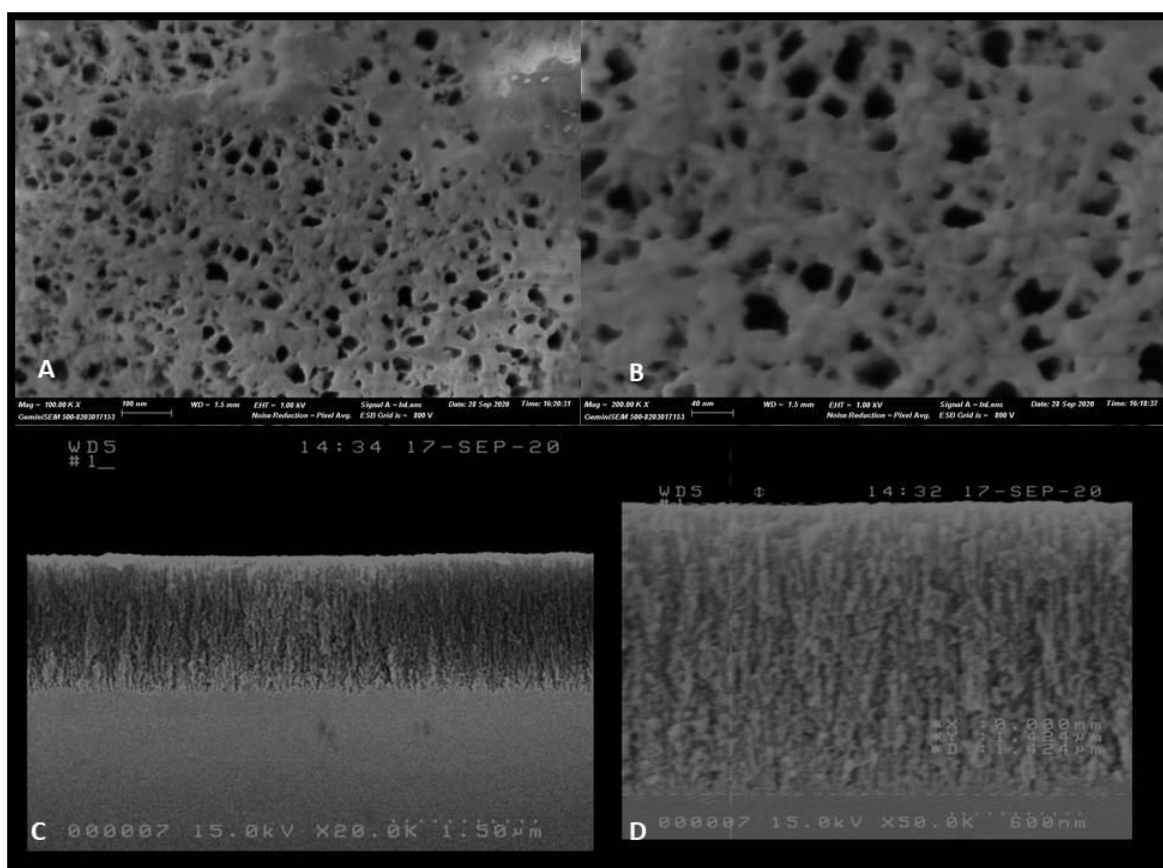


**Figure 41.** PSi view at SEM microscope. **A** and **B**: two images from the top of the sample. **C** and **D**: two image taken from the side of sample. The top view shows the pores that characterize the Porous silicon while the side view show the pores layers in thickness.

For the biosensor assembly, protein was firstly flowed into flow chambers for 30 minutes to perform the adsorption onto silicon surface. Tris Buffer 50 mM was flowed at the beginning and after protein flow, to create the baseline. Figure 42 shows that the adsorption occurred, because resonance shift took place. The resonance shift (from 0 to 4 nm approximately) demonstrate that protein was entered into Porous silicon surface.

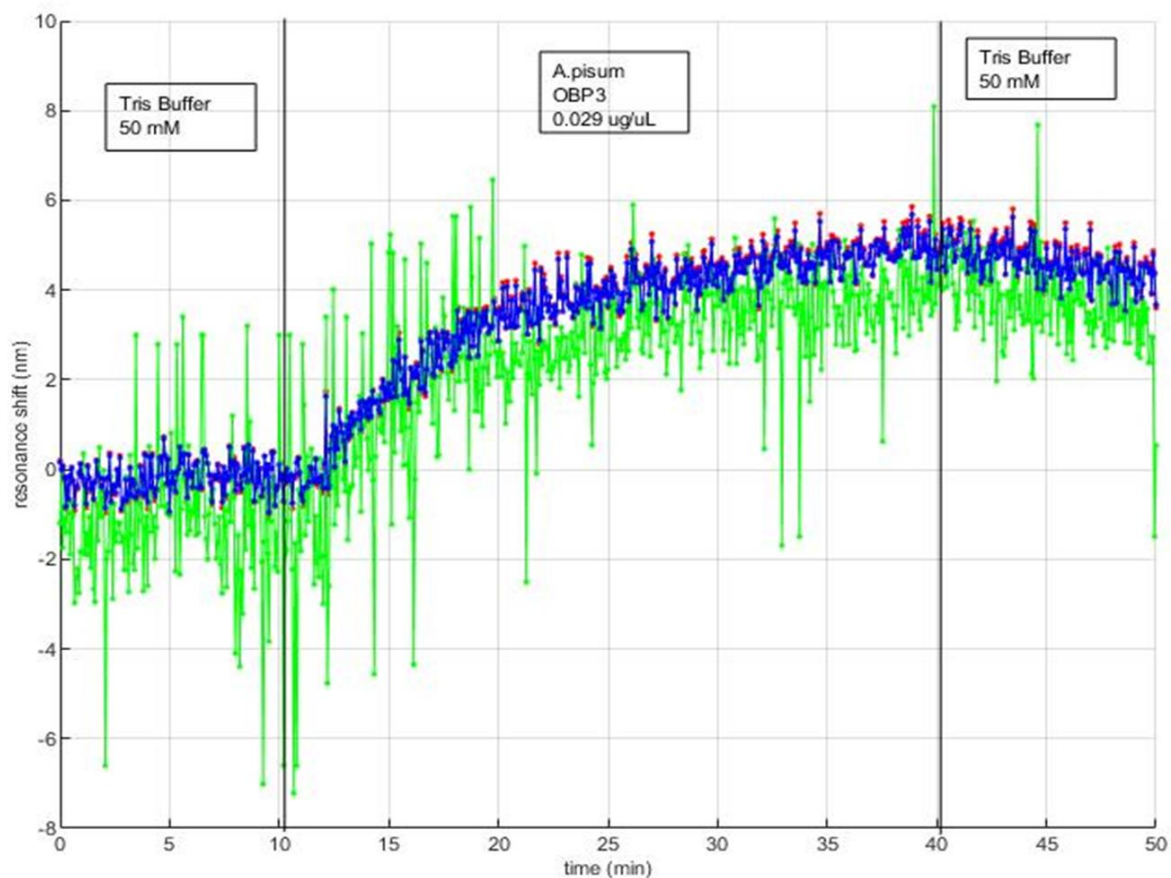


**Figure 42.** Resonance shift occurred during *Apis*OBP3 flowing. The behaviour of resonance shift shows the protein is inside the pores of silicon wafer.

The second step of biosensor assembly (Figure 43) was flowing the analyte (farnesol) to verify if a change of refractive index occurred. This is the biorecognition step. In theory, the protein was inside the pores and if it is able to bind analyte, a change in refractive index occurs also in this step. For this first experiment, 100  $\mu$ M farnesol (diluted in methanol) was used, just to be sure that the concentration was not a limiting factor. Methanol was used to dilute farnesol because the hydrophobic nature of terpene.

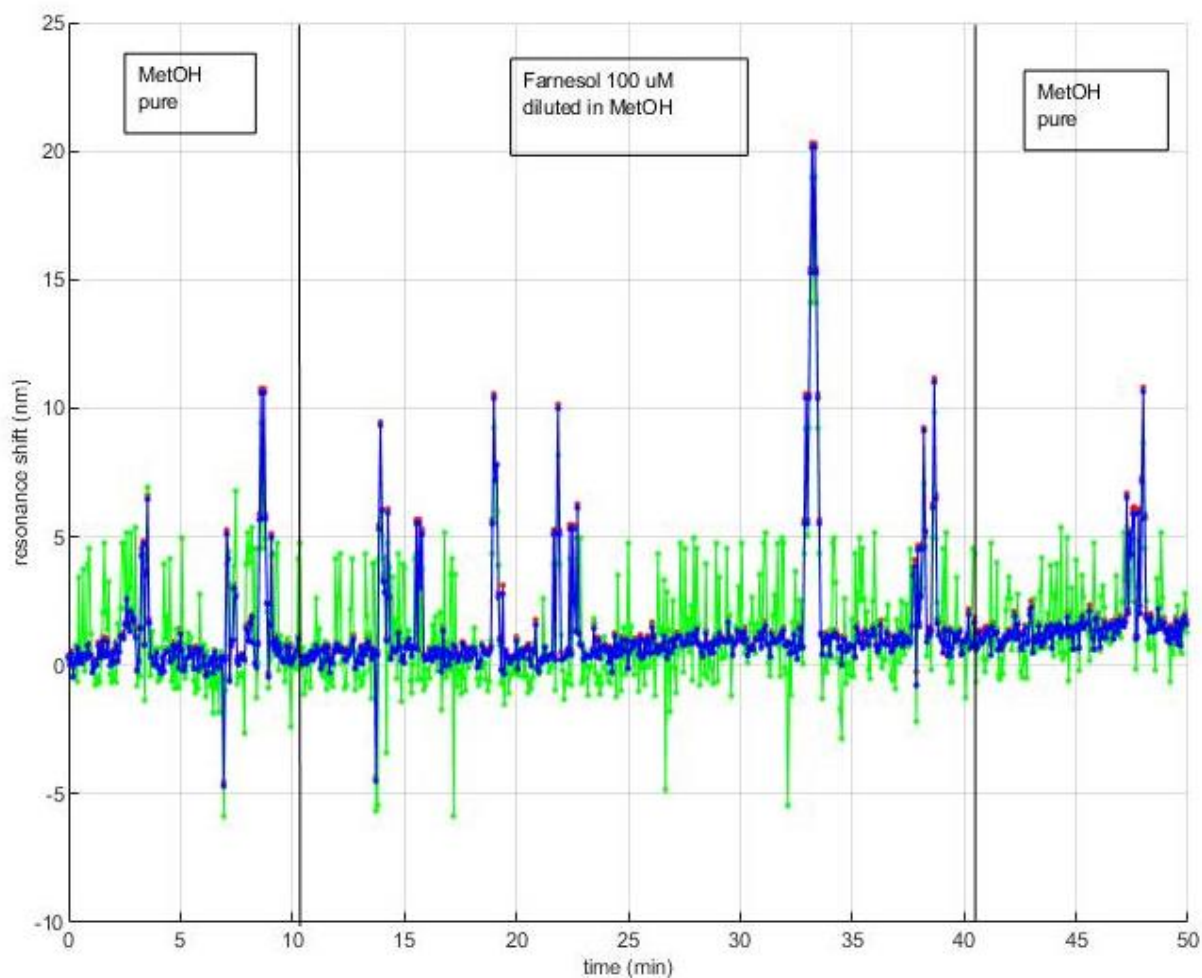


**Figure 43.** Sensing step. After protein flowing, the sensing step was performed using 100  $\mu\text{M}$  farnesol. An increase of refractive index (RI) occurred during farnesol flowing (from 0 to 1 approximately). In particular, the RI increase was observed 10 minutes after the start of farnesol flowing

Figure 43 showed that a change of refractive index occurs when farnesol flowed but this change seems to be stable even during the next methanol step.

It could be due to saturation of protein (higher concentration of analyte) or it could be an artefact caused by the adsorption of analyte by PSi surface.

To understand better the dynamics of the interaction among all the components, two negative controls were performed, in the same experiment, before protein flowing, using the same Porous silicon surface. The first negative control was based on the flowing of 100  $\mu\text{M}$  farnesol and the second one on flowing 400  $\mu\text{M}$  farnesol. The second negative control was performed to clarify the effect of an higher farnesol concentration on Psi.

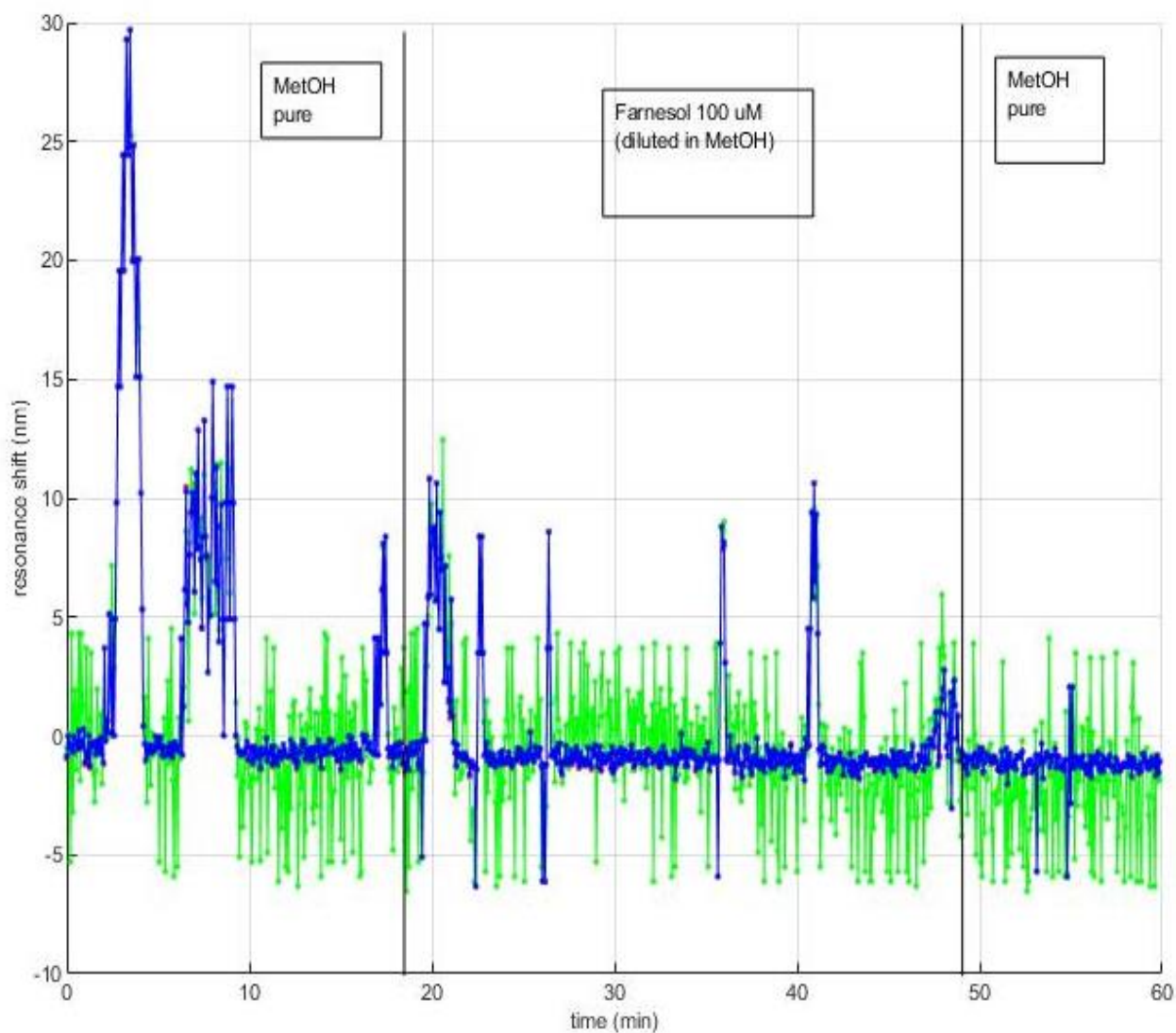


**Figure 44.** First negative control: the flowing step of 100  $\mu\text{M}$  farnesol. The baseline was created using methanol (Sigma-Aldrich, 34860) because farnesol (Sigma-Aldrich, 43348) was previous diluted in this alcohol. The spectrum did not show an increase of refractive index (RI) when the farnesol flowed. An increase of RI, happens when a different substance interact with the surface.

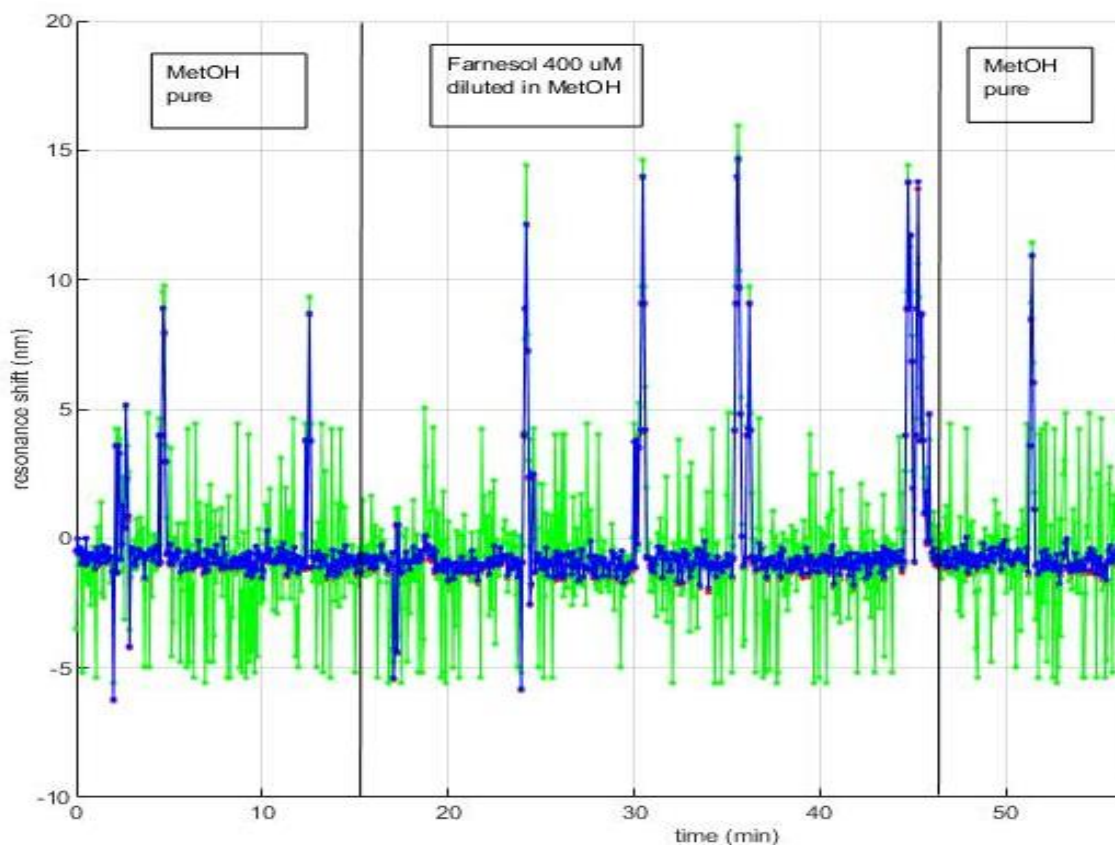


**Figure 45.** Second negative control: the flowing step of 400  $\mu\text{M}$  farnesol. The baseline was created using methanol (Sigma-Aldrich, 34860) because farnesol (Sigma-Aldrich, 43348) was previous diluted in this alcohol. The spectrum did not show an increase of refractive index (RI) when the farnesol flowed.

Both first (Figure 44) and second (Figure 45) negative control confirmed the non-influence of farnesol on the silicon surface. Both negative control spectra showed a different behaviour comparing them to the sensing spectrum. This difference allows us to deduce that the sensing took place.

In a following experiment (Figure 46 – 48) , different concentration of farnesol were flowed in the sensing step. This experiment was necessary as a preliminary test for sensor sensitivity. It is important to know which is the minimal concentration of terpene that biosensor can detect. In a first experiment, farnesol concentrations were selected in the range between 10  $\mu\text{M}$  and 400  $\mu\text{M}$ . The lower concentration can be detected by the system (Figure 46). In fact, an increase of RI seemed to occur in this sensing step (starting from the lower concentration) in contrast to what happened in the negative control showed in Figure 48 where the highest concentration did not provoke an increase of RI. The problem with this experiment relies on the use of methanol as diluent because it could affect the property of surface, influencing the results. Moreover methanol could affect the protein structure even if the role of methanol and

other organic solvent on protein folding is actually controversial (Yu et al., 2016).

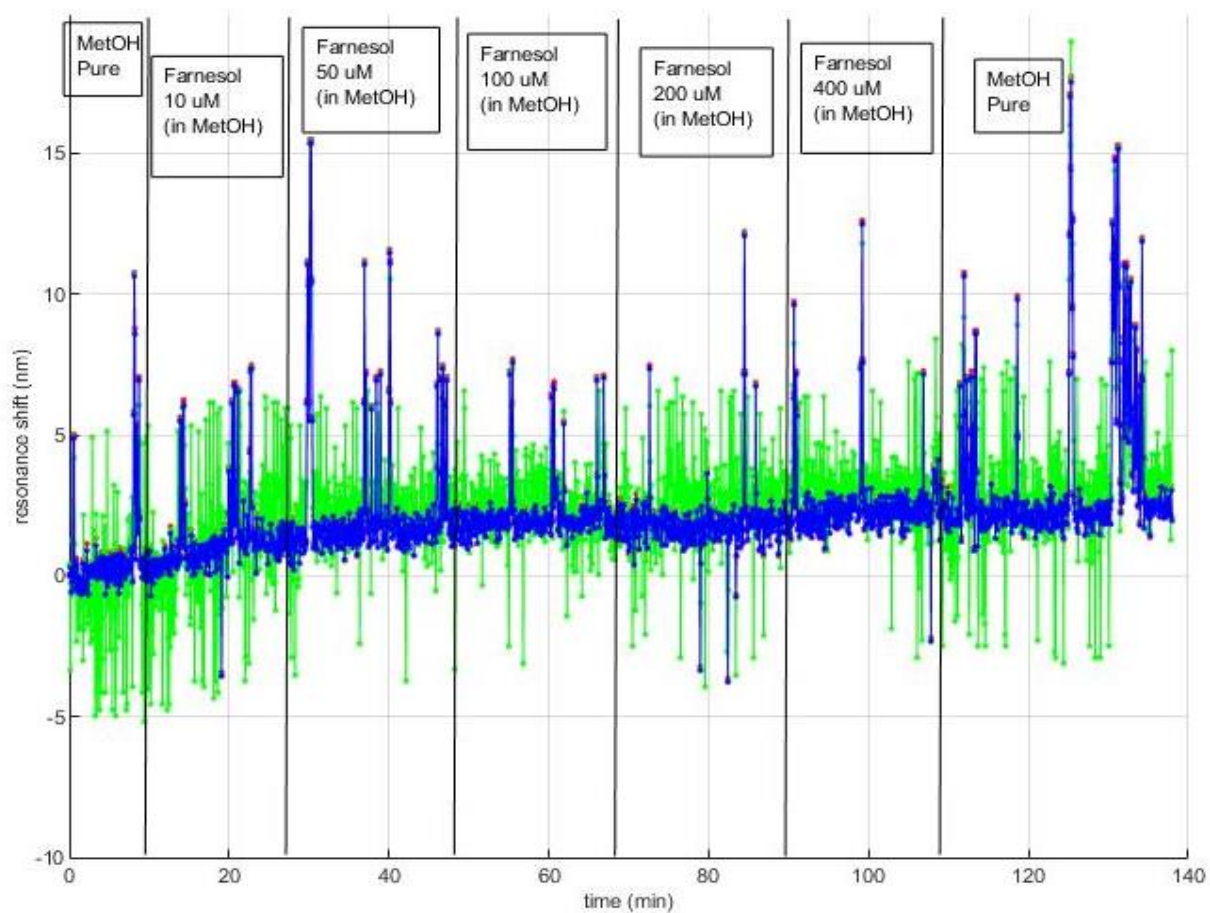


**Figure 46.** Sensing step. The spectrum shows an increase of refractive index during the flowing of all farnesol concentration tested.

The entrance of protein into Porous silicon surface, also in this case, was evaluated following the spectrum during protein flowing. This spectrum is shown in Figure 47.

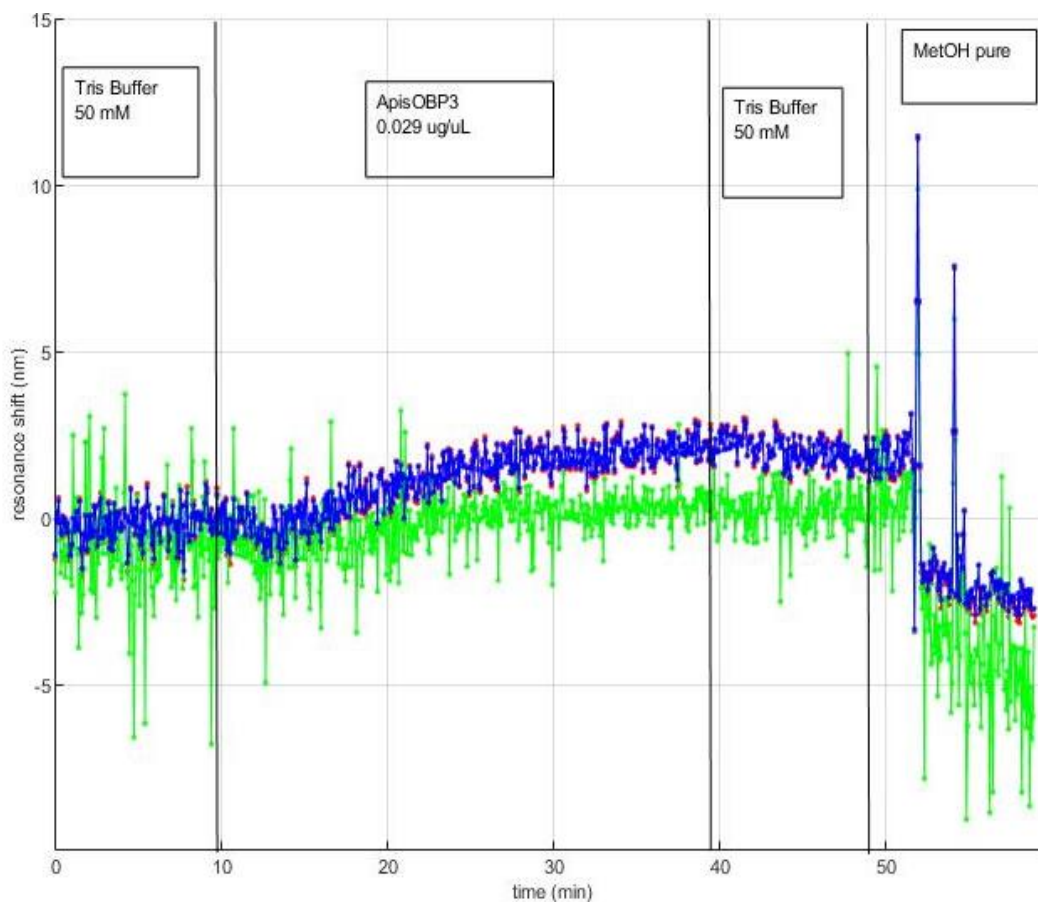


**Figure 47.** Protein adsorption step. The protein seems to be entered into Psi because there was an increase of refractive index during *ApisOBP3* flowing and in the following step (Tris Buffer flowing) this change remained similar (the protein had modified the original surface). The last flowing step was methanol flowing. It was necessary to create a baseline for the next step that was sensing step.

Moreover, an internal negative control was used to verify the effect of farnesol/methanol on surface (Figure 48). There was not an increase of refractive index, confirming that in the sensing step the increase could be due to the interaction between protein and farnesol.



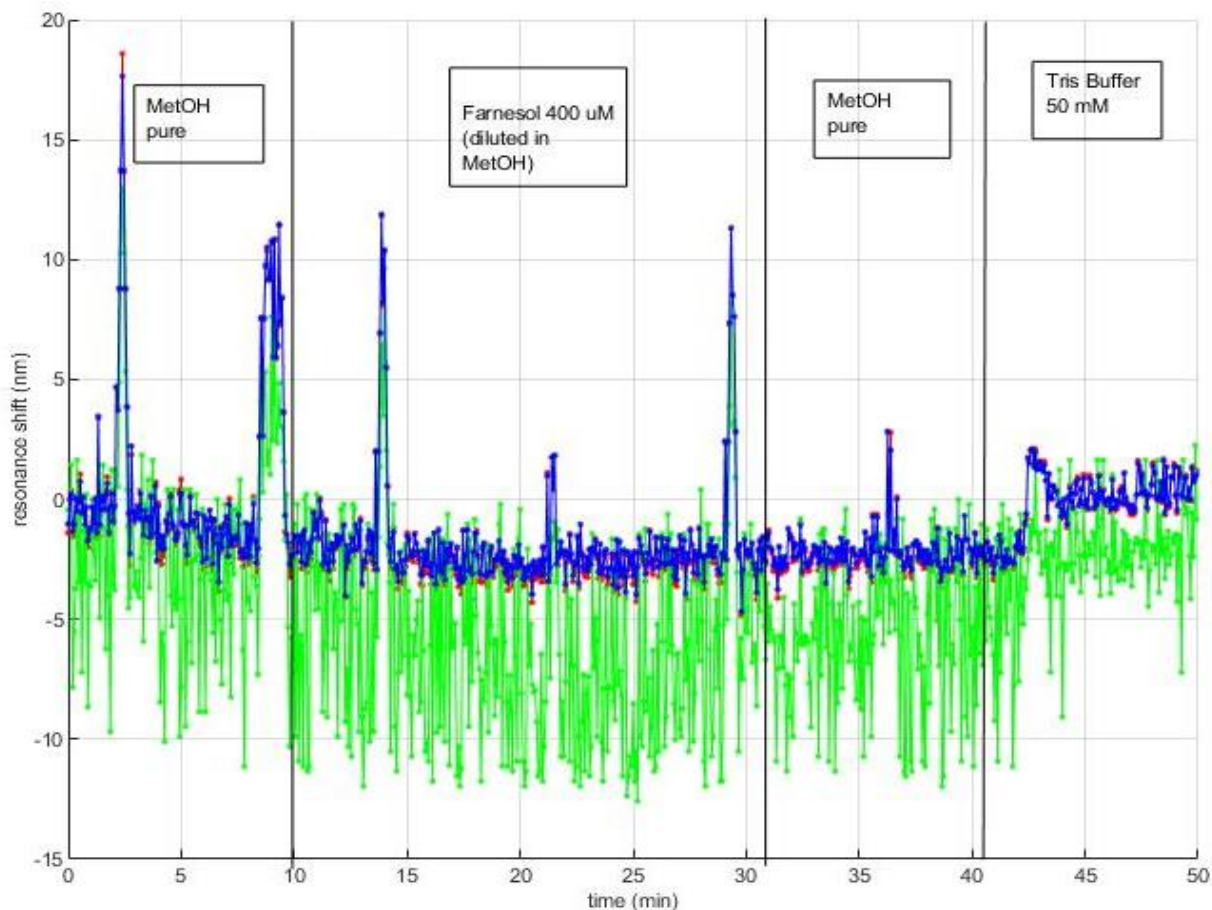


**Figure 48.** Negative control. Flowing the higher farnesol concentration, an increase of refractive index did not occur. Moreover, the spectrum behaviour seems to be very different from the sensing step spectrum.

Nevertheless, a calibration step was performed before starting with this last experiment. The reason of this additional step (made before the real experiment) was due to the fact that in the first experiment (Figures 42 – 45) bubbles were observed in all steps involving methanol and they were not in the protein flowing step where methanol was not used.

Figure 49 shows that methanol interacts with porous silicon surface in a peculiar way.

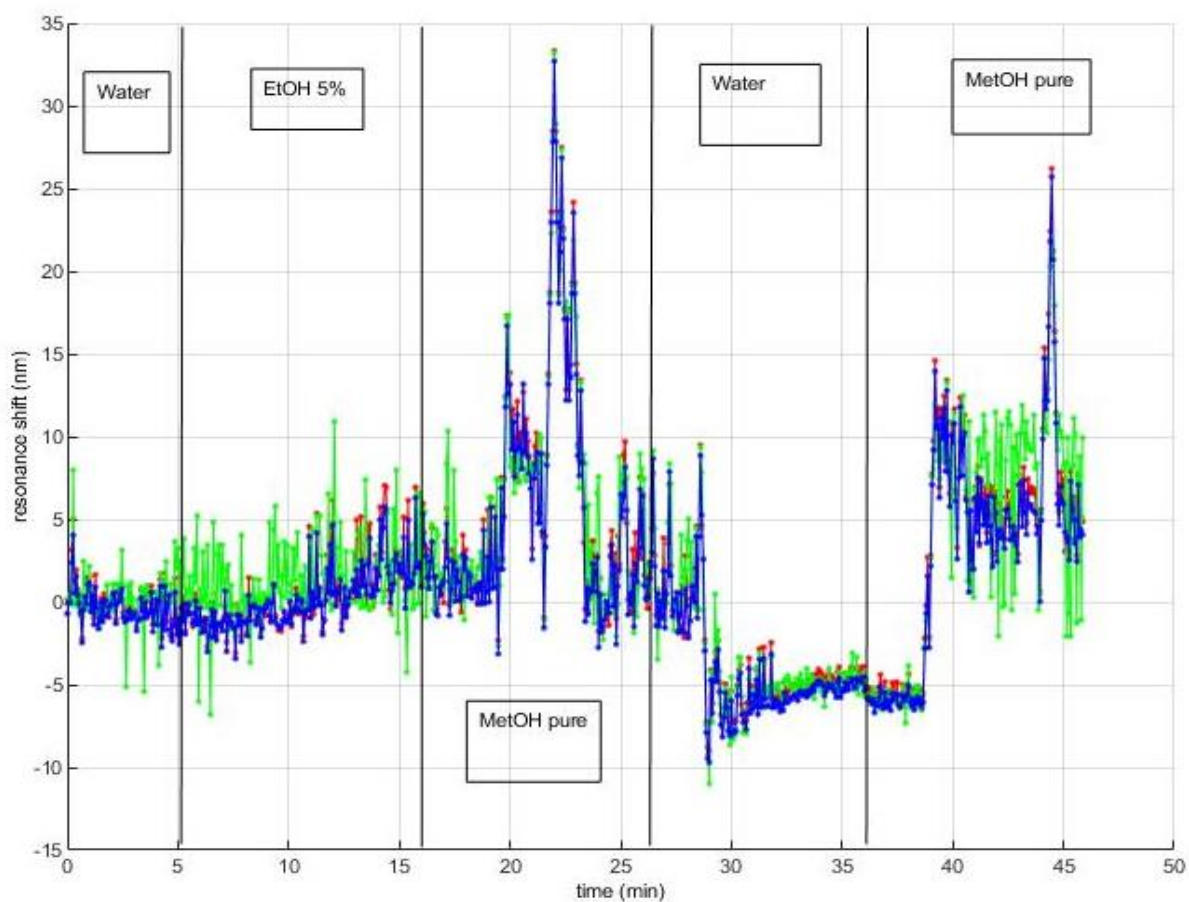


**Figure 49.** Calibration step. This step was useful to calculate sensor silicon surface sensitivity (for this purpose, Ethanol 5% was flowed) but also to understand the peculiar behaviour of Methanol. It is also noteworthy that when water is flowed after methanol there is a change of refractive index of approximately  $-5$ .

The peculiar behaviour of Methanol on Silicon surface has led to change the diluent of terpene. Ethanol was used instead Methanol.

A first attempt was conducted using  $100 \mu\text{M}$  farnesol diluted in Ethanol. All steps of experiment are showed in Figures 50 – 52. Unfortunately, this attempt was not successful.

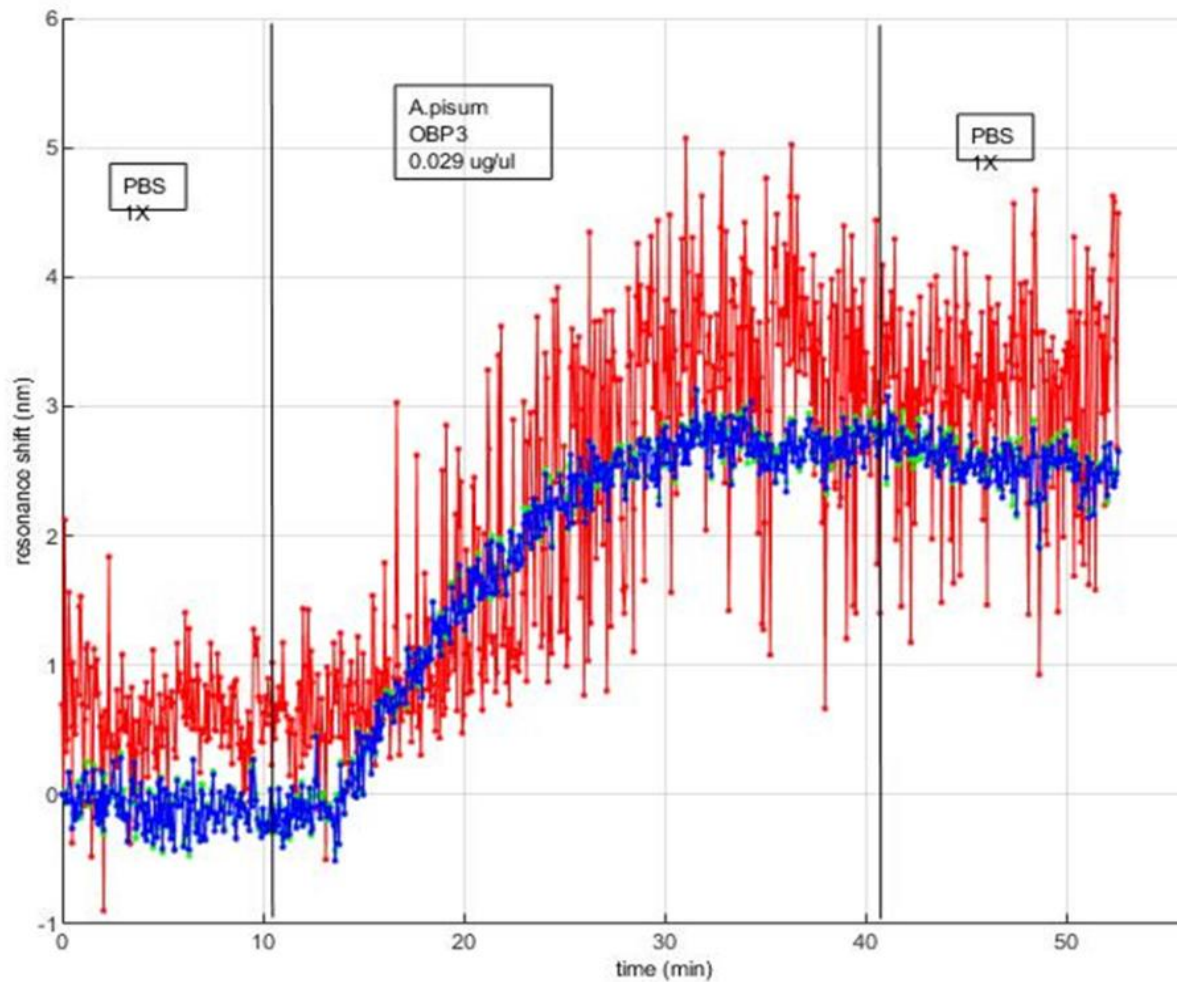


**Figure 50.** Resonance shift occurred during *Apis*OBP3 flowing. The behaviour of resonance shift shows the protein is inside the porous of silicon wafer. In this experiment, PBS1X was used to create a baseline (instead of Tris Buffer) to compare the effect of these two buffer on final results. In fact, the common buffer used at Nanophotonic Technology center, for biosensor assembly is PBS. The spectrum showed here, demonstrate that the different buffer do not influence, first of all, the entrance of protein. The amplitude of shift in this case is lower than the shift in Figure 42 but it is similar to shift in Figure 45. Despite the difference in amplitude, all spectra show the same behaviour typical of protein entrance. It is possible to deduce that the variability in amplitude is due to the porous silicon surface.

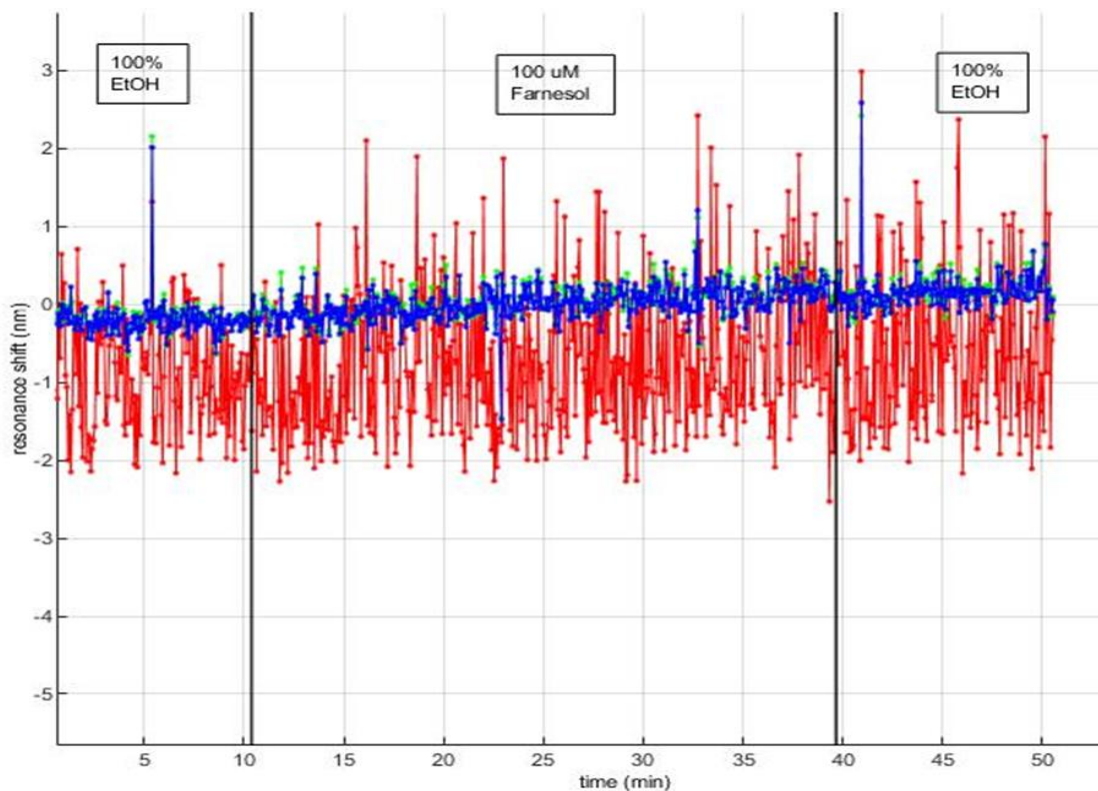


**Figure 51.** Sensing step. The spectrum shows a very little increase of refractive index during the farnesol flowing (from -0.5 to 0.5 approximately). However, also in this case, the behaviour of spectrum seems to indicate a saturation of protein.

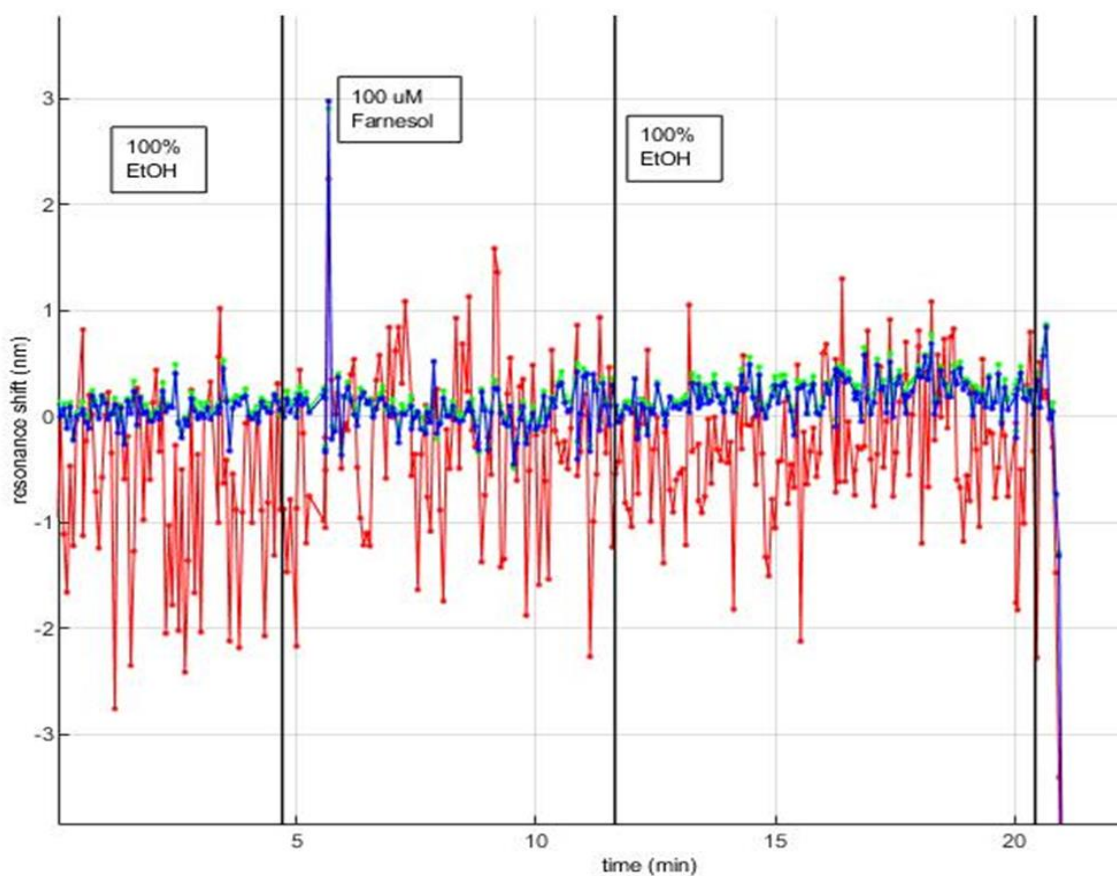


**Figure 52.** Negative control. This is the negative control realized flowing 100  $\mu$ M farnesol (diluted in Ethanol) before the protein adsorption step. This negative control is not completely

useful because the farnesol flowing time is less than one in sensing step. Hence, spectra are not completely comparable. However, the shift during farnesol seems to be approximately from 0 to 0.5 (less than sensing step).

This last experiment was not useful because the difference between negative control and sensing step is not really clear. Hence is not possible to conclude that a protein/analyte binding event occurred.

Another attempt was performed using different concentrations of farnesol (like experiment shows in Figures 46 - 48) diluted in pure ethanol, during the sensing step. Moreover in this case, the negative control spectrum (Figure 53) was different compared to sensing step spectrum (Figure 55). Nevertheless, the sensing step spectrum is difficult to understand because the spectrum for each concentration seemed to be very different from what was expected. For example, the shift corresponding to 50  $\mu\text{M}$  was a “negative” shift. There was not the increase due to the binding event. The only segment of spectrum consistent with the expectation were 10  $\mu\text{M}$  and 200  $\mu\text{M}$ .

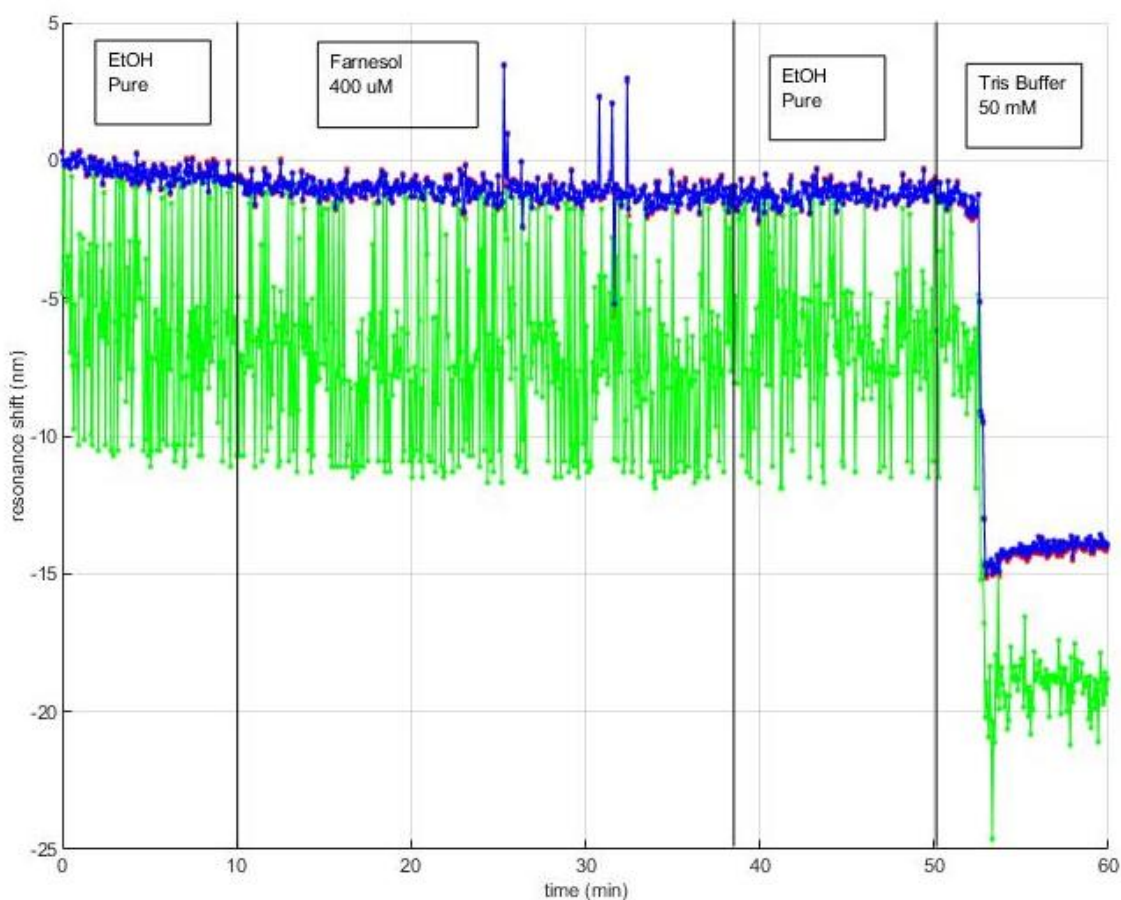


**Figure 53.** Negative control based on flowing 400  $\mu\text{M}$  farnesol diluted in ethanol. The spectrum of this negative control shows the same behaviour of negative control in Figure 48. When farnesol was flowing, no increase of refractive index occurred.

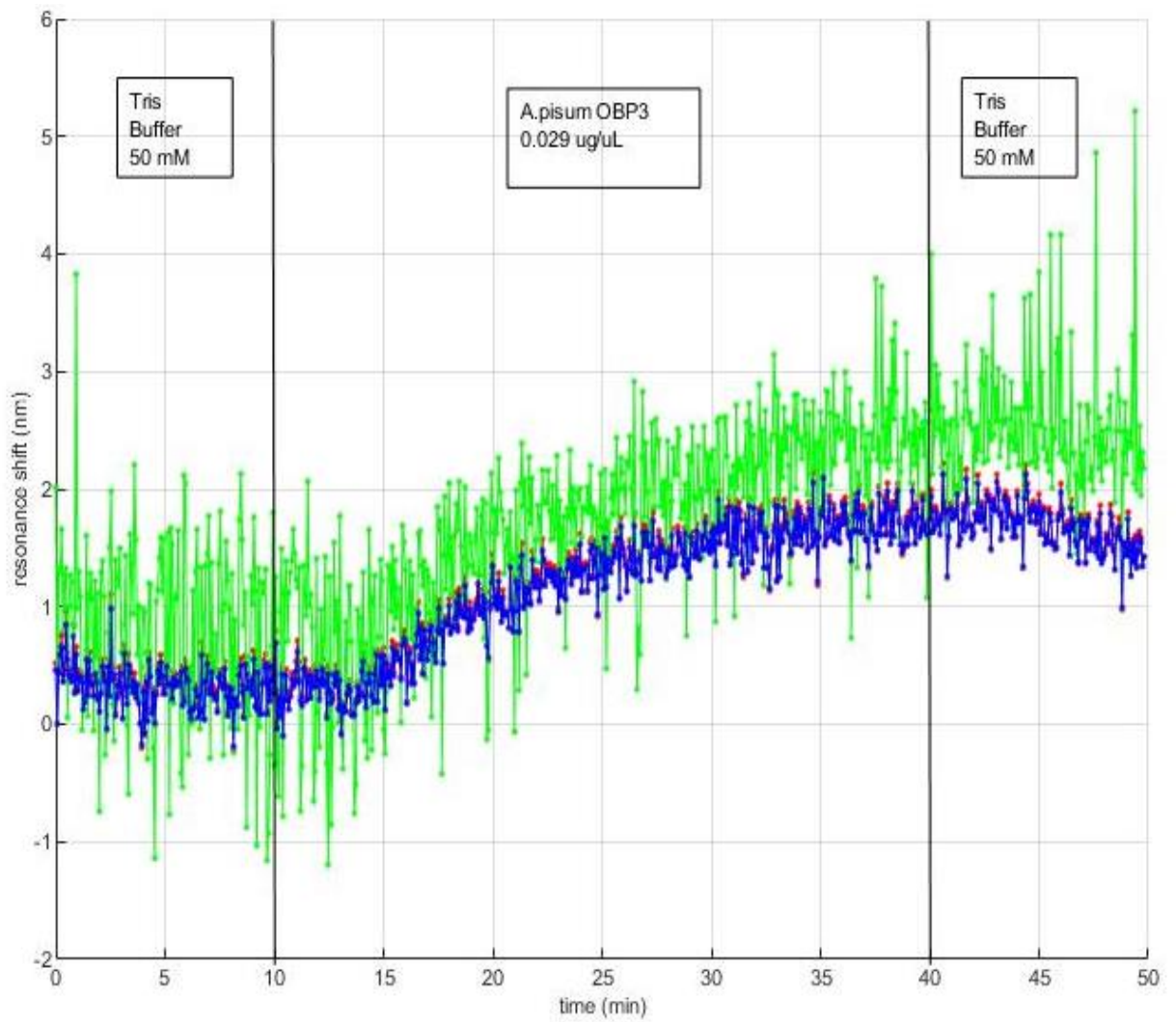


**Figure 54.** Protein adsorption. Also in this experiment, the spectrum related to protein adsorption is similar to previous ones. This confirm the entrance of protein in the pores.

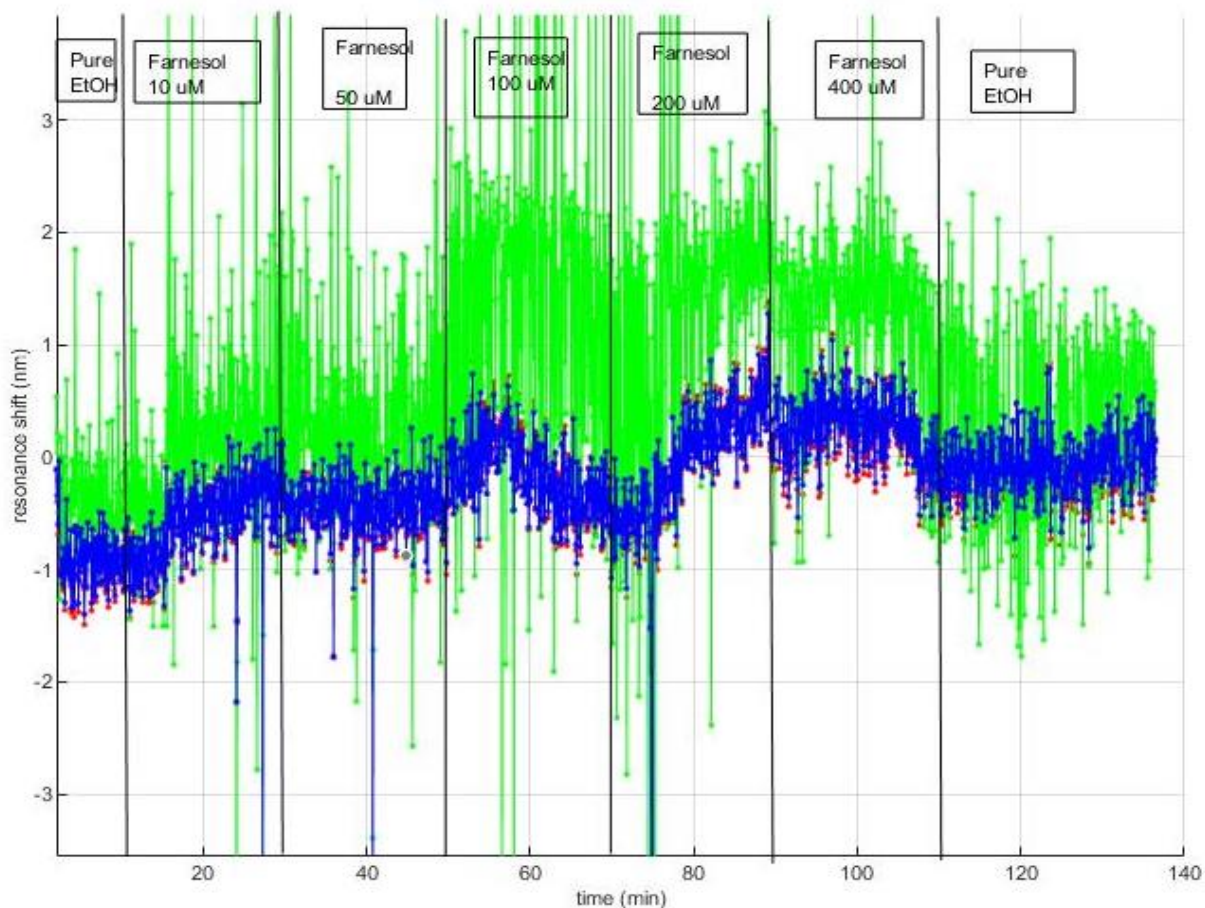


**Figure 55.** Sensing step. After protein flowing, the sensing step was performed using a range of farnesol concentration from 10  $\mu\text{M}$  to 400  $\mu\text{M}$ . All solution were prepared as serial dilution to minimize errors. An increase of refractive index (RI) occurred during the flowing of 10  $\mu\text{M}$  farnesol but the spectrum is not clear and showed a strange behaviour. The reason of this behaviour is not clear.

Actually more experiments are in progress at Nanophotonic Center of Valencia (Biophotonic unit), to investigate the reason why the sensing step do not happen correctly.

Indeed, despite the not clear results concerning the sensing step, P*Si* samples have proved to be optimum surface where introduce OBP.

Further experiments will concern an optimization of terpenes dilution.

## 4. DISCUSSION

Wine is very ancient alcoholic beverage and its history is dated to Prehistoric times. The most ancient proof (4100 B.C) of winemaking was founded in Armenia and it consists on the first winery in human society.

Vineyards and wine have always been an important part of human economy and culture and, at the date, they are important in national and international economies.

International wine trade has grown considerably in recent years, creating a more complex world market in which new producing countries (U.S.A., Australia, Chile) join the traditional ones (Italy, France, Spain).

World wine turnover is estimated to reach around 150 billion euro at the level of consumption and 60 billion concerning production.

On the other hand, wine exportations have a value of about 13 billion euros, making wine one of the most traded food products in international trade.

Considering these data, it is clear that it is necessary to introduce innovations within a traditional sector such as the wine industry.

Two important phenomena occur with the expansion of the market:

- An attempt of winemaker to improve his product to be more competitive in the market;
- An increase of wine falsification.

Wine fraud, in particular, is the most relevant plague in the word wine trade. The term fraud referred to wine means addition of low cost product (i.e juice) or chemical (i.e sweeteners) to confer some special feature to wine and put it in the market as valuable wine.

For example, in 1986, some Italian winemaking added methanol to wine describing it as PDO/DOC wine. This event provoked the death of consumers, wine market crash but also the consciousness of vulnerability of agro-food industries.

Concerning wine frauds, technology can be helpful to prevent them.

On the other hand, technology can help winemaker to monitor winemaking processes and improve his products concerning their quality (aroma, colours, sweetness).

Biosensors are examples of technology potentially helpful in winemaking.

This PhD Project, aimed to investigate how to develop a possible biosensor able to detect volatiles organic compounds that in wine are the major responsible of aroma (terpenes), with a look toward its application on wine of Basilicata region.

A biosensor is an analytical device based on 3 main components: biological receptor, transducer and electronics.



The selectivity and the specificity of biosensors rely mainly on biological receptor and for this reason the choice of the biological element is the most important.

First of all, an attempt to understand wine aroma was performed.

Wine is a very complex matrix and its aroma is due to several molecules but terpenes are the most relevant. In particular, aromatic terpenes, in wine, are only monoterpenes and sesquiterpenes.

Considering these data, aphids were the first source of biological element to use for biosensor development.

Aphids are naturally able to perceive terpene released by plants because of their phytophagous nature. In addition, different species of aphid use terpene as pheromone.

The common terpene in aphid alarm pheromone blend is  $\beta$ -farnesene, a sesquiterpene constituted by 3 consecutive isoprene units. It is a hydrocarbon lipid molecule. The  $\beta$ -farnesene is released by aphids as an alarm pheromone upon death to warn away other aphids. In *Acyrtosiphon pisum*,  $\beta$ -farnesene is the only alarm compound (Francis et al., 2005) but *Megoura viciae* synthesizes additional monoterpenes (Francis et al., 2005; Northey et al., 2016), including  $\alpha$ -pinene,  $\beta$ -pinene, and limonene.

To date, the perception of  $\beta$ -farnesene is known mediated by an odorant binding protein named OBP3 in both species. *Apis*OBP3 is also able to bind farnesol, a structural analogue of  $\beta$ -farnesene (Qiao et al., 2009); *Mvic*OBP3 is also able to bind limonene (Northey et al., 2016).

Farnesol and limonene are two typical wine terpenes.

Farnesol is a sesquiterpene, present in grape only in free form. It is the most representative terpenes in some grape variety such as white Muscat and Sangiovese (D'Onofrio, 2011). It confer to wine a floral aroma (rose) and it has a threshold of 20  $\mu\text{g/L}$  (Waterhouse et al., 2016). Limonene is a monoterpene present in wine such as Cabernet Sauvignon (Cheng et al., 2015) and in Muscat of Alexandria (Di Stefano, 2013) and it confer citrus aroma to wine.

Starting from this consideration both *Apis*OBP3 and *Mvic*OBP3 were obtain through recombinant procedure for their utilization in optical biosensor development to detect farnesol and limonene.

The affinity of these protein towards other terpenes was also tested *in silico* and *in vitro* with the purpose of verify they are able to bind some compound different from the already tested ones and investigate about their binding specificity.

*In silico* analysis relayed firstly on some structural consideration and comparison of *Apis*OBP3 and *Mvic*OBP3.

The three dimensional structure of each protein was obtained using I-TASSER software and

visualised using UCSF CHIMERA. Both proteins are composed by six  $\alpha$ -helices alternate to coil domains as classical insect OBPs. Then, the binding pocket of both was investigate to understand differences or similarity.

Using CASTp software the putative amino acids involved in the binding pocket formation were identified. This analysis was performed in order to understand how the ligand interacts with the protein and also to identify the correct strategy to immobilize them on silicon surface of the biosensor.

As *Apis*OBP3 and *Mvic*OBP3 share a high sequence identity (96%) (Bruno et al., 2018), the binding pocket results similar between the two proteins. They differ only for 2 amino acids, M42 e M60 (Section Results. Paragraph 3.6 Binding pocket analysis)

*Apis*OBP3 binding pocket is composed by 20 amino acids divided as follows:

- Hydrophobic: 14
- Hydrophilic: 3
- Basic: 3

*Mvic*OBP3 binding pocket is composed by 18 amino acids divided as follows:

- Hydrophobic: 12
- Hydrophilic: 3
- Basic: 3

The binding pockets share with each other also the position in the three dimensional structure. Most of them are localized in  $\alpha$ -helix domains excepting in  $\alpha$ -helix number 5. Moreover, Binding cavities seem to be located at the surface of proteins (Supplementary materials, Deepsite analysis) as occurs in most protein in nature (Nayal and Honing, 2006).

Comparing data obtain from CASTp and I TASSER software, it was possible to obtain other important information about binding pocket. In particular, Predicted Solvent Accessibility values referred to CASTp hypothetical binding pocket confirm their involvement in the formation of ligand cavity. I-TASSER predicting solvent accessibility values are regarded as a two element classification: exposed or buried and values range from 0 (buried residue) to 9 (highly exposed residue). All amino acids involved in binding pocket have values ranging from 0 and 4, confirming their involvement in the formation of ligand cavity in both OBPs.

The only residue, in both OBPs, with a high value of solvent accessibility is the arginine in position 1.

The three dimensional structure of each OBP was then used for docking of desired ligands.

Ligands were selected through a bibliographic approach and they are the most representative monoterpenes and sesquiterpenes in wines. Docking results allowed to select some terpenes, which should be tested *in vitro*. Using docking analyses, possible binding modes were

calculated for each complex OBP-terpene. In these virtual screening, terpenes (small organic compounds) are treated as possible ligands, and OBPs (target macromolecule) are treated as the receptor. In this case, energy scoring method was used to identify the most favourable binding modes of a given compound and then to rank the compounds. In detail, *in silico* analysis shows that for both *Apis*OBP3 and *Mvic*OBP3, energy values are negative for all compounds tested and for each of them the values are very similar. Only the complex OBP/ $\beta$  – caryophyllene shows a positive value of energy.

This result is important to speculate about binding pocket – ligand interaction. Indeed,  $\beta$  – caryophyllene is the only one terpene in the list that has a bicyclic structure, with a cyclobutane ring. Other terpenes that show an energy value near to the positive side are eucalyptol and linalool oxide, two epoxy monoterpenes.

The remaining terpenes show energy values comparable each other.

Correlating energy values of complexes to the structure of terpenes, it is interesting to speculate that:

- Epoxy terpenes (eucalyptol and linalool oxide) did not bind with good affinity aphid OBPs;
- Concerning cyclic terpenes, energy values are more negative regarding to carbon ring (limonene and  $\alpha$ -terpineol); terpenes with an heteroatom in the ring have a more positive energy value (rose oxide and nerol oxide);
- The length of linear chain could be involved in determining the affinity.

Concerning the latter point, it is interesting to note that energy value is higher for farnesol (12 carbon atoms) complexes than geraniol or nerol or citronellol (8 carbon atoms) or hotrienol (6 carbon atoms) complexes. This result is partially in agreement with results obtained by Qiao and colleagues (Qiao et al., 2009).

The last consideration is about energy values of farnesol complexes. For both *Apis*OBP3 and *Mvic*OBP3, a more negative energy value could be noted compared to  $\beta$ -farnesene/OBP complexes. Probably, the difference could be related to OH group at the end of farnesol (the two compound have the same chain length) that could be interact with the binding pocket.

The higher *in silico* affinity is in agreement with Sun et al., 2012.

Then, only complexes with energy values closer to energy value obtained using  $\beta$ -farnesene, were considered to perform *in vitro* assays.

For this reason, citronellol, geraniol and nerol were selected to be tested with *Apis*OBP3 (farnesol had already tested in Qiao et al. 2009); farnesol, nerol and geraniol were selected concerning *Mvic*OBP3 *in vitro* assays.

Unfortunately, these competitive binding assays did not work. Theoretically, these assays rely

on competition between a fluorescent probe and a selected ligand, resulting in a decrease a fluorescence if there is affinity between protein and ligand. In the competitive binding assays with *Apis*OBP3 and *Mvic*OBP3, an increase of fluorescence was observed even changing the concentration of probe. Therefore, results remained unsatisfactory but a possible explanation of this phenomenon can be found in recent articles that describe the formation of micelles that create an hydrophobic environment (like the binding pocket of protein) entrapping the probe and increasing the fluorescence.

The fluorescent approach has become the method of choice, being simple, rapid and requiring small amounts of proteins but recently some authors have showed, however, that there are criticisms about competitive fluorescent assays. The main problem is the reliability because of the strong dependence of fluorescence from the environment (Pelosi et al, 2018; Tan et al., 2019) such as pH or composition of buffer. Moreover, the nature of ligands used could be an affecting factor: some ligands such as long-chain fatty acids and other hydrophobic compounds can form micelles that encapsulate the probe thus generating additional fluorescence (Leal and Leal, 2015). Probably, the formation of micelles is the main reason of the unsuccessful experiments using terpenes. Indeed, all tested compounds are highly hydrophobic ( their logP values range from 2.16 of geraniol and nerol to 3.64 of farnesol).

However, another explanation of failure is the contemporary binding of fluorescent probe and ligand since the OBP binding pocket is so large (while the ligands are very small molecules) to accommodate them together and led them interacting with different regions in the core of protein (Tan et al. 2019).

This hypothesis has yet to be experimentally confirmed by scientific community but it is a plausible reason for the failure of competitive binding assays in this work, considering the involvement of only some amino acids in the formation of the most favourable protein-ligand complexes.

USCF CHIMERA visualization of OBP-terpene complexes (Results: Figure 36, Figure 37 and Figure 39) shows that not all residues of binding pocket are closer to the ligand (terpene) The distance is an essential factor concerning the interactions between a receptor and a ligand. The hypothesis is that amino acids far from terpene, could interact independently with fluorescent probe in the competitive assay. The visual analysis of three dimensional structure could be supported by the distance analysis of certain residues (Supplementary materials, Binding pocket residues distance). In fact, the distance between some OBP binding pocket residues and ligand was analysed using the USCF Chimera function “Show Distances to Nearby Residues” revealing that only some protein residues are spatially close to ligand atom (distance values are less than 4 Å). Distance between other binding pocket residues were

calculate with the function “Structure Measurement” and the values obtained were higher than 5 Å. The distance analysis is important to be considered because all interaction (hydrophobic or Van der Waals interaction, Hydrogen bonds) involved in ligand binding event are influenced by the distance.

In particular, comparing binding complexes formed by *Apis*OBP3/*Mvic*OBP3 and each terpene, it is emerged that residues L48, L60, L64, W68, W71, L08, L112 are far from ligand structure. Moreover, considering the surface images of OBPs and their complexes with terpenes (Supplementary materials, OBPs and OBP-ligand surface analysis), it is plausible to speculate that there is a difference in binding pocket structures due to the only two different amino acids in proteins mature form. Indeed, the three dimensional structure of *Apis*OBP3 seems to have a binding pocket more deep and having a channel that allows the ligand entry. *Mvic*OBP3 pocket, instead, is more flat and it could influence the accommodation of ligand. Moreover, considering the distance between ligand and binding pocket amino acids, *Mvic*OBP3 seems to interact mostly with the residues more exposed to surface rather than those buried.

The shape and the extension of the protein surface binding pocket dictates what interactions are possible with other macromolecules (Coleman and Sharp, 2010) but defining discrete pockets or possible interaction sites remains difficult.

Hence, other bioinformatics studies are needed to investigate the nature of the binding pocket and moreover these hypotheses will be supported by experimental approaches such as mutagenesis procedure, to better understand the role of each binding pocket residue in the interaction with ligand. The understanding of binding pocket will be functional to increase the specificity and selectivity of biosensor.

*Apis*OBP9 was also analysed concerning its structure, binding pocket and *in silico* affinity towards terpenes.

First of all, I-TASSER results show a different  $\alpha$ -helix domain pattern for *Apis*OBP9 (Supplementary materials, OBPs additional information). It shows shorter helix domains than *Apis*OBP3 and *Mvic*OBP3 with an increase of total number (the shortest is made by only 2 amino acids and the total number is 9, instead 6). Indeed, *Apis*OBP9 is classified as Plus – C OBP because of the presence of 8 cysteine residues.

Molecular docking simulations shows that *Apis*OBP9 has the same binding potential of *Apis*OBP3 and *Mvic*OBP3. Indeed, even if complexes energy values are a little lower than corresponding *Apis*OBP3/*Mvic*OBP3 complexes, the variation is the same according to terpene class (linear, cyclic or epoxy terpenes). Furthermore, it is interesting to observe a higher value of *Apis*OBP9/farnesol complex compared to *Apis*OBP9/ $\beta$ - farnesene, like

*Apis*OBP3 and *Mvic*OBP3. In general, we can assume that the introduction of a hydroxyl groups probably increase the possibility of interaction between ligand and protein, resulting in a more stable complex.

Analysing the distance between ligands atoms and binding pocket residues, also in *Apis*OBP9 only some residues have the right distance to interact with ligand.

The *Apis*OBP9 binding pocket residues closer to the ligand are I40, T41, Q42, A43, K44, E108, I113, F116. Moreover, in the complex OBP9/farnesol, another residue near to ligand (in the case of farnesol) is Q109. Probably the glutamine (with its NH<sub>2</sub> residue) interact with the double bound at the end of farnesol molecule (because of their closeness), getting stronger the interaction (dipole –  $\pi$  interaction).

In *Apis*OBP3 and *Mvic*OBP3 as well, another amino acid which is not part of binding pocket, is closer to the ligand (farnesol): A106. Probably it increases the hydrophobicity of binding pocket and it allows a better interaction of farnesol with OBPs.

These considerations could explain why the *in silico* energy values of OBP/farnesol complexes (regarding *Apis*OBP3, *Apis*OBP9 and *Mvic*OBP3) are higher than other terpenes.

Also, as regard *Apis*OBP9, Predicted Solvent Accessibility (PSA) values were analysed and also in this case the amino acids involved in binding pocket have PSA values ranging from 0 and 4, confirming their involvement in the formation of ligand cavity in this OBP.

*Apis*OBP9 binding pocket composition is as follows:

- Hydrophobic: 24
- Hydrophilic: 11
- Basic: 4
- Acid: 2

In *Apis*OBP9 binding pocket, amino acid number is higher than the other two proteins analysed in this work, with a number of 41 amino acids in total. Moreover, *Apis*OBP9 binding pocket shows a lower hydrophobic/hydrophilic amino acid ratio and the presence of 2 acidic amino acid (glutamate residues). Probably, these characteristics affect the binding affinity. In fact, hydrophobicity is one of the most important feature of binding site (Lijnzaad et al., 1996; Young et al., 1994).

After bioinformatics investigations, OBPs were used to realize optical biosensors in collaboration with Nanophotonic Technology Center of Valencia.

Optical biosensors are based on a change in optical propriety and in our case the change of refractive index. The surfaces used to assembly the device are Porous Silicon that are characterized by ease fabrication, highly tunable optical proprieties and biocompatibility (Karbassian, 2018).

The first attempt to realize an optical biosensor was conducted using *Apis*OBP3 and farnesol. It was necessary use this combination of protein/terpene as first couple because the binding between this two component was already detected (Sun et al., 2012).

They were used to verify the feasibility of this kind of biosensor and to optimize the assembly protocol. In fact, terpenes are very small molecules and the most important issue was about the possibility that there was not a visible change of refractive index.

The methods selected for protein entry in Porous Silicon surfaces was absorption. This procedure has the disadvantage of not permanent link of protein toward the surface but it has the advantage to allow the protein to maintain its three-dimensional structure. This is important for the correct binding with the analyte. The adsorption was selected also because it was the most appropriate technique because of its compatibility with the Tris Buffer where recombinant proteins were dissolved. In fact, the immobilisation with the classical coupling agent (ECD/NHS) was avoid because it is not totally compatible with the Tris Buffer, according to manufacture protocol.

A biosensor assembly attempt (Figure 42 – 45) was conducted using two negative control and methanol as terpenes diluent (an organic solvent was necessary because of terpene water insoluble nature). Interestingly, using methanol as diluent of terpenes a lot of bubbles appeared during analysis, only in those steps that require the use of this reagent. Probably, it is due to the reactivity of methanol onto the porous silicon surface and its adsorption mechanism (Glass et al., 1995; Miotto et al., 2004). Bubbles were present both in negative controls and in sensing step and they seem to not interfere with data evaluation because of the spectra. In fact, the negative control spectra are very different from sensing step spectra: an increase of refractive index (RI) was present only in sensing step. Just to be sure that the farnesol is not able to interact with porous silicon, a second negative control was used and also in this case, the spectrum did not show an increase of RI. This is important because it suggest that farnesol did not interact with surface even if there is an increase of concentration. In a following experiment, different concentrations of farnesol were flowed in the sensing step. This experiment was necessary as preliminary test for sensor sensitivity and to verify if the protocol adopted was optimal. Farnesol concentrations were selected in the range between 10  $\mu$ M and 400  $\mu$ M. The two extremes were selected because the lower concentration is in the range of ligand concentration generally used in competitive binding assay and the highest is derived from a preliminary test conducted at the Nanophotonic Technology Center of Valencia.

Results show that a possible binding between protein and farnesol occurred but there are doubts about the role of methanol on the surface. Indeed, in the calibration step (Figure 49),

something change when water is flowed after methanol. Ideally, when optical sensing is used, it is necessary to create a baseline to visualize the change in refractive index. In the calibration step, the baseline is created with water. When a solution is flowed after the water, a shift occurs because of the different nature of chemical composition. Subsequently, when water is flowed again the value returns to the initial one. In this case (Figure 49), the value did not return to baseline but it decreased by 5 (from 0 to -5 nm). An explanation could be that methanol could affect the superficial tension which means that water can go deeper into pore of silicon surface.

For this reason, an attempt to change the terpene diluent was performed. Especially, ethanol was used as new diluent. The choice of ethanol instead methanol could be justified by:

- Ethanol has been already studied concerning its reactivity on Psi (Garcia-Ruperez at al., 2010) and it is used generally to calculate the sensitivity of surface.
- Ethanol is considered an important matrix component that has physicochemical effects on other volatile compounds (Villamor and Ross, 2013); it acts as solubiliser of aroma compounds: the removal of ethanol from wine provokes the removal of a large quantity of chemical related to flavours ( Longo et al., 2015);

In view of the above, ethanol seemed to be a good and appropriated organic solvent to use for the biosensor design, instead methanol.

Anyway, at the beginning, methanol has been chosen because it is the most used alcohol to dilute volatile compounds, including the stock in competitive binding assay.

Therefore, the purpose is to understand what is the better protocol to assemble optical biosensors OBPs based, comparing results achieve using methanol and those using ethanol.

Unfortunately, also using ethanol as diluent, it was not possible to see a good signal in the sensing step (Figure 55).

In all experiments, an increase of refractive index occurred in the sensing step while it did not happen in all negative controls (the spectrum decreases or is similar to baseline when farnesol flowed, before protein adsorption). This result is encouraging but it is not possible to say for sure that the signal is due to the interaction between protein and farnesol. The increase of RI could be due to the physico-chemical modifications of porous silicon surface after protein adsorption.

Further experiments are necessary to clarify this point and optimize, in particular, the sensing step.

Despite the bad results in the sensing steps, these experiments confirm that Porous Silicon are good surface where introduce OBP. Indeed, in all attempts, the protein adsorption was successful. The success of protein adsorption was related also to the method used for the



oxidation. In a performed experiment which is not shown in this thesis, the oxidation methods were changed but the protein did not enter into pores, confirming the necessity to standardize and optimize a protocol for optical biosensor assembly.

## 5. CONCLUSION AND FUTURE PROSPECTIVE

The aim of this PhD project was the research and development of possible biosensors to be used in oenological field, particularly, to detect volatile organic compounds, such as terpenes, in wine. For this reason, the first attempt was to understand what kind of biological elements could be used. The better option was the use of aphids Odorant Binding Proteins (*Apis*OBP3, *Apis*OBP7, *Apis*OBP9, *Mvic*OBP3) because of the ability of these insect to perceive a terpene called  $\beta$  - farnesene. Concerning these proteins, bioinformatics analyses were carried out in order to better understand the binding pocket features of each protein and to highlight what amino acids could be essential in the ligand binding. Obviously, this study was only theoretical and, in the future, experimental data must be collected such as site specific mutagenesis data.

Subsequently, the idea was to use aphids OBPs to assembly an optical biosensor and verify protein behaviour in presence of ligands. A first attempt to realize a biosensor was made using *Apis*OBP3 (as bioreceptor) and farnesol (as analyte to detect). During the period abroad at Nanophotonic Technology Center in Valencia, Spain, several attempts were made to optimize the protocol of biosensor assembly. Actually, results are encouraging but more experiments are needed and they are already in progress.

This PhD research represents in its totality an attempt to introduce an innovation in one of the most ancient sector in economy. The purpose was not easy because of the complexity of wine aroma, a field that has been a challenge to wine researchers for the past 70 years.

The development of innovative devices able to monitoring chemicals that confer wine its peculiar aroma could contribute to an improvement of product organoleptic quality and winemaking procedure, too.

For example, a biosensor able to detect farnesol could be useful during winemaking.

Farnesol was found in beers and wines. In this last one beverage is responsible of sweet, floral (rose) odours. Detect and quantify this molecule could be interesting because farnesol has chemopreventative, antitumor, and antibacteria properties, with controversial allergic effects (Joo and Jetten, 2010; Kromidas et al., 2006).

Moreover, winemaking techniques (in particular yeast used during fermentation) affect the concentration of terpenes mainly concerning sesquiterpenes (as farnesol), producing themselves terpenes (Carrau et al., 2008).

Hence, the ability to alter the composition of sesquiterpenes in wine by winemaking techniques would allow winemakers to make wine with particular attributes. For example, a wine with a higher/lower concentration of farnesol. This concept is also important considering

the existence of non-aromatic grape varieties (like Aglianico del Vulture), characterized by a lower concentration of free aromas (consequently not detectable during tasting). Farnesol produced by yeast, for example, could contribute to increase the concentration of this aroma in wine obtained from non-aromatic grape.

In this context, the necessity of a small, simple-to-use, sensible and selective device as a biosensor is undoubted. Indeed, biosensors could be useful to detect/quantify chemical in *real time*, during all steps of winemaking from the maceration to aging, helping winemaker to improve quickly the quality and the customer appreciation of their products.

## 6. REFERENCES

- Adhikari, S., Manthana, P.V., Sajwan, K., Kota, K.K., Roy, R., 2010. A unified method for purification of basic proteins. *Anal Biochem* 400, 203–206. <https://doi.org/10.1016/j.ab.2010.01.011>
- Agelopoulos, N.G., Chamberlain, K., Pickett, J.A., 2000. Factors Affecting Volatile Emissions of Intact Potato Plants, *Solanum tuberosum*: Variability of Quantities and Stability of Ratios. *J Chem Ecol* 26, 497–511. <https://doi.org/10.1023/A:1005473825335>
- Agelopoulos, N.G., Hooper, A.M., Maniar, S.P., Pickett, J.A., Wadhams, L.J., 1999. A Novel Approach for Isolation of Volatile Chemicals Released by Individual Leaves of a Plant in situ. *J Chem Ecol* 25, 1411–1425. <https://doi.org/10.1023/A:1020939112234>
- Baietto, M., Wilson, A.D., 2015. Electronic-Nose Applications for fruit identification, ripeness and quality grading. *Sensors* 15, 899–931.
- Banuls, M.J., Puchades, R., Maquieira, A., 2013. Chemical surface modifications for the development of silicon-based label-free integrated optical (IO) biosensors: A review. *Analytica Chimica Acta* 1–16.
- Barker, S.A., 1989. Immobilization of the biological component of biosensors. *Biosensors: Fundamentals and Application*. Chapter n.6.
- Beck, J.J., Torto, B., Vannette, R.L., 2017. Eavesdropping on Plant-Insect-Microbe Chemical Communications in Agricultural Ecology: A Virtual Issue on Semiochemicals. *J. Agric. Food Chem.* 65, 5101–5103. <https://doi.org/10.1021/acs.jafc.7b02741>
- Beres, C., Costa, G.N.S., Cabezudo, I., da Silva-James, N.K., Teles, A.S.C., Cruz, A.P.G., Mellinger-Silva, C., Tonon, R.V., Cabral, L.M.C., Freitas, S.P., 2017. Towards integral utilization of grape pomace from winemaking process: A review. *Waste Management* 68, 581–594.

Bhalla, N., Jolly, P., Formisano, N., Estrela, P., 2016. Introduction to biosensors. *Essays in Biochemistry* 60, 1–8.

Birkett, M.A., Pickett, J.A., 2003. Aphid sex pheromones: from discovery to commercial production. *Phytochemistry* 62, 651–656. [https://doi.org/10.1016/s0031-9422\(02\)00568-x](https://doi.org/10.1016/s0031-9422(02)00568-x)

Bruno, D., Grossi, G., Salvia, R., Scala, A., Farina, D., Grimaldi, A., Zhou, J.-J., Bufo, S.A., Vogel, H., Grosse-Wilde, E., Hansson, B.S., Falabella, P., 2018. Sensilla Morphology and Complex Expression Pattern of Odorant Binding Proteins in the Vetch Aphid *Megoura viciae* (Hemiptera: Aphididae). *Front Physiol* 9. <https://doi.org/10.3389/fphys.2018.00777>

Caroselli, R., Sanchez, D.M., Alcantara, S.P., Prats Quilez, F., Torrijos Moran, L., Garcia-Ruperez, J., 2017. Real-Time and In - Flow Sensing using a High Sensitivity Porous Silicon Microcavity – Based Sensor. *Sensors* 17.

Carrau, F.M., Boido, E., Dellacassa, E., 2008. Terpenoids in Grapes and Wines: Origin and Chambers, J.P., Arulanandam, B.P., Matta, L.L., Weis, A., Valdes, J.J., 2008. Biosensor Recognition Elements. *Current Issues in Molecular Biology* 10, 1–12.

Chambers, J.P., Pretorius, I.S., 2010. Fermenting knowledge: the history of winemaking, science and yeast research. *EMBO reports* 11.

Cheng, G., Liu, Y., Yue, T.-X., Zhang, Z.-W., Cheng, G., Liu, Y., Yue, T.-X., Zhang, Z.-W., 2015. Comparison between aroma compounds in wines from four *Vitis vinifera* grape varieties grown in different shoot positions. *Food Science and Technology* 35, 237–246. <https://doi.org/10.1590/1678-457X.6438>

Coleman, R.G., Sharp, K.A., 2010. Protein Pockets: Inventory, Shape, and Comparison. *J Chem Inf Model* 50, 589–603. <https://doi.org/10.1021/ci900397t>

D'Onofrio, C., 2011. Caratterizzazione funzionale della biosintesi degli aromi delle uve durante lo sviluppo dell'acino e controllo della qualità aromatica delle uve. *Italus Hortus* 18 (2), 39–61.

Damberger, F., Nikonova, L., Horst, R., Peng, G., Leal, W.S., Wüthrich, K., 2000. NMR characterization of a pH-dependent equilibrium between two folded solution conformations of the pheromone binding protein from *Bombyx mori*. *Protein Sci.* 9, 1038–1041. <https://doi.org/10.1110/ps.9.5.1038>

Dawson, G.W., Pickett, J.A., Smiley, D.W., 1996. The aphid sex pheromone cyclopentanoids: synthesis in the elucidation of structure and biosynthetic pathways. *Bioorg. Med. Chem.* 4, 351–361. [https://doi.org/10.1016/0968-0896\(96\)00012-0](https://doi.org/10.1016/0968-0896(96)00012-0)

Dewhirst, S.Y., Pickett, J.A., Hardie, J., 2010. Aphid pheromones. *Vitam. Horm.* 83, 551–574. [https://doi.org/10.1016/S0083-6729\(10\)83022-5](https://doi.org/10.1016/S0083-6729(10)83022-5)

Dhanekar, S., Jain, S., 2013. Porous silicon biosensor: Current status. *Biosensors and Bioelectronics* 41, 54–64. <https://doi.org/10.1016/j.bios.2012.09.045>

Di Stefano, R., 2013. Gli aromi dei Moscati con particolare riferimento a quelli del Moscato Giallo., in: *Atti Accademia Italiana Della Vite e Del Vino*.

Dixon, A.F.G., 1998. *Aphid ecology : an optimization approach*, 2nd ed. ed. London : Chapman & Hall.

Escorihuela, J., Bañuls, M.J., Castelló, J.G., Toccafondo, V., García-Rupérez, J., Puchades, R., Maquieira, Á., 2012. Chemical silicon surface modification and bioreceptor attachment to develop competitive integrated photonic biosensors. *Anal Bioanal Chem* 404, 2831–2840. <https://doi.org/10.1007/s00216-012-6280-4>

Estevez, M.C., Alvarez, M., Lechuga, L.M., 2012. Integrated optical devices for lab-on-a-chip biosensing applications. *Laser & Photonics Reviews* 6, 463–487. <https://doi.org/10.1002/lpor.201100025>

Fan, J., Francis, F., Liu, Y., Chen, J.L., Cheng, D.F., 2011. An overview of odorant-binding protein functions in insect peripheral olfactory reception. *Genet. Mol. Res.* 10, 3056–3069. <https://doi.org/10.4238/2011.December.8.2>

Fleet, G.H., 2003. Yeast interactions and wine flavour. *International Journal of Food Microbiology* 86,11–22.

Fleet, G.H., 2007. *Wine*, 3rd Ed. ed. M.P.Doyle and L.R.Beuchat, ASM Press, Whashington, D.C.

Francis, F., Vandermoten, S., Verheggen, F., Lognay, G., Haubruge, E., 2005. Is the (E)- $\beta$ -farnesene onlyvolatile terpenoid in aphids? *Journal of Applied Entomology* 129, 6–11. <https://doi.org/10.1111/j.1439-0418.2005.00925.x>

Fregoni, M., Fregoni, C., Ferrarini, R., Spagnolli, F., 2008. *Chimica viticolo-enologica, con elementi di genetica e genomica della vite.*, Seconda edizione. ed. Reda Edizioni, Torino.

García-Rupérez, J., Toccafondo, V., Bañuls, M.J., Castelló, J.G., Griol, A., Peransi-Llopis, S., Maquieira, Á., 2010. Label-free antibody detection using band edge fringes in SOI planar photonic crystal waveguides in the slow-light regime. *Opt. Express*, OE 18, 24276–24286. <https://doi.org/10.1364/OE.18.024276>

Gorb, S.N., 2011. Insect-Inspired Technologies: Insects as a Source for Biomimetics, in: Vilcinskas, A.(Ed.), *Insect Biotechnology*. Springer Netherlands, Dordrecht, pp. 241–264. [https://doi.org/10.1007/978-90-481-9641-8\\_13](https://doi.org/10.1007/978-90-481-9641-8_13)

Griol, A., Peransi, S., Rodrigo, M., Hurtado, J., Bellieres, L., Ivanova, T., Zurita, D., Sánchez, C., Recuero, S., Hernández, A., Simón, S., Balka, G., Bossis, I., Capo, A., Camarca, A., D'Auria, S., Varriale, A., Giusti, A., 2019. Design and Development of Photonic Biosensors for Swine Viral Diseases Detection. *Sensors (Basel)* 19. <https://doi.org/10.3390/s19183985>

Große-Wilde, E., Svatoš, A., Krieger, J., 2006. A Pheromone-Binding Protein Mediates the Bombykol-Induced Activation of a Pheromone Receptor In Vitro. *Chem Senses* 31, 547–555. <https://doi.org/10.1093/chemse/bjj059>

Guerrieri, E., Digilio, M.C., 2008. Aphid-plant interactions: a review. *Journal of Plant Interactions* 3, 223–232. <https://doi.org/10.1080/17429140802567173>

Gullan PJ, Cranston PS. 2014. *The Insects: An Outline of Entomology*, 5th Edition. Wiley-Blackwell.

Hales, D.F., Tomiuk, J., Woehrmann, K., Sunnucks, P., 1997. Evolutionary and genetic aspects of aphid biology: A review. *EJE* 94, 1–55.

Hardie, J., Nottingham, S.F., Dawson, G.W., Harrington, R., Pickett, J.A., Wadhams, L.J., 1992. Attraction of field flying aphid males to synthetic sex pheromone. *Chemoecology* 3, 113–117.

Hargroves, K.J., Smith, M.H., 2006. Innovation inspired by nature: *Biomimicry* 4.

Hatano, E., Kunert, G., Bartram, S., Boland, W., Gershenzon, J., Weisser, W.W., 2008. Do Aphid Colonies Amplify their Emission of Alarm Pheromone? *J Chem Ecol* 34, 1149–1152. <https://doi.org/10.1007/s10886-008-9527-y>

Hopkins, W.G., Huner, N.P.A., 2007. *Fisiologia vegetale*, Edizione italiana sulla terza americana. ed.McGraw-Hill, Milano.

Horst, R., Damberger, F., Luginbühl, P., Güntert, P., Peng, G., Nikonova, L., Leal, W.S., Wüthrich, K., 2001. NMR structure reveals intramolecular regulation mechanism for pheromone binding and release. *Proc Natl Acad Sci U S A* 98, 14374–14379. <https://doi.org/10.1073/pnas.251532998>

Joo, J.H., Jetten, A.M., 2010. Molecular mechanisms involved in farnesol-induced apoptosis. *CancerLetters* 287, 123–135. <https://doi.org/10.1016/j.canlet.2009.05.015>

Karbassian, F., 2018. *Porous Silicon. Porosity - Process, Technologies and Applications*. <https://doi.org/10.5772/intechopen.72910>

Kaupp, U.B., 2010 Olfactory signalling in vertebrates and insects: differences and commonalities. *Nature* 11, 188–200.



Klowden, M.J., 2013. Communication Systems, in: *Physiological Systems in Insects*. Elsevier, pp.603–647. <https://doi.org/10.1016/B978-0-12-415819-1.00012-X>.

Klusák, V., Havlas, Z., Rulíšek, L., Vondrášek, J., Svatos, A., 2003. Sexual attraction in the silkworm moth. Nature of binding of bombykol in pheromone binding protein--an ab initio study. *Chem. Biol.* 10, 331–340. [https://doi.org/10.1016/s1074-5521\(03\)00074-7](https://doi.org/10.1016/s1074-5521(03)00074-7)

Krieger, J., von Nickisch-Roseneck, E., Mameli, M., Pelosi, P., Breer, H., 1996. Binding proteins from the antennae of *Bombyx mori*. *Insect Biochem. Mol. Biol.* 26, 297–307. [https://doi.org/10.1016/0965-1748\(95\)00096-8](https://doi.org/10.1016/0965-1748(95)00096-8)

Kromidas, L., Perrier, E., Flanagan, J., Rivero, R., Bonnet, I., 2006. Release of antimicrobial actives from microcapsules by the action of axillary bacteria. *International Journal of Cosmetic Science* 28,103–108. <https://doi.org/10.1111/j.1467-2494.2006.00283.x>

Kunert, G., Otto, S., Rose, U.S.R., Gershenzon, J., Weisser, W.W., 2005. Alarm pheromone mediates production of winged dispersal morphs in aphids. *Ecology Letters* 8, 596–603.

Laue, M., Steinbrecht, R.A., Ziegelberger, G., 1994. Immunocytochemical localization of general odorant-binding protein in olfactory sensilla of the silkworm *Antheraea polyphemus*. *Naturwissenschaften* 81, 178–180. <https://doi.org/10.1007/BF01134537>

Leal, G.M., Leal, W.S., 2015. Binding of a fluorescence reporter and a ligand to an odorant-binding protein of the yellow fever mosquito, *Aedes aegypti*. *F1000Res* 3, 305. <https://doi.org/10.12688/f1000research.5879.2>

Leal, W.S., 2013. Odorant reception in insects: roles of receptors, binding proteins, and degrading enzymes. *Annu. Rev. Entomol.* 58, 373–391. <https://doi.org/10.1146/annurev-ento-120811-153635>

Leal, W.S., Nikonova, L., Peng, G., 1999. Disulfide structure of the pheromone binding protein from the silkworm moth, *Bombyx mori*. *FEBS Lett.* 464, 85–90. [https://doi.org/10.1016/s0014-5793\(99\)01683-x](https://doi.org/10.1016/s0014-5793(99)01683-x)

- Lees, A.D., 1990. Dual photoperiodic timers controlling sex and female morph determination in the pea aphid *Acyrtosiphon pisum*. *Journal of Insect Physiology* 36, 585–591. [https://doi.org/10.1016/0022-1910\(90\)90027-D](https://doi.org/10.1016/0022-1910(90)90027-D)
- Lijnzaad, P., Berendsen, H.J.C., Argos, P., 1996. Hydrophobic patches on the surfaces of protein structures. *Proteins: Structure, Function, and Bioinformatics* 25, 389–397. <https://doi.org/10.1002>
- Longo, R., Blackman, J.W., Torley, P.J., Rogiers, S.Y., Schmidtke, L.M., 2017. Changes in volatile composition and sensory attributes of wines during alcohol content reduction: Changes in wines during alcohol content reduction. *J. Sci. Food Agric.* 97, 8–16. <https://doi.org/10.1002/jsfa.7757>
- MacKay, P.A., Reeleder, D.J., Lamb, R.J., 1983. Sexual morph production by apterous and alateviviparous *Acyrtosiphon pisum* (Harris) (Homoptera: Aphididae). *Can. J. Zool.* 61, 952–957. <https://doi.org/10.1139/z83-128>
- Malhotra, S., Verma, A., Tyagi, N., Kumar, V., 2017. Biosensors: principle, types and applications. *International Journal of Advance Research and Innovative Ideas in Education* Vol-3, 3639–3644.
- Marais, J., 1983. Terpenes in the aroma of grapes and wine: a review. *South African Journal for Enology and Viticulture* 4.
- Matsuo, T., Sugaya, S., Yasukawa, J., Aigaki, T., Fuyama, Y., 2007. Odorant-Binding Proteins OBP57d and OBP57e Affect Taste Perception and Host-Plant Preference in *Drosophila sechellia*. *PLOS Biology* 5, e118. <https://doi.org/10.1371/journal.pbio.0050118>
- Mauriello, G., Capece, A., D’Auria, M., Garde-Cerdan, T., Romano, P., 2009. SPME-GC method as a tool to differentiate VOC profiles in *Saccharomyces cerevisiae* wine yeasts. *Food Microbiology* 26, 246–252.
- Meyerhof, W., Korsching, S.I., 2016. *Chemosensory Systems in Mammals, Fishes, and Insects - Preamble*.

Micha, S.G., Wyss, U., 1996. Aphid alarm pheromone (E)- $\beta$ -farnesene: A host finding kairomone for the aphid primary parasitoid *Aphidius uzbekistanicus* (Hymenoptera: Aphidiinae). *Chemoecology* 7, 132–139. <https://doi.org/10.1007/BF01245965>

Micrometabolism during the Vinification Process. *Natural Product Communications* 3, 1934578X0800300. <https://doi.org/10.1177/1934578X0800300419>

Muñoz-González, C., Rodríguez-Bencomo, J.J., Moreno-Arribas, M.V., Pozo-Bayón, M.Á., 2011. Beyond the characterization of wine aroma compounds: looking for analytical approaches in trying to understand aroma perception during wine consumption. *Anal Bioanal Chem* 401, 1497–1512. <https://doi.org/10.1007/s00216-011-5078-0>

Nayal, M., Honig, B., 2006. On the nature of cavities on protein surfaces: Application to the identification of drug-binding sites. *Proteins: Structure, Function, and Bioinformatics* 63, 892–906. <https://doi.org/10.1002/prot.20897>

Northey, T., Venthur, H., De Biasio, F., Chauviac, F.-X., Cole, A., Ribeiro, K.A.L., Grossi, G., Falabella, P., Field, L.M., Keep, N.H., Zhou, J.-J., 2016. Crystal Structures and Binding Dynamics of Odorant-Binding Protein 3 from two aphid species *Megoura viciae* and *Nasonovia ribisnigri*. *Sci Rep* 6, 24739. <https://doi.org/10.1038/srep24739>

Pelosi, P., Calvello, M., Ban, L., 2005. Diversity of odorant-binding proteins and chemosensory proteins in insects. *Chem. Senses* 30 Suppl 1, i291-292. <https://doi.org/10.1093/chemse/bjh229>

Pelosi, P., Zhou, J.-J., Ban, L.P., Calvello, M., 2006. Soluble proteins in insect chemical communication. *Cell. Mol. Life Sci.* 63, 1658–1676. <https://doi.org/10.1007/s00018-005-5607-0>

Pelosi, P., Zhu, J., Knoll, W., 2018. Odorant-Binding Proteins as Sensing Elements for Odour Monitoring. *Sensors (Basel)* 18. <https://doi.org/10.3390/s18103248>

Pérez-Torrado, R., Barrio, E., Querol, A., 2017. Alternative yeasts for winemaking: *Saccharomyces noncerevisiae* and its hybrids. *Critical Reviews in Food Science and Nutrition* 58, 1780–1790.

- Pickett, J.A., Wadhams, L.J., Woodcock, C.M., Hardie, J., 1992. The Chemical Ecology of Aphids. *Annu. Rev. Entomol.* 37, 67–90. <https://doi.org/10.1146/annurev.en.37.010192.000435>
- Polásková, P., Herszage, J., Ebeler, S.E., 2008. Wine flavor: chemistry in a glass. *Chem Soc Rev* 37,2478–2489. <https://doi.org/10.1039/b714455p>
- Pophof, B., 2004. Pheromone-binding Proteins Contribute to the Activation of Olfactory Receptor Neurons in the Silkmoths *Antheraea polyphemus* and *Bombyx mori*. *Chemical Senses* 29, 117–125.
- Qiao, H., Tuccori, E., He, X., Gazzano, A., Field, L., Zhou, J.-J., Pelosi, P., 2009. Discrimination of alarm pheromone (E)-beta-farnesene by aphid odorant-binding proteins. *Insect Biochem. Mol. Biol.* 39, 414–419. <https://doi.org/10.1016/j.ibmb.2009.03.004>
- Rapp, A., Knipser, W., Engel, L., 1980. Identification of 3,7-dimethyl-octa-1,7-dien-3,6-diol in grae and wine aroma of Muscat varieties. *Vitis* 19, 226–229.
- Renou, M., 2014. Pheromones and General Odor Perception in Insects, in: Mucignat-Caretta, C. (Ed.), *Neurobiology of Chemical Communication, Frontiers in Neuroscience*. CRC Press/Taylor & Francis, Boca Raton (FL).
- Roitberg, B.D., Meyers, J.H. 1978. Adaptation of alarm pheromone responses of the pea aphid *Acyrtosiphon pisum* (Harris). *Can. J. Zool.* 56(1): 103–108 (1978).
- Ryan, M., 2002. *Insect Chemoreception: Fundamental and Applied*. Springer Netherlands. <https://doi.org/10.1007/0-306-47581-2>
- Sandler, B.H., Nikonova, L., Leal, W.S., Clardy, J. 2000. Sexual attraction in the silkworm moth: structure of the pheromone-binding-protein-bombykol complex. *Chem. Biol.* 7: 143-151.
- Simon, J.-C., Peccoud, J., 2018. Rapid evolution of aphid pests in agricultural environments. *Curr Opin Insect Sci* 26, 17–24. <https://doi.org/10.1016/j.cois.2017.12.009>

- Slogget, J., Weisser, W.W., 2004. A general mechanism for predator-and parasitoid-induced dispersal in the pea aphid, *Acyrtosiphon pisum*. *Aphids in a new millennium*.
- Steinbrecht, R.A., Laue, M., Ziegelberger, G., 1995. Immunolocalization of pheromone-binding protein and general odorant-binding protein in olfactory sensilla of the silk moths *Antheraea* and *Bombyx*. *Cell Tissue Res* 282, 203–217. <https://doi.org/10.1007/BF00319112>
- Steyer, D., Erny, C., Claudel, P., Riveill, G., Karst, F., Legras, J.-L., 2013. Genetic analysis of geraniol metabolism during fermentation. *Food Microbiology* 33, 228–234. <https://doi.org/10.1016/j.fm.2012.09.021>
- Stroble, J., Watkins, S., Stone, R., 2009. Biology-inspired sensor design. *IEEE Potentials* 28, 19–24. <https://doi.org/10.1109/MPOT.2009.934892>
- Su, C., Menuz, K., Carlson, J.R., 2009. Olfactory Perception: receptors, cells, and circuits. *Cell* 139, 45–59.
- Sun, Y.F., De Biasio, F., Qiao, H.L., Iovinella, I., Yang, S.X., Ling, Y., Riviello, L., Battaglia, D., Falabella, P., Yang, X.L., Pelosi, P., 2012. Two Odorant-Binding Proteins Mediate the Behavioural Response of Aphids to the Alarm Pheromone (E)- $\beta$ -farnesene and Structural Analogues. *PLoS One* 7. <https://doi.org/10.1371/journal.pone.0032759>
- Tan, J., Zaremska, V., Lim, S., Knoll, W., Pelosi, P., 2020. Probe-dependence of competitive fluorescent ligand binding assays to odorant-binding proteins. *Anal Bioanal Chem* 412, 547–554. <https://doi.org/10.1007/s00216-019-02309-9>
- Terracciano, M., Rea, I., Borbone, N., Moretta, R., Oliviero, G., Piccialli, G., De Stefano, L., 2019. Porous Silicon-Based Aptasensors: The Next Generation of Label-Free Devices for Health Monitoring. *Molecules* 24. <https://doi.org/10.3390/molecules24122216>
- Terrier, A., 1972. Thèse Université de Bordeaux n°162.
- Turlings, T.C.J., Ton, J. 2006. Exploiting scents of distress: The prospect of manipulating herbivore-induce plant odour to enhance the control of agricultural pests. *Curr. Opin. Plant Biol.* 9: 421–427.

Turner, A.P.F., 2013. Biosensors: sense and sensibility. *Chemical Society Reviews* 42, 3175–3648.

Usseglio-Tommaset, L., 1966. L'aroma di Moscato delle uve e dei vini, *Industrie Agrarie*.

Vandermoten, S., Mescher, M.C., Francis, F., Haubruge, E., Verheggen, F.J., 2012. Aphid alarm pheromone: An overview of current knowledge on biosynthesis and functions. *Insect Biochemistry and Molecular Biology* 42, 155–163. <https://doi.org/10.1016/j.ibmb.2011.11.008>

Verheggen, F.J., Arnaud, L., Bartram, S., Gohy, M., Haubruge, E., 2008. Aphid and Plant Volatiles Induce Oviposition in an Aphidophagous Hoverfly. *J Chem Ecol* 34, 301–307. <https://doi.org/10.1007/s10886-008-9434-2>

Vieira, F.G., Rozas, J., 2011. Comparative genomics of the odorant-binding and chemosensory protein gene families across the Arthropoda: origin and evolutionary history of the chemosensory system. *Genome Biol Evol* 3, 476–490. <https://doi.org/10.1093/gbe/evr033>

Villamor, R.R., Ross, C.F., 2013. Wine Matrix Compounds Affect Perception of Wine Aromas. *Annu.Rev. Food Sci. Technol.* 4, 1–20. <https://doi.org/10.1146/annurev-food-030212-182707>

Waterhouse, A.L., Sacks, G.L., Jeffery, D.W., 2016. *Understanding Wine Chemistry*. John Wiley & Sons.

Wilson, A.D., 2013. Diverse Applications of Electronic-nose Technologies in Agriculture and Forestry. *Sensors* 13, 2295–2348.

Young, L., Jernigan, R.L., Covell, D.G., 1994. A role for surface hydrophobicity in protein-protein recognition. *Protein Sci* 3, 717–729.

Yu, Y., Wang, J., Shao, Q., Shi, J., Weiland, Z. 2016. The effects of organic solvents on the folding pathway and associated thermodynamics of proteins: a microscopic view. *Sci Rep* 6, 19500. <https://doi.org/10.1038/srep19500>

Zhang, R., Wang, B., Grossi, G., Falabella, P., Liu, Y., Yan, S., et al. (2017). Molecular basis of alarm pheromone detection in aphids. *Curr. Biol.* 27, 55–61. doi: 10.1016/j.cub.2016.10.013

Zhang, S., Maida, R., Steinbrecht, R.A., 2001. Immunolocalization of odorant-binding proteins in noctuid moths (Insecta, Lepidoptera). *Chem. Senses* 26, 885–896. <https://doi.org/10.1093/chemse/26.7.885>

Zhou, J.-J., 2010. Chapter Ten - Odorant-Binding Proteins in Insects, in: Litwack, G. (Ed.), *Vitamins & Hormones, Pheromones*. Academic Press, pp. 241–272. [https://doi.org/10.1016/S0083-6729\(10\)83010-9](https://doi.org/10.1016/S0083-6729(10)83010-9)

Zhu, F., Du, B., Li, J., 2016. Aroma Compounds in Wine. *Grape and Wine Biotechnology*. <https://doi.org/10.5772/65102>

# SUPPLEMENTARY MATERIALS

## 1. Deepsite viewing

DeepSite is freely available at [www.playmolecule.org](http://www.playmolecule.org). and it is a software developed to predict protein-ligand binding sites. Users can submit jobs to the GPU equipped servers and get a full volumetric map of the most probable binding sites of the protein.

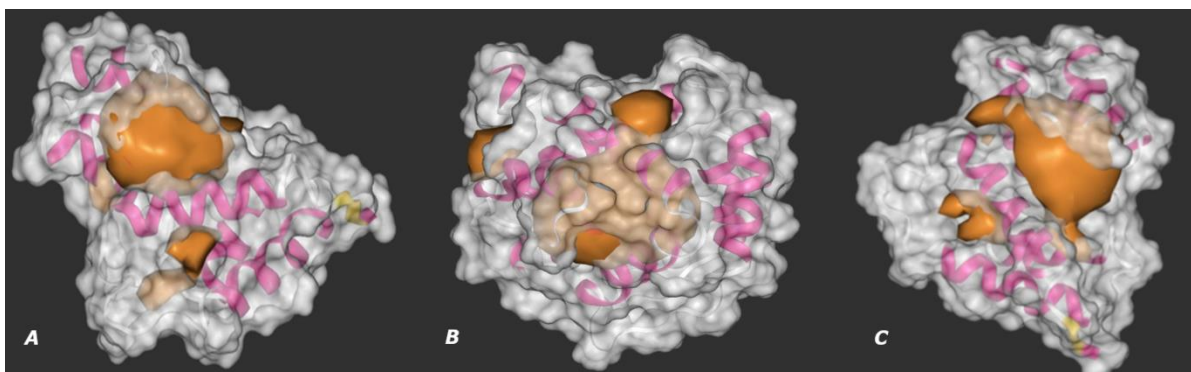


**Figure S1.** DeepSite view of aphid Odorant Binding Protein; **A.** *ApisOBP3*; **B.** *ApisOBP9*; **C.** *MvicOBP3*.

## 2. OBPs additional information.

### 2.1 I-TASSER results: domains and Predicted Solvent Accessibility.

#### I-TASSER results for job id S490529

(Click on [S490529\\_results.tar.bz2](#) to download the tarball file including all modeling results listed on this page. Click on [Annotation of I-TASSER Output](#) to read the in kept on the server for 60 days, there is no way to retrieve the modeling data older than 2 months).

Submitted Sequence in [FASTA format](#)

```
>protein
RFITTEQIDYYGKACNASEDDLWVKSYKVPTTETGKCLMKMITKLGLLNDDGGSYNKTM
EAGLKXKYNSEHSTEKIESINMKCYEALLVSKVWATCNYSYTVMACLNQDLDDKST
```

Predicted Secondary Structure

	20	40	60	80	100	
Sequence	RFITTEQIDYYGKACNASEDDLWVKSYKVPTTETGKCLMKMITKLGLLNDDGGSYNKTM	EAGLKXKYNSEHSTEKIESINMKCYEALLVSKVWATCNYSYTVMACLNQDLDDKST				
Prediction	CCCH+++++CCCC+++++CCCCCCCC+++++CCCCCCCC+++++CC+++++CCCCCCCC					
Conf.Score	9518999999875499999999999720899856430999999884636767770577799889987501427789999999988603789886430588999999987661644469					
	H:Helix; s:strand; c:coil					

Predicted Solvent Accessibility

	20	40	60	80	100	
Sequence	RFITTEQIDYYGKACNASEDDLWVKSYKVPTTETGKCLMKMITKLGLLNDDGGSYNKTM	EAGLKXKYNSEHSTEKIESINMKCYEALLVSKVWATCNYSYTVMACLNQDLDDKST				
Prediction	7343640451066172366204403644136365030013003432422477242436322530451365544640440153036414646474453142033114003633734678					
	Values range from 0 (buried residue) to 9 (highly exposed residue)					

**Figure S2.** *ApisOBP3* results.





## 2.2 OBPs binding pocket area and volume

Protein	Area	Volume
<i>Apis</i> OBP3	182.861	94.490
<i>Apis</i> OBP9	381.007	146.978
<i>Mvic</i> OBP3	140.573	90.001

**Table S1.** Additional information about aphid OBPs binding pocket

## 3. Binding pocket residues distance.

Here, USCF Chimera images are reported. They represent furthest binding pocket residues from ligand (more than 5 Amstrong). Ligands are stick and ball in light blue.

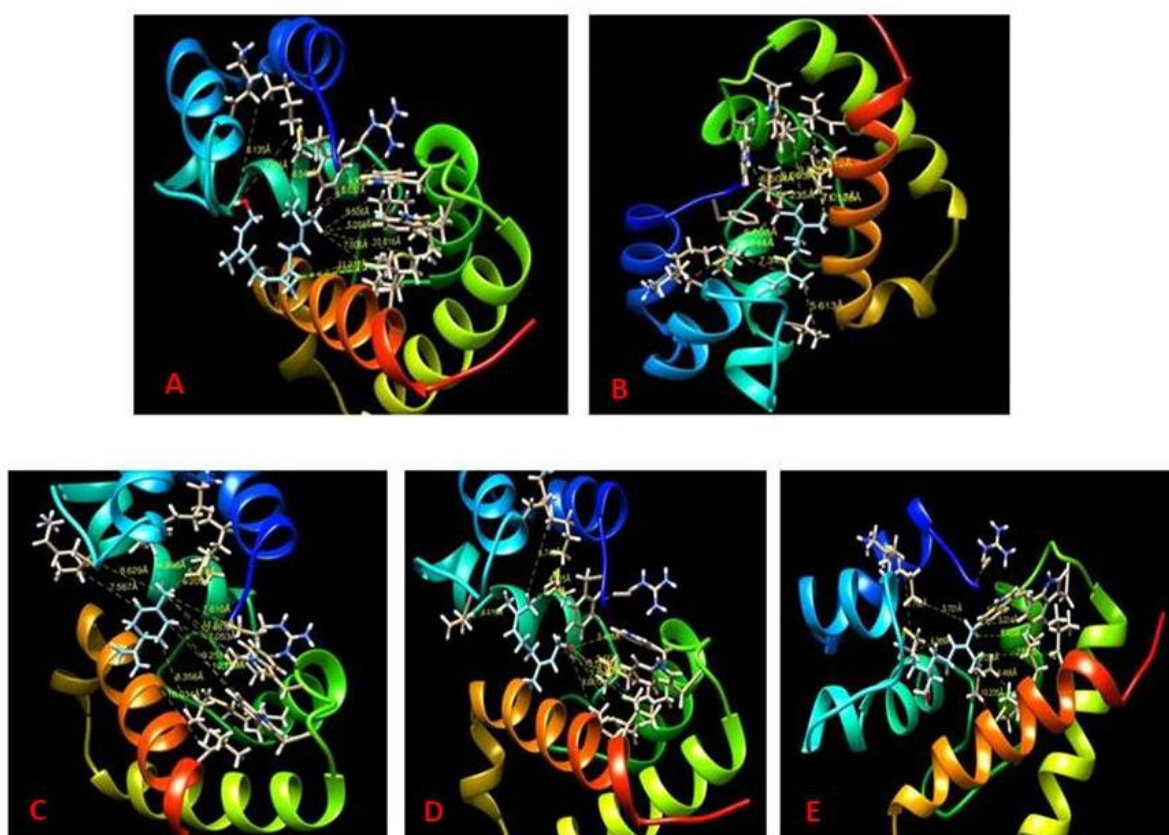


**Figure S5.** *Apis*OBP3 binding pocket residues far more than 5 Amstrong from ligand. **A.** farnesol; **B.** geraniol; **C.** limonene; **D.** nerol; **E.** citronellol.

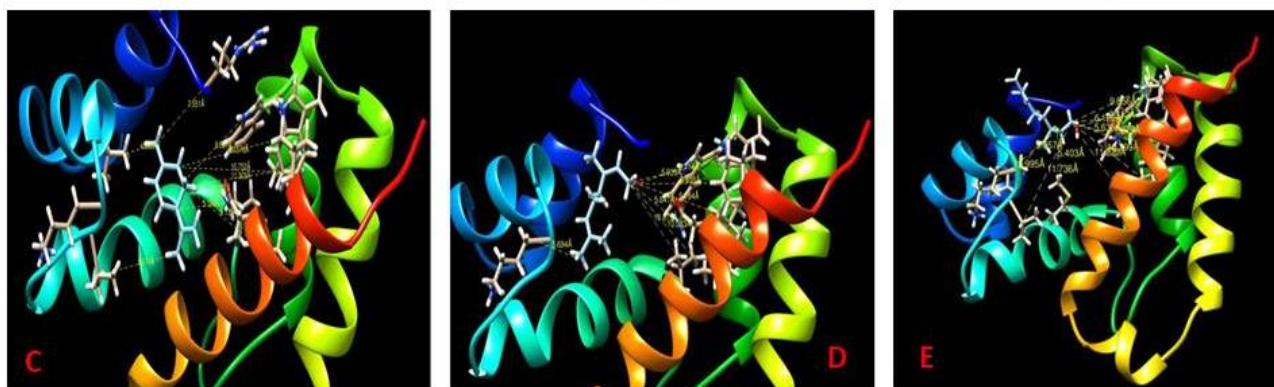
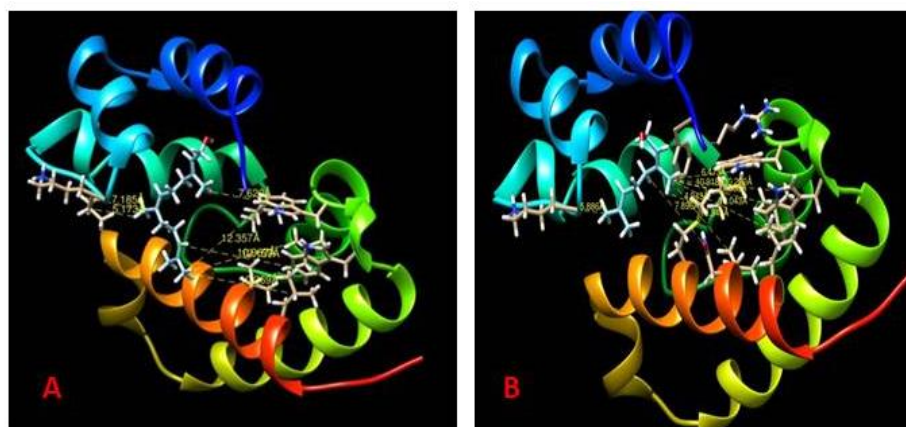


**Figure S6.** *MvicOBP3* binding pocket residues far more than 5 Angstroms from ligand. **A.** farnesol; **B.** geraniol; **C.** limonene; **D.** nerol; **E.** citronellol.

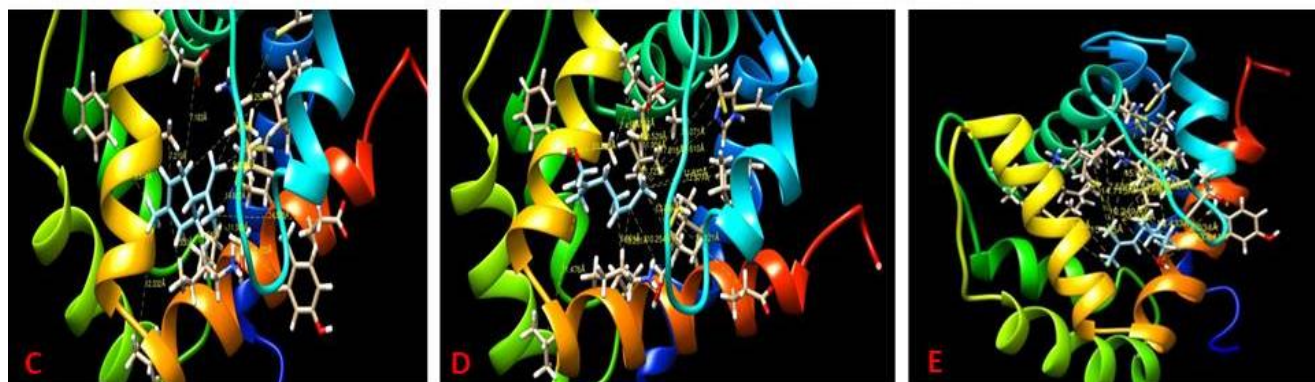
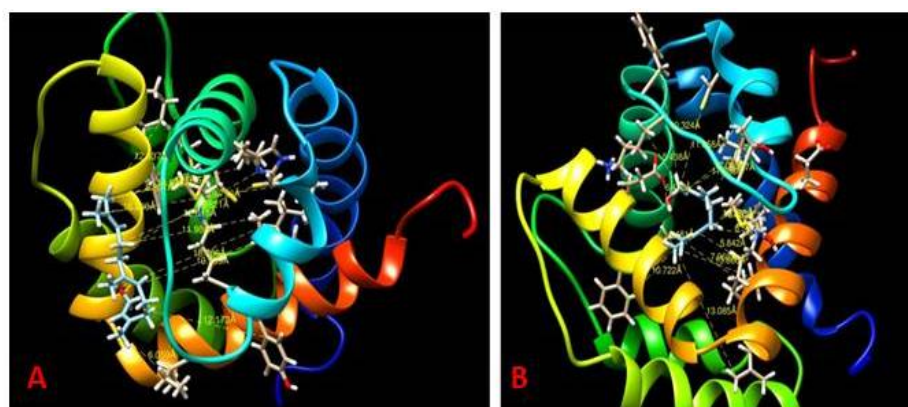


**Figure S7.** *ApisOBP3* binding pocket residues far more than 5 Angstroms from ligand. **A.** farnesol; **B.** geraniol; **C.** limonene; **D.** nerol; **E.** citronellol.

#### 4. OBPs and OBP-ligand surface analysis

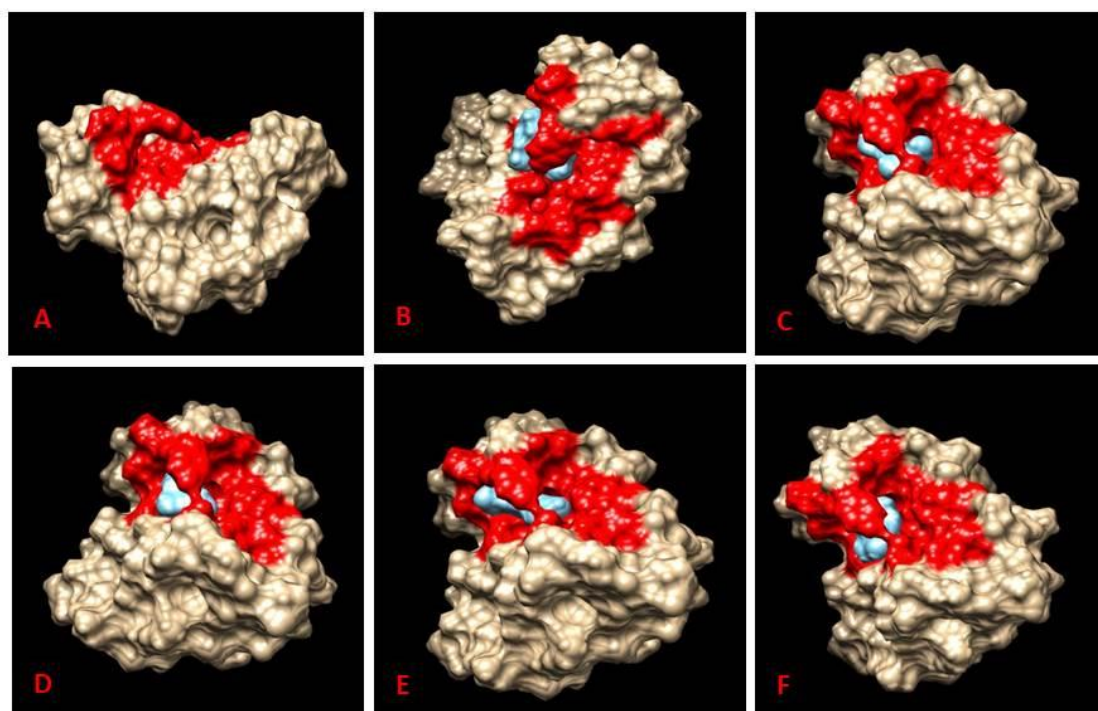


**Figure S8.** *Apis*OBP3 surface view. For all model, binding pocket surface is stained in red. **A.** *Apis*OBP3 only; **B.** OBP3 – farnesol; **C.** OBP3 - geraniol, **D.** OBP3 – nerol; **E.** OBP3 – citronellol; **F.** OBP3-limonene

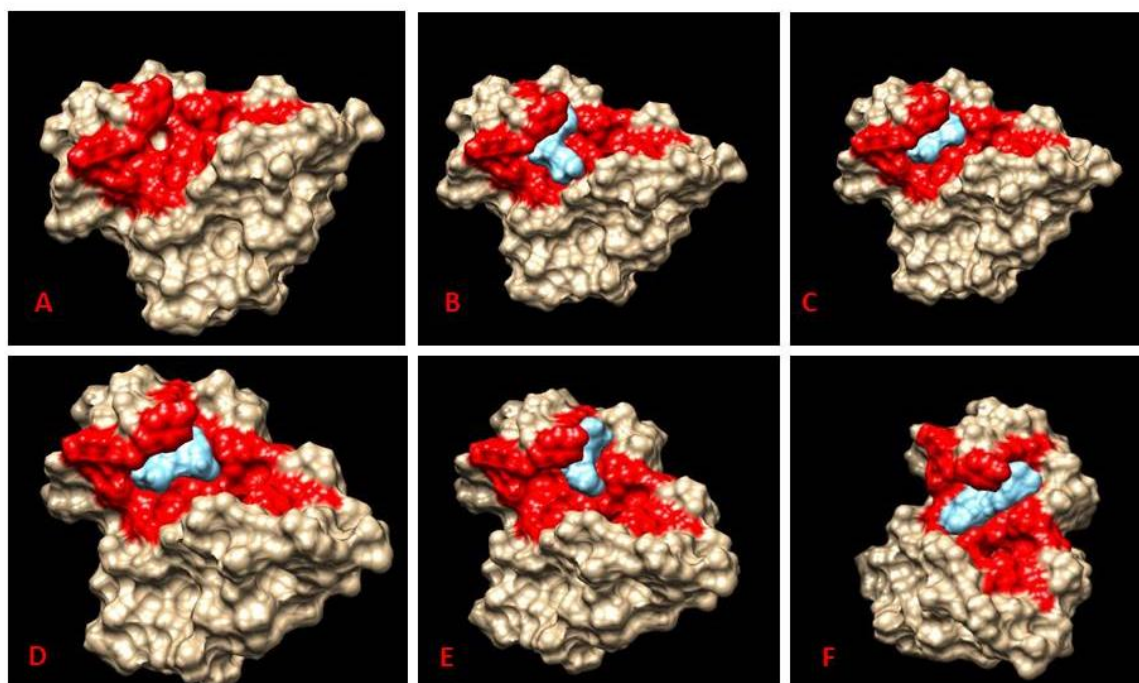


**Figure S9.** *Mvic*OBP3 surface view. For all model, binding pocket surface is stained in red. **A.** *Mvic*OBP3 only; **B.** OBP3 – farnesol; **C.** OBP3 - geraniol, **D.** OBP3 – nerol; **E.** OBP3 – citronellol; **F.** OBP3-limonene

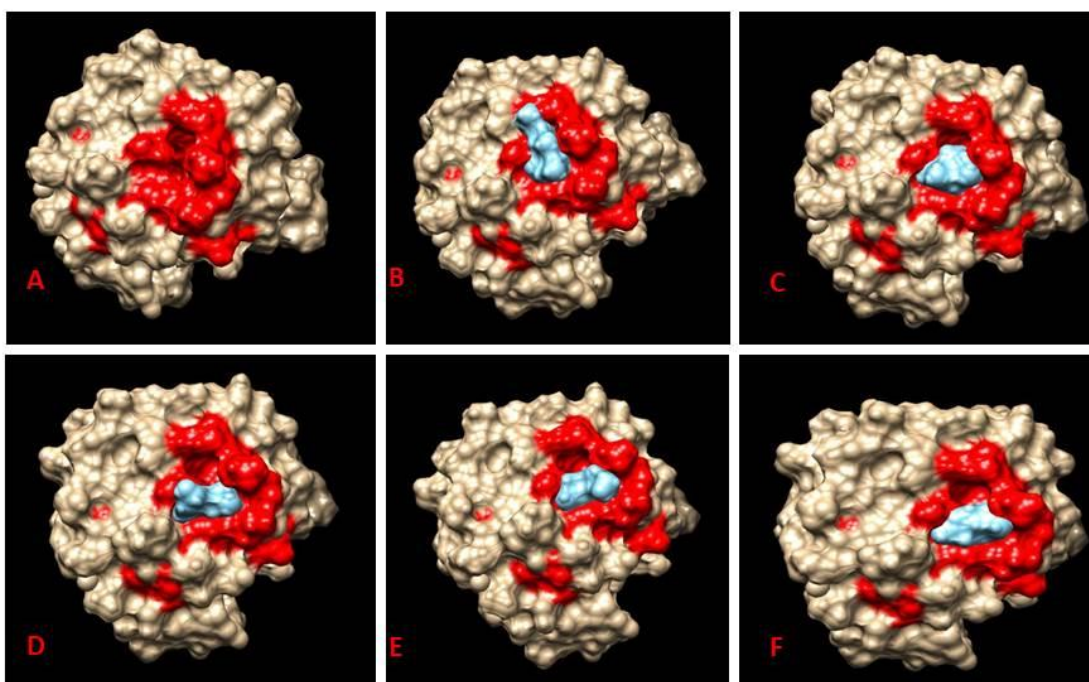


**Figure S10.** *Apis*OBP9 surface view. For all model, binding pocket surface is stained in red. **A.** *Apis*OBP9 only; **B.** OBP9 – farnesol; **C.** OBP9 - geraniol, **D.** OBP9 – nerol; **E.** OBP9 – citronellol; **F.** OBP9-limonene

## 5. Kd and Ki values obtained from competitive binding assay

PROTEIN	CHEMICAL	Ki (nM)	Kd ( $\mu$ M)
<i>Apis</i> OBP3	Nerol	50947	1,87E-17
	Geraniol	0.9992	4,92E-17
	Citronellol	87615	-6,86E-18
<i>Apis</i> OBP9	Farnesol	3127	-1,7871E-17
	Citronellol	1043	2,74E+01
	Nerol	43295	-387,334928
<i>Mvic</i> OBP3	Farnesol	87617	-4,28E-18
	Geraniol	29525	1,58E-16
	Nerol	92670	-1,15E-17

**Table S2.** Results of GraphPad (Ki) and SigmaPlot (kd) data analysis. The most reliable value is *Apis*OBP9 – citronellol Ki and Kd. However this data are not good because in the experimental performance of competitive assays there was an increase of fluorescence instead decrease.

## 6. Kd values of OBP-NPN complexes

<b>PROTEIN</b>	<b>Kd (<math>\mu</math>M)</b>
<i>Apisum</i> OBP3	5.9
<i>Apisum</i> OBP9	5.06
<i>Mvic</i> OBP3	1.9

# APPENDIX

## Appendix A: sequences

### A1. Aphids Odorant Binding Protein sequences

#### *Apis*OBP3 (Accession number: NM\_001160057.1)

AACCAGAATATTGTAATAAAAACAACGCGCACAGTCTTCTCCC GGCGGAGTGACG  
GAGTGATAATAACGACAGTAATAAAATTCTCCAGTCCGCAAAAAACGTGCGAAA  
TGATTTCTGTCGACGTTTTACATAACGTTGGTGTTCGGTATTGCGATGCTGATTTCA  
TGTGGCCACGGGCGATTTACGACGGAGCAAATCGATTATTATGGAAAAGCGTGC  
AACGCCAGCGAAGATGACCTCGTCGTAGTCAAATCCTACAAGGTGCCAACTACA  
GAAACTGGAAAGTGTCTGATGAAATGCATGATCACCAAAGTACTGCTGAAC  
GACGATGGTTCGTACAACAAAACCTGGCATGGAAGCGGGGTTAAAGAAATACTGG  
TCGGAATGGTCTACGGAGAAGATAGAGAGTATAAACAACAAGTGTATGAAGAA  
GCTTTACTTGTGTCAAAGGAGGTAGTAGCGACGTGCAATTACTCGTACACTGTGA  
TGCCATGTTTGAACAAGCAGTTGGATCTCGACAAGTCAACTTGAACCTCTTGAGC  
TGCATATTGAAGAGTAACCGAGTGGATCGAAACGAGAGTCAAACGTACCTACAT  
ATTATTTTTCATTTTAAAATCGTTTTATTTTCATACTCAAACATTTTATATTGTACA  
ATGAAGTCAGAAGTGTATTGTTTGATATAACAAAATATTATACATAATATATTA  
TATATAATATAACAATTAGTTTTTGGCTGTCACACTTTAGGATTTAAATGATATTTT  
CCGGTTTCCTTGATCCGACGACGATCACCTTGACACGTTTATGTATCGAATAAAA  
TTGTAATAAAAGCATCGGAATAATAATCATTATTATATACCTATATTATATTAACA  
ACGTTTTAATAAAAATACTATAATTCAATTGGTTAATGATGAAAAAAAAAAAAAAAAA  
AA

#### *Apis*OBP3 (Accession number: NM\_00116006)

AGTTTAAACACGGTCACCACAAACGTATGGTTCGAACTCAGTTTTATTCTCAAGTAA  
CGAGTTGAATAAAAAATATGTTGGTGTATCCGTTGCAGTAAAAAATTTGGTGCAGT  
GCAAATAGAAAAGGAACACAGCTGAAGTATGGTTCGCCCGGAAAAGAATGTATAA  
CATGTTACCAACGACCGTTTTTGTTCGCCATCATAGCGGCGACCGTCTTAAAGGAT  
TGCGACGCTTACTTGAGTGAAGCGGCCATCAAAAAACACAACAGATGTTGAAA  
ACCGTATGCTCCAAGAAACATTCGGTCGAAGAGGACGTATTTACGAACATCAA  
AAAGGAATATTTCCAGAGGACAACAACAATATAAAATGTTACTTTGCCTGTAATT  
TCAAAACTATGCAATTGATCAATCAAAAGGGAGTCATCGATAAAAAAATGTTCA  
AAGACAAGATGTTCGATGATGGCACCACGAACGTATACAAAATTTTGTACCAGT  
TATAGAACAGTGTACTGGAAAAGATAAAGGTGAAGAACTCTGTCAGTCTTCGTAC  
AACGTCATAAAGTGC GCGCACTCTGTTGATCCCAAAGTTTAGAGTTTCTACCAC  
TCTAGACGTCGTCACCTTCAATCAGCAGTTGATAGATCCCGGGTACAAAGAAACA  
TTAAGATTTATCGTCTGAAGTGTTTTTTTTATTGATAATAATTTGATTTATATTGTAG  
AACATATTTTTGTGTGTATTA AAAATTCAAATGCACGTTACAAAAAAAAAAAAAAAAA  
AA

#### *Apis*OBP9 (Accession number: NM\_001160063.1)

CCTAAAAAGTATCAAATATATATAACTCAAATTCTCGTACAATCAAATTTATTA  
TAACACTATAAATTTATTTGTTTGGTGTACCTGATTTATTACAACCAAACCTCAACA  
TGATAATCAAAAAGACATTGTTGCTATCAGTTTTCTGTTCTTTTCGGTTGTTTGTCT  
CAATCAATAAGGCTGATGATGCAGATGCAAAGGATAAGGAATTAATGTCAAAT

TATTCACTGTGGTTTTTAAATGCTTTAAGGATGCCGATTGGGGCACGTGCGGTGA  
AATGATAACAACATAAATATGACATAACTCAAGCTAAATATAAACAGTGTACATGT  
CACATGGCGTGTGCTGGGGAAGAACTTGGAAATGATAAACGCTTCGGGGCAACCA  
GAACCTGCGAAGTTCCTCGAATACGTGAACAAAATCAATAATCCAGACATTAAG  
AGTCAATTGCAACTTATTTACGACAAATGCCAAAATGTCAAAGGGTTCGGAGAAA  
TGCGATCTCGCAGAACAATTTGCCATATGTGCTTTTAAAGGAATCACCAGCACTGA  
AAGAACGCGTTTCTACGTTGATGGAAATGCTAGTGAAGATGAAACCAAAAATCAA  
AATAAATCTCTTCAGTCAACACATACACAGTTGCATCCGTTTTTCATATCTGTTTTT  
CCTAATAAATATTGTATTTGTAGGTACCGTTAATACCTACAAAACCAATAATAAT  
TATAATATATTTACAAATGTGATTAATAAATCAATGCAATTTCAATCAATTAATAA  
AAAAAAA

***MvicOBP3* (Accession number: MG596882.1)**

CCGCAGATAGCTTATTGTTAACCTTTGTATGTTATACACTACTCACACAATCACAA  
ACTCCAAAGTCTGTCTGGATGGTTGTTCAATTTGTACGTATTTAATGAATATTATT  
ATAATATTGTAATAAAAAAACGCGCACAGTCTTCTCCTGACGGACTGTACCGACA  
TAGTGATAATAACGACAATAATTCTCCAGCCCGCACAAACGCGATCAACGTGCG  
AAATGATTTTCGTCAACATTTTACTTTACGTTGCTGTTTCGGTATTGCGATGCTGATT  
TCATGTGGCTACGGGCGATTTACAACGGAACAAATCGATTATTACGGAAAAGCGT  
GCAACGCCAGCGAAGATGACCTCGTCGTAGTCAAATCCTACAAGGTACCATCTTC  
AGAAACTGGAAAGTGTCTGATGAAATGCATGATCACCAAACCTAGGACTGCTGAA  
CGACGATGGTTCGTACAACAAAACCTGGCATGGAAGCGGGGCTGAAGAAATACTG  
GTCCGAATGGTCTACGGAGAAAATCGAGTCTATAAACAACAAGTGTATGAAGA  
AGCTTTACTTGTGTCAAAAGAGGTAATAGCGACGTGCAATTATTCGTACACTGTG  
ATGGCATGTCTGAACAAACAGTTAGATCTCGACAAGTCAACTTGAAACTCTTGAG  
CATATTGAAGAGTTAACCGAGTGGACCAAATGAGAGTCAAACGTACATACATA  
TTATTTTTTCATTTTAAAATAATTTTATTTCTACTTTTATGATAGTTTTAATACTAC  
AACACTATACCTATATTATACAATAAAGTATATTGTTTGATATAACACAGAAATA  
TATATACAATTAGTTTTTGGTTGTCACACTTTAGGATTTAAATGATATTTTCCGGT  
TTCCTTGATCTGACAGCGATCACCTTGACACGTTTATGTATCGAATAAAATTGTAA  
AAAAACGTAGGATTAATAATTACTATTATATACTACATTAACCTTTTAAATAAAT  
ACTATAATTC AATTGGTTAAAA

**A2.Vector primers**

NAME	SEQUENCE
T7 promoter, forward primer	5'- TAATACGACTCACTATAGGG – 3'
T7 terminator, reverse primer	5'- GCTAGTTATTGCTCAGCGG – 3'



### A3. Sequencing alignment

- *Acyrtosiphon pisum* OBP3. **A**: nucleotide sequence **B** amino acid sequence.

```
>191021-005_I24_1D05ZAA245.ab1
Sequence ID: Query_27359 Length: 1578
Range 1: 61 to 414

Score:638 bits(345), Expect:0.0,
Identities:351/354(99%), Gaps:0/354(0%), Strand: Plus/Plus

Query 1      CGATTTACGACGGAGCAAAATCGATTATTATGAAAAAGCGTCAACGCAGCGAAGATGAC 60
Sbjct 61      ||| ||||| ||| ||| ||| ||| ||| ||| ||| ||| ||| ||| ||| ||| ||| |||
CGATTTTCGACGGAACAATCGATTATTATGAAAAAGCGTCAACGCAGCGAAGATGAC 120

Query 61      CTCGTCGTAGTCAAATCCTACAAGGTGCCAACTACAGAAACTGGAAAGTGTCTGATGAAA 120
Sbjct 121     CTCGTCGTAGTCAAATCCTACAAGGTGCCAACTACAGAAACTGGAAAGTGTCTGATGAAA 180

Query 121     TGCATGATCACCAAACTAGGACTGCTGAACGACGATGGTTCTGATACAAAACTGGCATG 180
Sbjct 181     TGCATGATCACCAAACTAGGACTGTTGAACGACGATGGTTCTGATACAAAACTGGCATG 240

Query 181     GAAGCGGGGTTAAAGAAATACTGGTCGGAATGGTCTACGGAGAAGATAGAGAGTATAAAC 240
Sbjct 241     GAAGCGGGGTTAAAGAAATACTGGTCGGAATGGTCTACGGAGAAGATAGAGAGTATAAAC 300

Query 241     AACAAAGTGTATTGAAGAAAGCTTTACTTGTGTCAAAGGAGGTAGTAGCGACGTCGAATTAC 300
Sbjct 301     AACAAAGTGTATTGAAGAAAGCTTTACTTGTGTCAAAGGAGGTAGTAGCGACGTCGAATTAC 360

Query 301     TCGTACACTGTGATGGCATGTTGAACAAGCAGTTGGATCTGCAACAGTCAACT 354
Sbjct 361     TCGTACACTGTGATGGCATGTTGAACAAGCAGTTGGATCTGCAACAGTCAACT 414
```

```
>191021-005_I24_1D05ZAA245.ab1
Sequence ID: Query_58441 Length: 1578
Range 1: 61 to 414

Score:284 bits(623), Expect:3e-81,
Method:,
Identities:117/118(99%), Positives:118/118(100%), Gaps:0/118(0%)

Query 1      RFTTEQIDYYGKACHASEDDLWVKSYPVTTETGKCLMKCMITKLGLLNDGGSYRKTM 180
Sbjct 61      RF+TEQIDYYGKACHASEDDLWVKSYPVTTETGKCLMKCMITKLGLLNDGGSYRKTM 240

Query 181     EAGLKKYSEWSETEKIESINMKCYEALLVSKVWATCNYSYTMALNKQLDLDKST 354
Sbjct 241     EAGLKKYSEWSETEKIESINMKCYEALLVSKVWATCNYSYTMALNKQLDLDKST 414
```

- *Acyrtosiphon pisum* OBP7 **A**: nucleotide sequence; **B** amino acid sequence

```
>191122-023_M24_1DD5ZAA243.ab1
Sequence ID: Query_913 Length: 1467
Range 1: 65 to 439

Score:693 bits(375), Expect:0.0,
Identities:375/375(100%), Gaps:0/375(0%), Strand: Plus/Plus

Query 1      TACTTGAGTGAAGCGGCCATcaaaaaaCACAACAGATGTTGAAAACCGTATGCTCCAAG 60
Sbjct 65      TACTTGAGTGAAGCGGCCATCAAAAAACACAACAGATGTTGAAAACCGTATGCTCCAAG 124

Query 61      AACATTGGTGAAGAGGACGATTACGAACATCAAAAAAGGAATATTTCCAGAGGAC 120
Sbjct 125     AACATTGGTGAAGAGGACGATTACGAACATCAAAAAAGGAATATTTCCAGAGGAC 184

Query 121     AACAAATATAAAATGTTACTTTGCTGTAATTTCAAACATGCAATGATCAATCAA 180
Sbjct 185     AACAAATATAAAATGTTACTTTGCTGTAATTTCAAACATGCAATGATCAATCAA 244

Query 181     AAGGGAGTCATCGATAaaaaaaTGTCAAAGACAAGATGTCGATGATGGCACCACCGAAC 240
Sbjct 245     AAGGGAGTCATCGATAAAAAAATGTTCAAAGACAAGATGTCGATGATGGCACCACCGAAC 304

Query 241     GTATACAAAATTTGTTACAGTTATAGAACAGTGTACTGAAAAAGATAAAGGTGAAGAA 300
Sbjct 305     GTATACAAAATTTGTTACAGTTATAGAACAGTGTACTGAAAAAGATAAAGGTGAAGAA 364

Query 301     CTCTGTCAGTCTTCTACAACGTCATAAAGTGCAGCAGTCTGTTGATCCCAAAAAGTTTA 360
Sbjct 365     CTCTGTCAGTCTTCTACAACGTCATAAAGTGCAGCAGTCTGTTGATCCCAAAAAGTTTA 424

Query 361     GAGTTTCTACCACTC 375
Sbjct 425     GAGTTTCTACCACTC 439
```

```
>191122-023_M24_1DD5ZAA243.ab1
Sequence ID: Query_62989 Length: 1467
Range 6: 65 to 439

Score:271 bits(586), Expect:2e-77,
Method:,
Identities:125/125(100%), Positives:125/125(100%), Gaps:0/125(0%)

Query 1      YLSEAAIKKQQMLKTVCSKKSVEEDVFTNIKKGIFPEDNNIKCYFACNFKTMQLINQ 180
Sbjct 65      YLSEAAIKKQQMLKTVCSKKSVEEDVFTNIKKGIFPEDNNIKCYFACNFKTMQLINQ 244

Query 181     KGVIdkkmfkdkmsmmAPPNVYKILLPVIEQCTGKDKGEELCQSSYNVIKCAHSVDPKSL 360
Sbjct 245     KGVIdkkmfkdkmsmmAPPNVYKILLPVIEQCTGKDKGEELCQSSYNVIKCAHSVDPKSL 424

Query 361     EFLPL 375
Sbjct 425     EFLPL 439
```

- *Acyrtosiphon pisum* OBP9 **A**: nucleotide sequence; **B** aminoacid sequence

```
>191122-023_024_1005ZAA244.ab1
Sequence ID: Query_9495 Length: 1482
Range 1: 128 to 550
Score:776 bits(420), Expect:0.0,
Identities:423/423(100%), Gaps:0/423(0%), Strand: Plus/Plus
Query 1 GATGATGCAGATGCAAAGGATAAGGAATTAATGTCAAATATTCACTGTGGTTTTTAAA 60
Sbjct 128 GATGATGCAGATGCAAAGGATAAGGAATTAATGTCAAATATTCACTGTGGTTTTTAAA 187
Query 61 TGCTTTAAGGATGCCGATTGGGGCACGTGCGGTGAAATGATAACAACATAAATATGACATA 120
Sbjct 188 TGCTTTAAGGATGCCGATTGGGGCACGTGCGGTGAAATGATAACAACATAAATATGACATA 247
Query 121 ACTCAAGCTAAATATAAACAGTGATCATGTACATGGCGTGTGGGGAAGAACTTGA 180
Sbjct 248 ACTCAAGCTAAATATAAACAGTGATCATGTACATGGCGTGTGGGGAAGAACTTGA 307
Query 181 ATGATAAACGCTTCGGGGCAACGAGAACCTGCGAAGTTCCTGAATACGTGAACAAAATC 240
Sbjct 308 ATGATAAACGCTTCGGGGCAACGAGAACCTGCGAAGTTCCTGAATACGTGAACAAAATC 367
Query 241 AATAATCCAGACATTAAGAGTCAATTGCAACTTATTACGACAAATGCCAAAATGTCAA 300
Sbjct 368 AATAATCCAGACATTAAGAGTCAATTGCAACTTATTACGACAAATGCCAAAATGTCAA 427
Query 301 GGGTCGGAGAAATGCGCATCTCGCAGAAACAATTTGCCATATGTGCTTTAAGGAATCACCA 360
Sbjct 428 GGGTCGGAGAAATGCGCATCTCGCAGAAACAATTTGCCATATGTGCTTTAAGGAATCACCA 487
Query 361 CCACTGAAAGAACGCTTTCTACGTGATGGAATGCTAGTGAAGATGAAACAAAATCA 420
Sbjct 488 CCACTGAAAGAACGCTTTCTACGTGATGGAATGCTAGTGAAGATGAAACAAAATCA 547
```

```
>191122-023_024_1005ZAA244.ab1
Sequence ID: Query_27909 Length: 1482
Range 1: 128 to 550
Score:344 bits(745), Expect:3e-99,
Method:,
Identities:141/141(100%), Positives:141/141(100%), Gaps:0/141(0%)
Query 1 DDADAKDELMSKLFVVFKCFKADWGTGCEMITTKYDIQAKYKQCTCHMACAGEELG 180
Sbjct 128 DDADAKDELMSKLFVVFKCFKADWGTGCEMITTKYDIQAKYKQCTCHMACAGEELG 307
Query 181 MINASGQPEPAKFLFYVNHINHPDIKSQLIYDKCQHWKSEKDLAEQFAICAFKESP 360
Sbjct 308 MINASGQPEPAKFLFYVNHINHPDIKSQLIYDKCQHWKSEKDLAEQFAICAFKESP 487
Query 361 ALKERVSTLMEHLV0MKPKSK 423
Sbjct 488 ALKERVSTLMEHLV0MKPKSK 550
```

- *Megoura viciae* OBP3. **A**: nucleotidic sequence **B** aminoacidic sequence

```
>191021-005_M24_1005ZAA246.ab1
Sequence ID: Query_47679 Length: 1179
Range 1: 62 to 415
Score:643 bits(348), Expect:0.0,
Identities:352/354(99%), Gaps:0/354(0%), Strand: Plus/Plus
Query 1 CGATTTACAACGGAACAATCGATTATTACGAAAAGCTGCAACGCCAGCAGAGATGAC 60
Sbjct 62 CGATTTACACGGAGCAATCGATTATTACGAAAAGCTGCAACGCCAGCAGAGATGAC 121
Query 61 CTCGTCGTAGTCAAATCTACAAGGTACCATCTTACGAAAAGTGGAAAGTGTCTGATGAAA 120
Sbjct 122 CTCGTCGTAGTCAAATCTACAAGGTACCATCTTACGAAAAGTGGAAAGTGTCTGATGAAA 181
Query 121 TGCATGATCACCAAACTAGGACTGCTGAACGACGATGGTTCGTACAAACAAACTGGCATG 180
Sbjct 182 TGCATGATCACCAAACTAGGACTGCTGAACGACGATGGTTCGTACAAACAAACTGGCATG 241
Query 181 GAAGCGGGCTGAAGAAATACTGGTCCGAATGGTCTACGGAGAAAATCGAGTCTATAAAC 240
Sbjct 242 GAAGCGGGCTGAAGAAATACTGGTCCGAATGGTCTACGGAGAAAATCGAGTCTATAAAC 301
Query 241 AACAAAGTTATGAAGAAGCTTTACTTGTGTCAAAGAGGTAATAGCGACGTGCAATTAT 300
Sbjct 302 AACAAAGTTATGAAGAAGCTTTACTTGTGTCAAAGAGGTAATAGCGACGTGCAATTAT 361
Query 301 TCGTACACTGTGATGGCATGTCTGAACAACAGTTAGATCTCGACAAGTCAACT 354
Sbjct 362 TCGTACACTGTGATGGCATGTCTGAACAACAGTTAGATCTCGACAAGTCAACT 415
```

```
>191021-005_M24_1005ZAA246.ab1
Sequence ID: Query_26517 Length: 1179
Range 1: 62 to 415
Score:285 bits(625), Expect:1e-81,
Method:,
Identities:118/118(100%), Positives:118/118(100%), Gaps:0/118(0%)
Query 1 RFTTEQIDYYGKACNASIEDDLVVKSYKVPSETGKCLMKMITKLGLLNDDGSYNKTM 180
Sbjct 62 RFTTEQIDYYGKACNASIEDDLVVKSYKVPSETGKCLMKMITKLGLLNDDGSYNKTM 241
Query 181 EAGLKKYSEWSTEKIESINNKCYEALLVSKEVIATCHNSYTVMACLNKQLDLKST 354
Sbjct 242 EAGLKKYSEWSTEKIESINNKCYEALLVSKEVIATCHNSYTVMACLNKQLDLKST 415
```

## **Appendix B: protocols**

### **B1. Plasmid dephosphorylation**

Dephosphorylation is a common step in traditional cloning workflows to ensure that the vector does not re-circularize during ligation. It consists on the following steps:

1. Add Reaction Buffer to linear plasmid (NEBuffer #3, B7203S).
2. Add CIP (Alkaline Phosphatase, Calf Intestinal ; # M0290).
3. Incubate 1 hour at 37°C.
4. Incubate 30 minutes at 55°C.
5. Repeat step 2, step 3 and step 4.
6. Purify DNA by phenol extraction.

### **B2. DNA Extraction from Agarose Gel**

Purification of double-stranded DNA from TAE agarose gel was conducted using Quantum Prep™ Freeze 'N Squeeze DNA gel Extraction Spin column.

1. Excise the band of interest using a clean razor blade and trim excess of agarose from all sides.
2. Chop the trimmed gel slice and place it into the filter cup.
3. Freeze 5 minutes at -20°C.
4. Centrifuge the sample at 13000 x g for 3 minutes at room temperature.
5. Collect the purified DNA.

Ethanol precipitation of the purified DNA was performed to further purify the sample.

### **B3. Ca<sup>2+</sup> competent cells transformation**

Transformation is a key process in molecular cloning, by which multiple copies of recombinant DNA molecules are produced. The ability to take up free, extracellular genetic material is the prerequisite for bacterial competent cells to undergo transformation. The objective is to obtain the replication of sequence of interest of a recombinant plasmid.

It consists on the following steps:

1. Thaw cells in ice.
2. Pipet max 30 ng of DNA into cells.
3. Mix gently.
4. Ice for 30 minutes.
5. Incubate at 42°C for 45 seconds.
6. Ice for 15 minutes.

7. Add SOC (Super Optimal broth with Catabolite repression) up to 1 mL.
8. Incubate 1 hour at 37°C.
9. Plate on LB agar medium containing appropriate antibiotic

#### **B4. Mini-prep procedure**

Mini-preparation of plasmid DNA is a rapid, small-scale isolation of plasmid DNA from bacteria. Mini-preps are used in the process of molecular cloning to analyse bacterial clones.

The kit used for mini-prep was Fast Plasmid Mini Kit and it consist on:

1. Pellet 1.5 ml of fresh bacterial culture at maximum speed for 1 minute in the provided 2 ml Culture Tube.
2. Remove medium by decanting, taking care not to disturb bacterial pellet.
3. Add 400 µL of ICE-COLD Complete Lysis Solution.
4. Mix thoroughly by constant vortexing at the highest setting for a full 30 seconds. This step is critical for obtaining maximum yield.
5. Incubate the lysate at room temperature for 3 minutes.
6. Transfer the lysate to a Spin Column Assembly by decanting or pipetting.
7. Centrifuge the Spin Column Assembly for 60 seconds at maximum speed.
8. Add 400 µL of DILUTED Wash Buffer to the Spin Column Assembly.
9. Centrifuge the Spin Column Assembly for 60 seconds at maximum speed.
10. Remove the Spin Column from the centrifuge and decant the filtrate from the Spin Column Assembly Waste Tube. Place the Spin Column back into the Waste Tube and return it to the centrifuge.
11. Centrifuge at maximum speed for 1 minute to dry the Spin Column.
12. Transfer the Spin Column into a Collection Tube.
13. Add 50 µL of Elution Buffer directly to the centre of the Spin Column membrane and cap the Collection Tube over the Spin Column.
14. Centrifuge at maximum speed for 60 seconds.
15. Remove and discard the Spin Column.
16. The eluted DNA can be used immediately for downstream applications or stored at -20°C

#### **B5. Midi-prep procedure**

Midi-preparation of plasmid DNA is a plasmid DNA isolation technique from bacteria. It differ from mini-prep because of the initial bacteria culture used. It leads to get more plasmid DNA. The kit used for midi-prep was the HiPure PureLink™ Plasmid Midiprep and it consist

on:

1. Harvest 50 mL bacterial culture by centrifuging the overnight LB culture at  $4000 \times g$  for 10 minutes. Remove all medium.
2. Add 4 mL Resuspension Buffer (R3) with RNase A to the cell pellet and resuspend the cells until homogeneous.
3. Add 4 mL Lysis Buffer (L7). Mix gently by inverting the capped tube until the lysate mixture is thoroughly homogenous.
4. Incubate at room temperature for 5 minutes.
5. Add 4 mL Precipitation Buffer (N3) and mix immediately by inverting the capped tube until the mixture is thoroughly homogeneous.
6. Centrifuge the mixture at  $>12000 \times g$  for 10 minutes at room temperature.
7. Load the supernatant onto the equilibrated (EQ Buffer) column. Allow the solution in the column to drain by gravity flow.
8. Wash the column twice with 10 mL Wash Buffer (W8). Allow the solution in the column to drain by gravity flow after each wash. Discard the flow-through.
9. Proceed to Elute and precipitate DNA using 5 mL Elution Buffer (E4) to the column and allow the solution to drain by gravity flow.
10. The elution tube contains the purified DNA.
11. Discard the column and add 3.5 mL isopropanol to the elution tube. Mix well.
12. Centrifuge the tube at  $>12000 \times g$  for 30 minutes at  $4^{\circ}\text{C}$ .
13. Carefully remove and discard the supernatant and resuspend the pellet in 3 mL 70% ethanol.
14. Centrifuge the tube at  $>12000 \times g$  for 5 minutes at  $4^{\circ}\text{C}$ .
15. Carefully remove and discard the supernatant and air-dry the pellet for 10 minutes.
16. Resuspend the DNA pellet in TE Buffer (TE).

### **B6. Denaturing protocol extraction**

Cell lysis was obtained using denaturing lysis buffer containing 8 M Urea.

After induction, cells were harvested and centrifuged at  $4000 \times g$  for 20 minutes at  $4^{\circ}\text{C}$ . the supernatant was discarded and the pellet resuspended in denaturing lysis buffer (5ml/g).

Samples were incubated at room temperature for 20 minutes and then centrifuged at  $13000 \times g$  for 20 minutes at  $4^{\circ}\text{C}$ . The supernatant was collected and analysed using SDS-page. Pellet was also analysed to verify the presence of recombinant protein.

## **B7. Solubilisation and refolding of recombinant protein.**

Recombinant protein were already checked in inclusion bodies. For this reason denaturing protocol extraction was used instead sonication.

Denaturing buffer containing 8 M Urea allows to destroy cell wall and cytoplasmatic membrane. Urea also solubilised the inclusion bodies.

Inclusion bodies contain very little host protein, ribosomal components or DNA/RNA fragments. They often almost exclusively contain the over expressed protein.

Protein inclusion bodies are classically thought to contain misfolded protein but in the last decades researcher find a way to refold protein in IBs.

The protocol used in this work consist on “oxido-shuffling” reagents, cysteine-cystine:

1. Add 10 mM DTT dissolved in Tris-HCl pH 8.0 (250  $\mu$ L/100 mL of cells culture).
2. Incubate at room temperature for 1 hour.
3. Add 100 mM cystine dissolved in 0.5 M NaOH (100  $\mu$ L/100 mL of cells culture).
4. Incubate at room temperature for 10 minutes.
5. Add 5 mM cysteine dissolved in 100 mM Tris-HCl, pH 8.0 (1 mL/100 mL of cells culture).
6. Incubate for 16 hours at a 4°C, under stirring.
7. Dialyzed against appropriate buffer.

## **B8. SDS-PAGE**

In order to check all protein samples obtained, a 5% stacking and 12% separation polyacrylamide gels were made (Sambrook and Russel, 1989)

After polymerisation, the polyacrylamide gel was washed with distilled water and immersed in 1x Running Buffer. 19  $\mu$ L of each sample was prepared for running on polyacrylamide gels, supplemented with 4x Laemmli sample buffer up to a final volume of 25  $\mu$ L.

All samples were heated at 100°C for 5 min and loaded onto the wells of stacking gel, with a molecular weight marker for reference. Proteins were visualised on separation gel thanks to Coomassie staining solution and then by rinsing gel with a Destaining solution until blue bands were clearly visible.

## **B9. Anion exchange chromatography**

Anion-exchange chromatography is a process that separates substances based on their charges using an ion-exchange resin containing positively charged groups. In this work, DEAE-Sepharose resin was used. Purification was performed using a bench column and 1,5 mL elution fraction were obtained thanks to gravity flow.

1 mL of resin was loaded into polypropylene column and equilibrate with 50mM Tris Buffer pH 7.4 until the output pH was the same of input. Then sample was loaded and an incubation time of 15 minutes occurs. 10 mL of 50mM Tris Buffer pH 7.4 were used to elute the recombinant protein and 10 mL 50mM Tris Buffer pH 7.4/ 1M NaCl were used to elute bacterial proteins. This protocol was used for *Apis*OBP3, *Mvic*OBP3 and *Apis*OBP7.

For *Apis*OBP7, a different pH of buffer was used (10.8 instead 7.4).

Ionic exchange purification exploit the isoelectric point of recombinant proteins. The isoelectric point (pI) is the pH at which a molecule carries no net electrical charge. The net charge on the molecule is affected by pH of its surrounding environment and can become more positively or negatively charged due to the gain or loss, respectively, of protons (H<sup>+</sup>). At a pH below their pI, proteins carry a net positive charge; above their pI they carry a net negative charge. For *Apis*OBP3 and *Mvic*OBP3, elution was performed using a buffer with pH 2 time above their pI (5.20) to allow the binding of sample to the positively charged resin. At pH 7.4, the two proteins have a negative charge and can bound the positively charged resin. For *Apis*OBP7 (pI = 8.8) two anionic exchange strategies were adopted. The first attempt consisted on using elution buffer with pH 10.8; the second was based on using a elution buffer with pH 7.4. In the first case, the pH was 2 time above pI and in this condition, the negative charge of protein allowed the binding of sample to the positively charged resin. The second attempt was conducted using buffer with pH 7.4 according to consideration on acidic nature of bacterial proteins (Adhikari et al., 2010) and the basic nature of *Apis*OBP7. At this pH value, bacterial protein are virtually negative charged and OBP7 virtually has positive net charge.

### **B10. Gel filtration chromatography**

Gel filtration chromatography is a chromatographic method in which molecules in solution are separated by their size and molecular weight.

2 g of Sephadex G50 were swollen in 30 mM Tris Buffer pH 8, overnight at 4°C.

The next day the resin was loaded into propylene column creating a packed column.

Sample was loaded into column and 10 mL of 30 mM Tris Buffer pH 8 were used as mobile phase and 1.5 mL fraction were collected under gravity flow.

### **B11. Ni-NTA chromatography**

Ni-NTA resin was used to purify the His-tagged *Apis*OBP9. The procedure was conducted in batch. The protocol used was:

1. Add 1 ml of the 50% Ni-NTA slurry to 4 ml cleared lysate and mix gently by shaking (200 rpm on a rotary shaker) at 4°C for 60 min.
2. Load the lysate–Ni-NTA mixture into a column with the bottom outlet capped.
3. Remove bottom cap and collect the column flow-through. Save flow-through for SDS-PAGE analysis.
4. Wash twice with 4 ml wash buffer; collect wash fractions for SDS-PAGE analysis.
5. Elute the protein 4 times with 0.5 ml elution buffer. Collect the eluate in four tubes and analyse them by SDS-PAGE.



## Appendix C: solutions

### C1. Bacterial medium

- **Liquid bacterial culture:** LB (Luria – Bertani) Broth  
10 g Tryptone enzymatic digest from Casein (Fluka Analytical, #95039)  
5 g Selected yeast extract (Sigma Aldrich, #Y0875)  
10 g Sodium chloride (Sigma Aldrich, #31434)  
Final volume: 1 L distilled water  
Autoclave (Compact 40 Benchtop Priorclave): 121°C 15 min
- **Solid bacterial culture:** LB Agar 1,5%  
1.5 g Agar bacteriological (OXOID, LP0011)  
100 mL Luria Bertani (LB) broth  
Autoclave (Compact 40 Benchtop Priorclave): 121°C 15 min.

### C2. Denaturing Lysis Buffer

Volume: 1 liter

100 mM NaH<sub>2</sub>PO<sub>4</sub> [13.8 g NaH<sub>2</sub>PO<sub>4</sub>·H<sub>2</sub>O (MW 137.99 g/mol)]

10 mM Tris [1.2 g Tris base (MW 121.1 g/mol)]

8 M urea [480.5 g (MW 60.06 g/mol)]

Adjust pH to 8.0 using NaOH.

### C3. Native Lysis Buffer

Volume: 1 liter

50 mM NaH<sub>2</sub>PO<sub>4</sub> [6.90 g NaH<sub>2</sub>PO<sub>4</sub>·H<sub>2</sub>O (MW 137.99 g/mol)]

300 mM NaCl [17.54 g NaCl (MW 58.44 g/mol)]

10 mM imidazole [0.68 g imidazole (MW 68.08 g/mol)]

Adjust pH to 8.0 using NaOH.

### C4. Purification Buffers

- **Tris Buffer (Anionic exchange chromatography and gel filtration)**

**Stock solution:** 1M, Volume 1 Liter

1M Tris base [121.14 g (MW 121.14 g/mol)]

Adjust solution to desired pH using HCl

30 mM and 50 mM dilutions were prepared from the stock.

- **Elution Buffer, denaturing conditions (Ni-NTA purification)**

**Buffer D**

Volume: 1 Liter

100 mM NaH<sub>2</sub>PO<sub>4</sub> [13.8 g NaH<sub>2</sub>PO<sub>4</sub>·H<sub>2</sub>O (MW 137.99 g/mol)]

10 mM Tris·Cl [1.2 g Tris base (MW 121.1 g/mol)]

8 M urea [480.5 g (MW 60.06 g/mol)]

Adjust pH to 5.9 using HCl.

**Buffer E**

Volume: 1 Liter

100 mM NaH<sub>2</sub>PO<sub>4</sub> [13.8 g NaH<sub>2</sub>PO<sub>4</sub>·H<sub>2</sub>O (MW 137.99 g/mol)]

10 mM Tris·Cl [1.2 g Tris base (MW 121.1 g/mol)]

8 M urea [480.5 g (MW 60.06 g/mol)]

Adjust pH to 4.5 using HCl.

- **Elution Buffer, native conditions (Ni-NTA purification)**

Volume: 1 Liter

50 mM NaH<sub>2</sub>PO<sub>4</sub> [6.90 g NaH<sub>2</sub>PO<sub>4</sub>·H<sub>2</sub>O (MW 137.99 g/mol)]

300 mM NaCl [17.54 g NaCl (MW 58.44 g/mol)]

250 mM imidazole [17.00 g imidazole (MW 68.08 g/mol)]

Adjust pH to 8.0 using NaOH.

## **C5. Protein electrophoresis solution**

- **Running buffer (10X)**

60 g Trizma base (248 mM) (Sigma Aldrich, #T1503)

288 g Glycine (1.92 M) (Sigma Aldrich, #50046)

20 g Sodium Dodecyl Sulfate (1 % w/v) (Bio-Rad #1610302)

Final volume: 2 L distilled water

- **Laemli 4X**

25% v/v Glycerol (Sigma Aldrich, #56-81-5)

5% β-mercaptoethanol (Sigma Aldrich, #60-24-2)

2% w/v Sodium Dodecyl Sulfate (1 % w/v) (Bio-Rad #1610302)

0.01% w/v bromophenol blue (Bio-Rad #1610404)

65 mM TrisHCl, pH 6.8

- **Destaining solution**

300 mL Methanol (30%) (Sigma Aldrich, #322415) or alternatively Ethanol (30%) (Sigma Aldrich, #16368)

100 mL Glacial acetic acid (10%) (Sigma Aldrich, #33209)

600 mL distilled water

- **Comassie solution**

1.25 g Coomassie blue brilliant R-250 (Bio-Rad, # 1610400)

225 mL Methanol (Sigma Aldrich, #322415)

50 mL Glacial acetic acid (Sigma Aldrich, #33209)

225 mL distilled water